I - EXECUTIVE SUMMARY

This synthesis, initiated during the meeting, was consolidated therafter by inputs received from the workshop participants, and in particular from John Allen, Isabel Ambar, Isabelle Taupier Letage, Marlon Lewis, Ananda Pascual and Volker Strass. Jordi Font and Frederic Briand, assisted by Carolyn Scheurle and Paula Moschella, took care of the final editing, while Valérie Gollino did oversee the physical production process.

1. INTRODUCTION

A workshop focused on the observation, understanding and prediction of mesoscale processes in the Mediterranean Sea was held from 25 to 28 May 2005 at the historical Station Zoologique, part of the Observatoire Océanologique de Villefranche-sur-mer. Nineteen scientists originating from twelve countries attended the meeting at the invitation of CIESM.

In welcoming the participants, Frédéric Briand, Director General of the Commission, stressed the exploratory nature of CIESM workshops, seeking as much as possible to capture emerging concepts and hypotheses. This guided the choice of the guests – physicists, biologists and modelers – assembled here to reflect upon the challenges raised, and the best tools available for the study of mesoscale biological and physical processes, now increasingly recognized as highly significant in the Mediterranean Sea and elsewhere. He expressed his thanks and appreciation to Michel Glass[1], Director of the Observatory, and to his staff for facilitating the preparation of the meeting. He then invited Jordi Font, Chair of the CIESM Committee on Physics and Climate of the Ocean who initially conceived the theme of the workshop, to present the scientific background and objectives of the meeting.

As revealed by many studies during the last two decades, the Mediterranean Sea is an ocean region where intermediate scales (mesoscale) play a key role in determining the characteristics of the basin-wide marine circulation, the distribution of water masses, and even ecosystem functioning. A multidisciplinary approach in the study of mesoscale structures and processes is an increasing demand of researchers. Specialists from different disciplines and with complementary backgrounds were therefore invited to this workshop to review the main issues of mesoscale research in the Mediterranean, and to propose new foci and techniques to help the entire Mediterranean community to significantly advance in this field.

Two days of individual presentations were followed by two days of general discussions and recommendations for future work. The presentations covered a wide range of topics and raised exciting discussions, including debate on issues regarding interpretation of available data and conceptual models that reveal open questions and highlight the need for collaborative efforts in mesoscale research. In the following, the main conclusions of the workshop are summarized, followed by extended abstracts of the different presentations.

1 On the following day Dr Glass presented a survey of the fascinating history of the research carried out at the Station, from the early days traced by Russian plankton scientists, to nowadays when it has emerged as a major multi-disciplinary Center.

Mesoscale features represent the internal weather systems of the ocean. As such, their role in the distribution of water properties and life in the ocean is as important as that of the atmospheric weather in the distribution of air properties and terrestrial life.

Almost every satellite image of sea surface height, sea surface temperature or ocean colour reveals mesoscale meanders, filaments and eddies. Mesoscale eddies are low or high pressure systems associated with cyclonic or anticyclonic circulation, respectively. Like their atmospheric counterparts, they are mostly formed by baroclinic instability of larger-scale fronts. The mesoscale motions draw their kinetic energy from the reservoir of available potential energy. Additional input of kinetic energy can come from the horizontal shear of larger-scale currents through barotropic instability. As a result of the conversion of available potential energy, spectra for horizontal motions in the ocean generally reveal a maximum of kinetic energy in the mesoscale range. Because of their analogy to atmospheric weather systems, mesoscale phenomena of the ocean are occasionally also called synoptic (e.g. Kamenkovich *et al*., 1986).

The horizontal scale of mesoscale features is set solely by internal properties of the ocean, as measured by the internal Rossby radius of deformation; it is not imposed by external forcing or topography, for instance. The range of mesoscale horizontal dimensions extends from a few kilometers to a few hundreds of kilometers, where the restoring ß-effect exerts a limiting control. The vertical extent ranges from few tens to a few thousands of meters (i.e. down to the bottom). The timescales associated with mesoscale motions are typically in the range of a few days to several months (yet can reach several years).

Mesoscale dynamics is governed by quasi-geostrophic balances. While the associated motions are thus mainly horizontal, small deviations from geostrophy make a significant difference. In places where the flow changes in time, and where eddies interact with each other or with the mean flow, frontogenesis or frontolysis results, and the conservation of potential vorticity consequently induces vertical motions. Such upwelling or downwelling events can be strong enough (tens of meters per day) and last long enough (several days) to affect biological processes. The primary production by planktonic algae in particular can be affected, for instance as a result of the displacement of phytoplankton cells along the vertical light profile or as a result of a vertical flux of plant nutrients. This leads to another analogy with atmospheric weather processes, namely the creation of (phytoplankton) clouds and their subsequent (sedimentation) precipitation. That the mesoscale circulation also accounts for the advection of organisms, and hence either accomplishes or hinders completion of their life cycles, is obvious.

Although the length scale of mesoscale motions is set by internal properties of the ocean, mesoscale eddies can become trapped by topographic structures if these have matching dimensions. In the Mediterranean this seems to happen quite regularly, so that eddies attain the characteristics of stationary gyres. Prominent examples are the Alboran gyres. The Alboran Sea[2] is the region of the western Mediterranean basin adjacent to the Strait of Gibraltar, through which a two layer exchange takes place with an inflow of fresher Atlantic water in the upper layer and an outflow of saltier Mediterranean Water below. Due to the mesoscale motions that are superimposed on the thermohaline circulation, which is driven by the Mediterranean basin-scale dominance of evaporation over river runoff and precipitation, the surface inflow at Gibraltar occurs, most generally, in a narrow (25-30 km wide) north-eastward jet that later forms a meandering front, coupled to one or two large (100 km diameter) anticyclonic gyres trapped by the topography. The incoming Atlantic water mixes with the surface resident water, giving rise to the modified Atlantic waters (Gascard and Richez, 1985), known as Atlantic Water (AW – see www.ciesm.org/catalog/WaterMassAcronyms.pdf) within the Mediterranean. It fills the southern Alboran and then flows eastward to the whole Mediterranean Sea (Font *et al*., 2002; Millot and Taupier-Letage, 2005a).

On the western side of the Strait of Gibraltar, the out-flowing Mediterranean Water (MW) creates a water mass signature that can be traced throughout the Atlantic Ocean and even beyond.

2 One will remark through the course of this Monograph that different authors may use different terms to name identical type of maritime regions (sea, basin, sub-basin, etc.). CIESM is seeking ways to reach harmonization.

Mesoscale dynamics contributes significantly to the spreading of MW in the Atlantic, as a substantial fraction of this water penetrates into the Atlantic by way of the so-called meddies (for a recent account see Siedler *et al*., 2005). Meddies are long-lived, sub-surface eddies or lenses containing high-salinity water of Mediterranean origin with anticyclonic rotation and approximate diameters of 100 km, which have been observed to form off the southwestern coast of Portugal (Bower *et al*., 1995). The spreading of the Mediterranean Water in the world ocean is an example of the diffusive effect that mesoscale eddies can have in the mean over larger space and time scales.

It follows that any endeavour to improve the skill of operational modeling and forecasting requires a sufficient understanding of mesoscale processes. Developing the best strategies for observing, analyzing, and forecasting mesoscale processes was hence the aim of this workshop.

Compared to synoptic meteorology, resolving and forecasting the 'ocean weather' is complicated by the fact that the scale of the ocean weather systems is much smaller (~ 10 - 100 km) than that of the atmospheric weather systems (~ 100 - 1000 km). Per unit area, numerical ocean forecast models thus need hundred times as many grid points as atmosphere forecast models. Since computer power still is a constraint, an acceptable model resolution will be more easily achieved for an ocean basin that is as confined as the Mediterranean Sea. This, combined with the fact that the lateral boundaries are rather small and the surface forcing is comparably well defined, makes the Mediterranean Sea an ideal test bed for the improvement of ocean forecasting models. Furthermore Mediterranean waters are quite easily accessible for collecting the relevant mesoscale data sets needed for model validation.

2. TIME SCALES, LENGTH SCALES AND BIOLOGICAL IMPACT

Lewis (2002) provided a review of 50 years of research recognizing and explaining the relationship between scales of biological patchiness and physical mechanisms in the open ocean (see also LeBlanc *et al*., 2004; Strass, 1992; Steemann Nielsen, 1952). We do not attempt to summarise this here: instead we introduce some recent arguments and observations which were the subject of very recent publication and/or discussion at this CIESM workshop.

At the mesoscale, spatially considered to be 10-100 km and temporally weeks to months, the vertical disturbance of isopycnal surfaces has been referred to as 'eddy pumping' (Falkowski *et al*., 1991). On its own, this represents a single stochastic source of nutrients to the euphotic zone related to the growth component of cyclonic (in the case of a mode 1 vertical dynamic height profile) or anticyclonic (in the case of a mode 2 vertical dynamic height profile) vorticity (Gill, 1982).

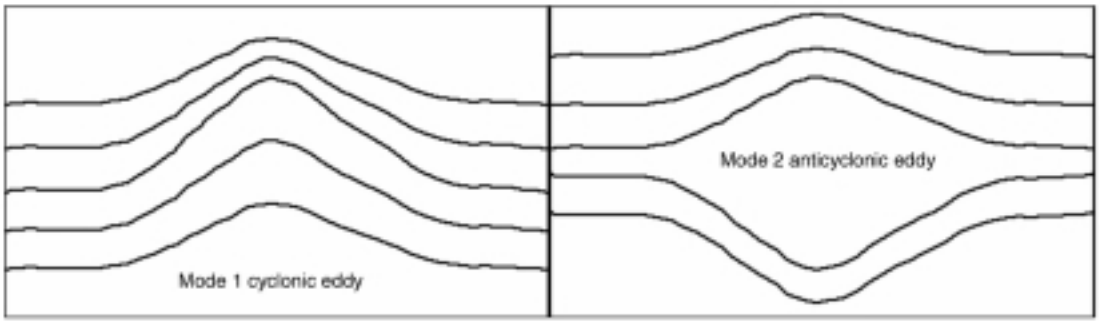

Fig. 1. Vertical structure of ocean eddies as depicted by the dynamic height isolines (from Gill, 1982).

A more sustained source of new nutrients to the euphotic layer comes from the wave propagation model of mesoscale eddies in which water is not trapped within the eddies but is moved up and down on isopycnal surfaces displaced vertically by the propagation of the eddies. This passing perturbation mode of influence for eddies has been discussed in the context of eddy permitting/resolving general circulation coupled ecosystem models (Oschlies, 2002; McGillicuddy *et al*., 2003). However, this mechanism still fails to supply enough new nutrients

into the euphotic zone to get anywhere near the Jenkins (1982) estimates of new production inferred from oxygen utilization. Part of the problem with this model of eddy scale processes is that the same isopycnal surfaces are brought up and down through the base of the euphotic zone and are steadily depleted of nutrients. A further restoring mechanism is required to replenish the nutrients; along isopycnal (effectively horizontal) mixing is the logical choice, although it is difficult to see how this could achieve the restoring time scales claimed (e.g. 10 days, Seigel *et al*., 2003).

More recent studies of internal wave driven turbulent mixing and a proper parameterisation of vertical diffusivity, taking into account the inherently double diffusive nature of the Atlantic (Dietze *et al*., 2004; Schmitt *et al*., 2005), make a significant contribution to the budgets but continue to fall short of finding the nutrients to satisfy the apparent requirements for export flux based on geochemical signals in deeper waters.

Of course it may be that the approach of Jenkins (1982) was simply in error: however, there is an eddy scale mechanism that is not well represented in even the highest resolution general circulation coupled ecosystem models, and which may hold the secret to the missing production. The ubiquity of mesoscale eddies in the open ocean has been demonstrated in the length scale and persistence of sea surface height anomaly data from satellite altimeters (Kuragano and Kamachi, 2000), in eddy kinetic energy spectra (Stammer, 1997; Wunsch, 1997; Wunsch and Stammer, 1995), and most obviously in the striped nature of ADCP data plotted for trans-basin WOCE like ocean sections (Bryden *et al*., 2002). The existence of these eddies predominantly results from baroclinic instability (Stammer, 1997). Although the impact of baroclinic instability is global, it is expressed at what Lévy *et al*. (2001) termed the 'sub-mesoscale' (1-10 km spatially, and perhaps days temporally). In the atmosphere this process drives weather scales. In the ocean, baroclinic instability creates eddies and meanders in water mass boundaries (Allen and Smeed, 1996; Munk *et al*., 2000). In baroclinic instability, potential energy is released, this happens through the real exchange of water vertically, higher density waters descending under less dense waters, not a closed circulation (Lévy *et al*., 2001; Allen *et al*., 2005).

General circulation models do not explicitly ignore baroclinic instability, but the discrete resolution (10-15 km or greater) of the model 'reality' prevents them from reproducing physical structures at scales much smaller than 50 km. Higher resolution process models (Lévy *et al*., 2001; Lévy, 2003; Nurser and Zhang, 2000, Allen *et al*., 2001a) clearly show that the cross front and vertical exchanges driven by baroclinic instability occur at much smaller scales. Although the net large scale tendency of baroclinic instability is to flatten sloping isopycnal surfaces (Pollard and Regier, 1992), the release of this potential energy happens through filamentary tongues extending along isopycnal surfaces where the along-isopycnal potential vorticity (angular momentum for a stratified fluid) gradient is low (Allen and Smeed, 1996; Allen *et al*., 2001b). These filaments are typically 1-10 km in width but may be many tens to hundreds of km in length and extend to hundreds of metres in depth. Releasing potential energy by carrying salt and heat, these filaments also carry biogeochemical signatures; exchanging nutrient-replete with nutrient-exhausted waters (Nurser and Zhang, 2000, Allen *et al*., 2005), and stripping organic material out of the surface layers (Videau *et al*., 1994; Fielding *et al*., 2001).

Mesoscale dynamics has time scales similar to biological growth rates

Individual atmospheric weather systems generally have little ecological impact on terrestrial or marine biological systems. Grass grows, algae blooms and herbivores graze through many low pressure (cyclonic) and high pressure (anticyclonic) weather systems. In the open ocean we have a very different picture. The primary producers and herbivores have shorter life time scales (days); time scales that coincide with those of mesoscale eddies and fronts, i.e. oceanographic 'weather'. This suggests that plankton can have either good or bad weather lifetimes associated with just a single cyclonic or anticyclonic eddy system. It also suggests that species or groups may be adapted to rapid acclimation rather than niche exploitation. The magnitude of vertical motions associated with baroclinic instability is significant on biological timescales both for phytoplankton growth and the development of zooplankton grazing pressure.

True mixing, buoyancy vs. diapycnal turbulent mixing

The gravitational sinking of organic particles results from the mortality of phytoplankton populations or faecal pellet residue following zooplankton grazing. In-vitro experiments on single diatom cells indicate very low sinking rates, generally < 1 m/ day (Smayda, 1970; Bienfang and Harrison, 1984). However delicate phytoplankton aggregates may have sinking velocities ≥ 100 m/ day resulting from a critical change in flow regime and thus drag coefficient (DiTullio *et al*., 2000). A commonly held misconception is that turbulence may help to support negatively buoyant phytoplankton cells, however, the simple consideration of a random motion against a constant gravitational force can be used to dismiss this view. Indeed the most recent experimental work on the impacts of turbulence (Ruiz *et al*., 2004) shows that on the contrary, turbulence acts to increase the net sinking velocity; resulting from the particles following rotational paths and converging in regions with the same flow direction as the gravity/buoyancy force. However, Rodriguez *et al*. (2001) showed that quite small advective upward vertical velocities, < 5 m/ day, were required to support a size structure spectrum biased towards the large (less buoyant) phytoplankton particles in the Alboran Sea, and such upward velocities are commonly induced by mesoscale phenomena.

3. OBSERVING TECHNOLOGIES AND METHODS

A recurrent problem in many oceanographic mesoscale studies is the difficulty to adapt the sampling needs of different aspects of a multidisciplinary program in a unique coherent observational strategy. Physical oceanographers are used to profile the ocean with CTD probes in such a rapid way that they can most often cover a 3D area affected by a mesoscale process in a time compatible with the scale of the phenomena under study. However, the classical techniques to determine chemical and biological properties are usually more time consuming and in many occasions provide data where the effects of spatial and temporal variability in a rapidly evolving mesoscale process/structure cannot be separated. The use of remotely sensed information, the development of new sensors and sampling platforms, and the availability of elaborated data analysis techniques and numerical models, are drawing an emerging scenario where building up a coherent full strategy to understand mesoscale phenomena starts to be a reality.

3.1. Remote sensing

Remote sensing has played and continues to play a key role in observing mesoscale dynamics, and thus in understanding the observed variability. Indeed satellite images provide a synoptic view at basin-scale, with resolutions in space (~ km) and time scales (day to week) that allow a correct description of the mesoscale phenomena such as filaments, fronts, eddies and gyres. Insofar as the general circulation of the water masses consists of unstable currents generating mesoscale meanders and eddies, remote sensing is also an excellent tool to study the former. Images - more generally remotely-sensed information - can be collected to build time series (duration up to several years, e.g. Marullo *et al*., 1999b; Larnicol *et al*., 2002; Antoine *et al*., 2005), making it possible to track mesoscale features (e.g. Puillat *et al*., 2002). With technological improvements it is easy now to receive the remotely-sensed information on-board oceanographic research vessels in (near) real-time, so that the sampling strategy of a cruise can be adequately defined, taking into account the mesoscale phenomena which impact both the dynamical and the biogeochemical /biological fields.

3.1.1. Data types

Exhaustive lists of available platforms and sensors, including the basic principles of the measure, are readily available (see for instance http://rst.gsfc.nasa.gov/). Here we will only offer a summary covering the most-widely used data types.

• Thermal imagery:

The AVHRR (Advanced Very High Resolution Radiometer) sensor is the most widely used to map the SST (Sea Surface Temperature). The spatial resolution (pixel) is about 1km and the thermal resolution ~0.13°C. The swath is ~2,000 km. Since several satellites fly simultaneously, most of the Mediterranean Sea can be covered several times per day. The SST retrieval is fairly easy, and data processing is mostly uniform in the receiving centers. (Near)real-time products are

commonly available. Since the thermal signal only comes from the upper layer, precautions must be taken to infer circulation and mesoscale features. Examples of tracking mesoscale structures with SST will be found in the papers of Ambar and Serra, or Taupier-Letage and Millot, in this volume. Note that other sensors (e.g. most of those dedicated to ocean colour) also have a thermal band, as the ATSR (Along Track Scanning Radiometer) on board the European ERS and Envisat satellites or MODIS (Moderate Resolution Imaging Spectroradiometer) on board the NASA EOS Terra and Aqua satellites.

• Visible/ocean colour imagery:

After a long gap between CZCS (Coastal Zone Color Scanner, 1978-1986) and SeaWiFS (Sea-viewing Wide Field-of-view Sensor, launched in 1997), nowadays there are several sensors flying simultaneously to map the surface distribution of algal pigments, dissolved organic matter and particulate matter. For a review of the parameters that can be computed and the sensors available see http://www.ioccg.org/. Examples of such images can be seen in the papers by Allen, Oguz, Poulain, Ribera *et al*., or Taupier-Letage and Millot, in this volume. The spatial resolution (pixel) ranges from less than 1km to ~4km. The Mediterranean is fully covered within 1-2 daytime period(s). The retrieval of the marine signal which amounts to less than 10% of the total is complex, and the nature of the matter (living- non living, particulate-dissolved) can be so specific, that algorithms are likely to be site-specific, and/or specific to a processing center. Due also to the longer processing chain, commercial concerns or administrative roadblocks, (near) real time products at full spatial resolution are seldom proposed on a regular basis. Because of the close relationship between physical and biological phenomena at mesoscale, the distribution of phytoplankton can also be used to infer horizontal advection, as shown by the correlation of both signatures on Figure 2 *(SST and CHL 28 Feb. 1998)*. Ocean colour images are even a better tracer than SSTs, since the signal comes from a thicker layer (1 optical depth, nominally 2-30 meters in the Mediterranean, depending on the level of biomass).

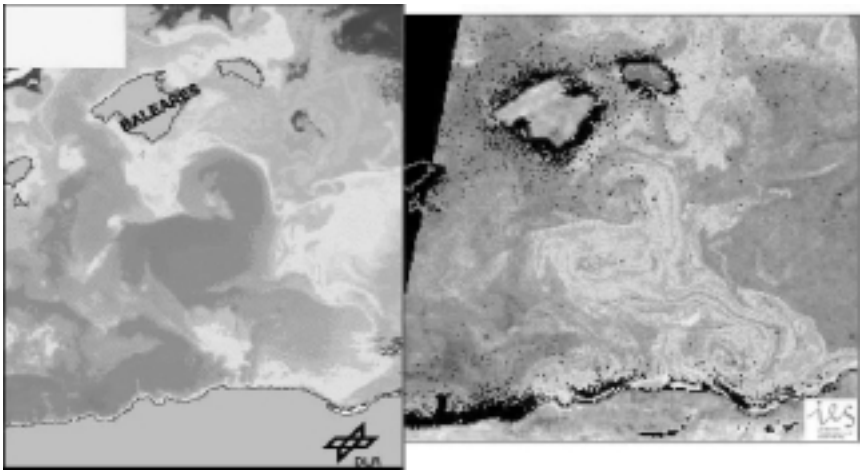

Fig.2. (See page 108 for original color plate) Thermal/SST (left, NOAA/AVHRR image, processed at DLR and LOB) and biological (right, SeaWiFS image, processed at IES/JRC) signatures of Algerian mesoscale (anticyclonic) eddies, on 28 February 1998. Temperature and chlorophyll content increase from blue to red.

• Altimetry:

Satellite altimetry is a useful tool providing sea surface topography measurements from which geostrophic velocities can be estimated. One of the big advantages of altimetry is that it can be used independently of cloud conditions. However the spatial and temporal resolutions are lower than for SST products. Typically, the along-track spatial resolution is 7 km whereas the distance between adjacent tracks is about 240 km at the latitudes of the Mediterranean for a mission like Jason-1 and TOPEX/POSEIDON, with a 10-day repeat orbit. Other altimeters, like ERS-1/2 or ENVISAT, are characterized by a higher spatial resolution at the expenses of a lower temporal

resolution (35 days). Thus, in almost all the applications of altimetry, several missions are merged in order to increase both the temporal and spatial sampling and to produce gridded fields (see Larnicol *et al*., 2002, for the merging of TOPEX/POSEIDON and ERS-1/2 and Pascual *et al*., 2005 for the combination of up to four altimeters).

• Scatterometry:

Scatterometers are used to estimate the vector wind fields at the sea surface, from which gridded wind stress fields can be generated and used to force the momentum equation at the sea surface. Models of surface wave dynamics and air-sea gas exchange critically depend on the wind stress field at the sea-surface as well, and mesoscale variations in SST can generate feedback into the atmosphere and induce wind stress curls at the same scale. The current SeaWinds instrument onboard the NASA QuikSCAT satellite generates standard vector wind data products at 25 km resolution based on measurements of the radar backscatter at the sea surface (see http://podaac.jpl.nasa.gov/cgi-bin/dcatalog/fam_summary.pl?ovw+qscat). Coastal products have been achieved with a resolution to 12.5 km on a near-to-real time basis in support of operational oceanography, albeit with somewhat greater errors. In comparison with surface buoy observations, accuracies of 0.8 m/s in wind speed and 5.4 degrees in direction are achieved with the satellite observations, with root mean square deviations of ~1.6 m/s and 30 degrees respectively.

• Shore-based radars:

The measurement of surface currents in nearshore environments has been repeatedly identified as critical for future ocean observing systems. Surface currents can be mapped with a radio Doppler-frequency technique called variously HF Radar, surface current radar, or CODAR (the dominant commercial system), which operates at 3-50 MHz. These are remote sensing observations, albeit with observing stations situated on the coast looking out to sea, or alternatively fixed onto stable buoys or platforms. A backbone-level coverage network requires shore installation sites spaced about every 100 km along the coast, assuming offshore ranges of 100-180 km. Radial currents relative to individual sites are derived by microwave scattering; vector currents are available for the region of overlapping coverage from two or more individual sites. At present there are over forty individual HF radar systems presently operated in US EEZ waters by research institutions with many more planned, and also in Europe there is an increasing deployment either in fixed or mobile locations. While many are long-range (~200 km) others are more regional-scale (30-60 km), higher resolution systems (see, for example: http://www.gomoos.org/codar/). The ultimate objective is to provide full coverage of coastal waters for operational purposes. Such highly resolved observations in time and space complement the less frequent and broader scale satellite scatterometer measurements, and as well, permit observations near the coast which are problematic for scatterometers.

3.1.2. Remote sensing products for end-users available on the Mediterranean

In the following table we provide information on satellite derived products (sea surface temperature, ocean colour, surface wind, and sea surface height) over the Mediterranean Sea that can be downloaded for research use. We list here only the products that i) cover the Mediterranean, ii) are ready-to-use, and iii) are freely available (possibly after registration). They can be either images or data files, and include real time and archived data.

A first version of this table (near-real time products only) was prepared by the European MAMA research network (Mediterranean network to Assess and upgrade Monitoring and forecasting Activity in the region, http://www.mama-net.org/).

In http://vosdata.santateresa.enea.it:54321/mfs/mama/id19.htm examples will be found of the products and readme files with downloading instructions. In a few cases where specific arrangements were achieved to allow data access to MAMA partners for evaluation purposes (e.g. with the Coastwatch project http://www.enviport.org/GMES/services/coastal/index.htm through ACRI), these might not be available after the conclusion of Coastwatch and MAMA.

Table 1. Satellite products available over the Mediterranean region.

Product and provider	Images	Data files	Spatial resolution	Time step	Area	Coverage of a single map	Web site for download
SST							
ICM-CSIC	*		1.1 km	several per day	35N-46.2N 15W-16.5E	Western Barcelona at Nadir Mediterranean + part Atlantic (depending on pass)	http://ers.cmima.csic.es/saidin/
CYCOFOS Univ. of Cyprus	*	* (free, users can register)	1.85 km	daily night time	30N-41N 15E-36E	Eastern Mediterranean	http://www.ucy.ac.cy/cyocean/
GOS-ISAC Rome / ADRICOSM	*	* (passwd)	1.1 km at Nadir	daily	39N-46N 12E-20E	Adriatic sea	http://gos.ifa.rm.cnr.it/adricosm/
GOS-ISAC Rome	*		5 km	several per day	30N-48N 10W-40E	entire Mediterranean	http://gos.ifa.rm.cnr.it/index.php?id=292
LOS-IFREMER Brest	*	* 400 Kb	2 km	several per day	NE Atlantic + Mediterranean	E + W Med. (uncomplete)	http://www.ifremer.fr/cersat/en/index.htm
GOS- ISAC + CMS / MFSTEP		*	1/16° (~7 km)	daily optimally interpolated map	30.25S-46N 18.125W- 36.25E	entire Mediterranean +East Atlantic	http://www.bo.ingv.it/mfstep/WP3/
CMS +GOS- ISAC / MFSPP	*	* (free, users can register)	1/8° (11-14 km)	weekly composite	30N-46N 5W-37E	entire Mediterranean	http://www.bo.ingv.it/mfstep/WP8/sst.htm
ACRI Sophia-Antipolis	*	* 5-10 Mb	1 km	weekly composite (updated daily)	30N-45N 6W-37E	entire Mediterranean	http://www.acri.fr/ + icm server to download images and data
ESA/MEDSPIRATION	*	*	L2P 2-10 km L4 -2 km	daily L2P L4	30N-46N 5W-37E	L2P entire Mediterranean + Atlantic L4 entire Mediterranean	http://www.medspiration.org/
OGS/ Trieste	*		1.1 km at Nadir	several per day	30N-48N 10W-40E	entire Mediterranean, Adriatic, Gulf of Trieste	http://doga.ogs.trieste.it/doga/sire/sato.html
DLR/Oberpfaffenhofen	* gif (free, re-gistration) 03/1993-present		1.1 km	daily, weekly and montly composites		entire Mediterranean	http://eoweb.dlr.de needs color contrast adjustment
Ocean Colour							
ACRI Sophie-Antipolis	*	* 5-10 Mb	1 km	weekly composite (updated daily)	30N-45N 6W-37E	entire Mediterranean	http://www.acri.fr/ + icm server to download images and data
GOS-ISAC	* (free)	* (available on agree-ment)	1 km	daily MODIS passages	30N-46N 5W-37E	entire Mediterranean + Adriatic	http://gos.ifa.rm.cnr.it/index.php?id=373
IES-JRC Ispra	*		2 km	single, ten-day, monthly	30N-46N 6W-36.5E	entire Mediterranean	http://marine.jrc.cec.eu.int/frames/archive_seawifs.htm
Wind							
KNMI Netherlands / QuikSCAT	*	* (passwd)	100 km	3 days or less	30N-46N 6W-37E	1700 Km wide strip	http://www.knmi.nl/scatterometer/qscat_prod/
KNMI Netherlands / ERS-2	*	*	25 km	daily (30 min delay)	global	variable	images in http://www.knmi.nl/scatterometer/ers_prod/ data files in ftp://scatuser:Scat4any@ftp.knmi.nl/prescat1_0
LOS-IFREMER Brest		* 3 Mb per orbit	25 km	daily (5-6 day delay)	global	along swath	http://www.ifremer.fr/cersat/en/data/overview/swath/l2b.htm
LOS-IFREMER Brest	*	* 2100 Kb	0.5°	daily (6-7 day delay)	global	gridded data	http://www.ifremer.fr/cersat/en/data/overview/gridded/mwfqscat.htm
SSH							
CLS Toulouse / MFSTEP		* real time	1/8° (11-14 km)	twice per week	30N-46N 5W -35E	entire Mediterranean	http://www.cls.fr/html/oceano/general/applications/mfstep_en.html ftp://ftp.cls.fr/pub/oceano/Mfs_Ingv274F4P2D6K8G/maps/oer/merged/h/
CLS Toulouse		*delayed. Time from 1993 (avai-lable on agreement)	1/8° (11-14 km)	weekly maps	30N-46N 5W-35E	entire Mediterranean	http://www.cls.fr on request to Gilles Larnicol: *Gilles.Larnicol@cls.fr*

3.2. *In situ* technologies

The mesoscale variations observed in the Mediterranean Sea are generated largely by baroclinic instabilities, with spatial scales order 10-100 km and time scales order 10 to 100 days. In turn, variance at these scales cascades to higher wave-numbers. As a result, isopycnals can be locally uplifted, nutrients are brought near the surface, and the resulting primary production of organic matter then propagates to higher trophic levels. Resolution of the physical and biological dynamics associated with mesoscale processes requires both an adequate observational base, and appropriate parameterizations of mesoscale variability for inclusion in larger scale climate and food chain models.

Shipboard observations are and will remain extremely useful for process oriented studies and for a wide variety of oceanographic experiments which cannot be carried out without them. However, by themselves they are not suitable for resolution of biogeochemical variability over the mesoscale. Autonomous platforms, instrumented with appropriate sensor arrays, hold the most promise for complementing ship-based systems for observation of mesoscale variability.

3.2.1. Sensors for observation of biogeochemical variability

In addition to the routine measurement of the four dimensional temperature and salinity fields, new technologies have emerged for the measurement of key biogeochemical properties and processes from autonomous platforms. General requirements for such instruments are a solid theoretical and practical basis for the measurement and its relationship to the property or process of interest, low power, resistance to environmental degradation (e.g. biofouling, corrosion), an ability to maintain calibration for extended periods, and a general robustness for untended operations. As the numbers of autonomous platforms increases, costs will decrease as well.

A number of sensors either currently deployed on in development are listed in Table 2.

Table 2. Current sensors for autonomous platforms.

Sensor	Principle	Product	Power	Data	Relative Cost	Status
Meteorological Sensor Suite	Varied	Wind speed, Direction, Air temperature, Humidity, Solar Radiation, Air pressure	Low	Low	Low	Mature
CTD	Varied	Conductivity, Temperature, Salinity, Depth (Pressure)	Low	Moderate	Moderate	Mature
ADCP	Doppler shift	Depth-resolved currents	Moderate	High	Moderate-High	Mature
Radiometer	Photodiode, CCD	Solar irradiance, upwelling radiance (ocean color), light attenuation, penetration, and reflectance, particle size/type	Low	Low-Moderate	Low-Moderate	Mature
Scattering/Absorption Sensors, Optical	Photodiode, CCD	Spectral absorption and scattering, particle size/type, POC, PIC	Low	Low-Moderate	Low-Moderate	Mature
Nutrient Sensors	Optical, and Chemical	Concentration of nutrients	Moderate	Low-Moderate	Moderate-High	Experimental
Oxygen, pCO_2	Varied	Concentration of gases	Low-Moderate	Low	Low-Moderate	Experimental-Mature
Fluorometers	Fluorometric	Concentration of Chlorophyll, CDOM	Low	Low	Low	Mature
Fluorescence Induction , Pulsed Fluorometers	Fluorometric	Properties of photosynthesis	Moderate	Moderate-High	High	Experimental
Scattering Sensors, Acoustic	Acoustic	Particle size/type	Moderate	Low-Moderate	Moderate	Mature
Sediment Traps	Gravity collection	Sediment fluxes and type	Low	Low	Moderate	Mature-Experimental
Plankton Recorder (e.g. CPR)	Net	Particle concentration/type	Low	Low	Moderate	Mature
Flow Cytometer	Laser enhanced microscope	Particle concentration/type	High	High	High	Experimental
Microstructure	Piezoelectric, thermistor, inductive	Velocity, temperature, conductivity microstructure/turbulence	Moderate	High	Moderate	Mature-Experimental
Imagers, Optical Plankton Counter	Optical, Varied	Particle Type/Concentration	High	High	High	Mature-Experimental

3.2.2. Observational platforms

There are a variety of autonomous observation platforms available, which can provide complementary approaches to the resolution of mesoscale variability in biogeochemical and physical processes. These include ships of opportunity, fixed moorings, drifting buoys, profiling floats, gliders and powered autonomous vehicles. Current capabilities of platforms are summarized in Table 3.

Table 3. Observational platforms for autonomous deployment.

Type	Deployment	Spatial Scales	Power Available	Payload Mass	Cost	Strengths	Weaknesses	Maturity
Ships of Opportunity	Instrumented ferries, cargo vessels	Small along track	High	High	Moderate for inst. only	Repeat transect, low cost	Restricted track, no spatial control	Mature
Fixed Moorings	Anchored instrument package	N/A, fixed location	Low-Moderate	Moderate – High	Moderate – High	Long time series at high temporal resolution	Limited spatial resolution unless arrays	Mature
Drifting surface buoys	Floating instrument package	Regional, global if arrays	Limited	Low	Low	Surface properties, velocity	Limited depth resolution, power, payload	Mature
Profiling Floats	Profiling instrument package	Regional, global if arrays	Limited	Low	Moderate-Low	Time – series w/ vertical resolution	Limited power, payload	Experimental – mature
Gliders	Profiling instrument package with limited lateral control.	Regional to global if arrays	Limited	Low	Moderate	Time-series with resolution in horizontal and vertical	Limited power, payload	Experimental
Powered AUV's	Profiling package with powered control of position	Small, unless in swarm	Moderate	Moderate	High	Can execute defined mapping, high payload	High cost	Experimental

3.2.3. Future directions

The unbiased sampling of the oceanic mesoscale variability will require a complementary array of platforms, with autonomous instrumented devices playing a useful role. Future efforts to reduce the size, power and cost of instruments will remain a high priority, as well as integration of data into information products that relate directly to outstanding questions regarding the importance of mesoscale processes in the ocean.

3.3. Sampling strategies

For nearly three decades it has become increasingly common place to make physical (hydrographic) measurements of regions of the oceans sufficient to observe horizontal scales of order (10 km) and in a time frame that, to a first approximation, allows us to assume synchronism of the measurements (Tintoré *et al*., 1991; Pollard *et al*., 1995 and others). As a result, our knowledge of the storm (eddy) scale in the ocean has increased dramatically. Just like storms in the atmosphere, eddies in the ocean are created by, and affect, the release of energy across a front and the eventual mixing of two adjacent water masses (Hoskins *et al*., 1985; Gill, 1982). Similarly, large vertical circulations are associated with eddies, and frontogenetic processes in general (Leach, 1987; Pollard and Regier, 1992; Viudez *et al*., 1996; Allen and Smeed, 1996); these were hitherto only predicted through applied mathematical theory. In the past decade we began to develop and deploy novel instrumentation and analysis techniques to make biogeochemical measurements synchronised with the physical (hydrographic) measurements (Griffiths and Roe, 1993; Fielding *et al*., 2001). The resulting interdisciplinary observations demonstrated that frontogenetic physical processes play a significant role in the vertical and horizontal transport of phytoplankton, and either directly transport zooplankton or indirectly interfere with their behavioural habits (Fielding *et al*., 2001).

At the mesoscale, a significant component of the flow cannot be measured directly; this includes the vertical flow. Instead we derive this flow from a combination of our primitive equations of motion, a suitable balance condition and some assumptions about the conditions on the boundary of our region of interest. Thus the hydrographic and biogeochemical data follow a very different analysis/processing route than the derived three-dimensional flow field. Our first approximation, that the measurements were synoptic, is no longer wholly valid. The error in this approximation

affects the hydrographic and biogeochemical data through a route different from that in which it affects the derived three dimensional flow field.

In situ observations of mesoscale processes in the ocean are traditionally both difficult and expensive to make. The trade-off between spatial resolution, vertical excursion and synopticity of the measurements leads to compromises which, although frequently assumed to be acceptable, in practice rarely are. Satellite observations may be made at the required temporal and spatial resolution but the connection between surface signature and subsurface flow is often not clear and in many areas there is no unique solution. New techniques however, for re-locating data relative to the observed motion, for designing optimum sampling strategies and for making *in situ* observations from autonomous vehicles, are being developed to overcome these difficulties in the immediate future if they are suitably exploited.

An attempt to examine the impact of a lack of synopticity on the computation of derived parameters such as the vertical velocity was undertaken by Allen *et al*. (2001). Rixen *et al*. (2003) checked the errors derived from different sampling strategies such as 'cross-front' and 'along-front' radiator style surveys. Pascual *et al*. (2004) used the QG tendency equation to estimate the propagation velocity of a meander sampled during an intensive survey. The estimated propagation speed was then used to relocate stations in order to produce a 'synoptic' map. More recently, Gomis *et al*. (2005) have evaluated synopticity errors for different sampling strategies applied to simulated unstable baroclinic waves and have proposed and tested two methods aimed at reducing the impact of the lack of synopticity. Counter-intuitively, Rixen *et al*. (2003), showed that downstream and upstream 'cross-front' sampling can produce larger errors than' along-front' sampling. In their particular case study, the along-front sampling resulted in errors in vertical velocity of more than 50% in places. These values are significantly higher than those obtained for typical observation errors and sampling limitations (between 15 and 30% for vertical velocity as obtained in Gomis and Pedder, 2005). By combining the relocation of stations (based on a system velocity) and the correction of observations (through the estimation of a growth rate), the authors were then able to eliminate practically all synopticity errors in the case of the along-front sampling. In practice, the error reduction is likely to be less effective, since actual fields cannot be expected to have a system velocity as homogeneous as for the single-mode waves simulated in this work.

3.4. Modeling support

Financial, technical and human resource constraints demand efficient measurements, an issue of particular concern in oceanography. Efficient sampling requires *a priori* knowledge of scales, for the physical processes, life cycles and trophic interactions of the pelagic ecosystem. The adaptive sampling brings together *in situ* sampling and multiple platforms including remote (satellites, aircraft and shore-based), stationary (moorings), moveable (ships and AUVs), and drifting (surface or vertically mobile) with advanced ocean models to improve our ability to observe and predict the ocean. The operational data collection system relays information to a shore and/or to a ship in near real-time (hours) where it is assimilated into numerical models that create four dimensional fields and predict future conditions. The time series of the sea conditions derived from operational forecasting and observing systems may show trends and changes in mesoscale features, and thus helps adaptive sampling to focus on places where the data will be most useful and well matched to the phenomena of interest for the ability to predict ocean properties.

In general, there is a tendency for environmental systems to be 'patchy' that is, the ecological constituents, their structure and their relationships vary from place to place according to the influences of the local dynamics. They also tend to be highly heterogeneous, with biogeochemical characteristics varying rapidly over space and time. The data collection exercise itself adds uncertainty due to human and instrumentation errors as well as by limitations involved in the resolution and the synopticity of measurements. Trying to capture all of that variability in a field survey is incredibly challenging. Time and resource constraints for most field exercises limit the number of sample points which we can realistically visit and measure.

If scales are known for intermittent episodic phenomena, adequate uniform and efficient sampling is possible. Coarser sampling misses entirely, or aliases the phenomena. Finer sampling

is redundant and time consuming especially for many biogeochemical parameters, and rates. The adaptive sampling strategy attempts to minimize a selected error measure which depends on data type, sampling and assimilation scheme and a suite of interdisciplinary dynamical models. During the 1990s, the opportunities and requirements for multi-scale, interdisciplinary ocean forecasting have sharpened, the term 'adaptive sampling' for ocean observational networks was articulated, and the concept of Ocean Observing and Prediction Systems has firmly emerged. The systematic and long term observations of mesoscale phenomena cannot be done without the existence of a network of monitoring and or forecasting systems on local, sub-regional and regional level. Operational oceanography, which is defined as the activity of routine observations and forecasting of the sea water conditions and their near real time interpretation and dissemination on-line, may contribute substantially to the study of mesoscale phenomena.

Data assimilation, which melds observations with dynamics, provides the only feasible basis for obtaining accurate synoptic mesoscale realizations over the space-time scales and domains of interest. The near real time transmission and assimilation of the observed in-situ or remotely sensed data into the numerical models has made it possible to provide nowcasts on the present state of the sea characteristics, forecasts on the near future (days and weeks) conditions of the sea and hindcasts on the past state of the sea conditions.

Data assimilation dynamically adjusts and interpolates data inserted into models. In modern ocean adaptive sampling, a goal is to characterize the ideal future sampling among the possible choices in an adaptive accord with the constraints and available forecasts that have assimilated all of the past data. This goal can be achieved either subjectively, with forecast information being combined with the a priori experience to intuitively choose the future sampling, or quantitatively, where forecast capabilities serve as input to a mathematical sampling criterion whose real-time, continued, optimization routines predict the adaptive sampling. The parameters of the adaptive sampling procedure are therefore the available forecasts, new data acquired during the forecast, the constraints and the goal, i.e. the properties to be optimized and the metrics used to measure these properties.

The rapid development of operational ocean monitoring and forecasting systems will obviously support a better management of the marine environment and assist decision makers and public end-users against problems that arise from the various economic activities in the marine sector. It will also assist scientists in studying the spatial and temporal variability of the mesoscale phenomena, as for example the major flow dynamic features in the Eastern Mediterranean, such as the Rhodes gyre, the so-called Mid Mediterranean Jet, etc.

Today adaptive sampling is in its infancy and methodological advances in the forthcoming years will be related to advances in the observing and prediction systems components, the overall system concept and system integration, as well as dedicated theoretical research on objective, automated sampling. The experience gathered in recent decades suggests that the first decade of this century should result in the maturing and evolution of the ocean observing and prediction system concept, which ultimately provide the basis for effective and efficient management of multi-use of the Mediterranean Sea. In Europe, several operational oceanographic forecasting and observing systems (such as MERCATOR, FOAM, MFS, CYCOFOS, POSEIDON, TOPAZ) have been implemented recently, providing regularly on-line in-situ, remote sensing and numerical products, useful also for mesoscale studies on coastal, sub-regional and regional level.

3.5. Information retrieval

Over the past 30 years, a major effort has been made to describe mesoscale variability at global ocean scale. To a large extent, this is the result of new satellite sensors that are able to measure parameters like sea surface temperature, surface elevation or ocean colour at enough high resolution to resolve mesoscale variability with global coverage. Monitoring the seas with these powerful sensors reveals the presence of mesoscale features everywhere. The overall impact of these ubiquitous features on the ocean ecosystem and on the role this has in the biogeochemical cycles of the earth is a research challenge which cannot be ignored, since satellites show an ocean pregnant with mesoscale eddies, jets, filaments and dipoles.

The analysis of sea surface temperature maps has proven to be essential in order to identify and track these structures and to support the description of surface circulation features from large to sub-basin and mesoscale (see Ambar and Serra, Taupier-Letage and Millot, this volume). Similarly, the possibility to accurately measure the sea surface elevation through satellite altimeter data has led to a much deeper comprehension of the ocean circulation in terms of energy involved in mesoscale processes and direct estimates of the surface velocities, at an increased space and time resolution, in the last years, due to the simultaneous flight of several altimeter missions. In this context, it is clear that the number of active sensors available and the merging techniques used represent a crucial issue for the future scientific and operational plans (Pascual *et al*., this volume). As a consequence, a serious concern related to the uncertainties of future altimeter missions (both mounting traditional sensors and introducing innovative concepts as the Wide Swath Ocean Altimeter or Ka-band sensor constellations) was expressed during the workshop.

Actually, much has already been learnt from the remote sensing data by themselves, but the analyses of single sensors and parameters cannot clearly be considered exhaustive. In some sense, the merging of complementary information coming from different platforms, both space-borne and *in situ*, is a key tool to extend our knowledge, for example, from the sea surface to the deeper layers (Buongiorno Nardelli, this volume). To this aim, several methods have already been proposed, that are mainly based on statistical or empirical techniques. However, there is a clear need to optimize and extend the existing methodologies, also exploring the possibility to identify simpler descriptors or parameterizations of the system from theoretical considerations.

Within this context, two complementary approaches can be generally followed. One concerns the assimilation of observed data in the numerical models. The other approach is purely observational, and consists in the attempt to retrieve as much information as possible from the measurements alone. The complementarity of these two paths lies in the necessity for the experimental oceanographers to learn from the more consolidated experience of modelers in the statistical treatment of multivariate data, and in the need for the modelers to fully understand what information is contained in the observations which they must assimilate, in order to design more efficient algorithms.

In addition, encouraging results have already been obtained in retrieving relevant information from across disciplines, as a natural consequence of the strengthened collaboration between physicists, biologists, chemists, etc. A few straightforward examples were presented during the workshop: it has now become quite common for any physical oceanographer to use phytoplankton distribution estimated from space-borne ocean colour measurements as a tracer of the surface dynamics. Similarly, simplified biological models have allowed estimating the vertical velocities associated to upwelling events through sequences of satellite images of SST and chlorophyll concentration (Ruiz and Navarro, this volume).

Nevertheless, the fundamental issue concerning the impact of mesoscale processes on the global ecosystem dynamics still remains almost completely unanswered. Our present inability to provide a reliable answer to such a complicated question is not only due to the many unknown processes relating the biological responses to the different scales of ocean variability, but also, largely, to the limited data coverage of the global oceans at these scales (as satellites only provide surface measurements of a few variables). This lack of data makes it quite difficult to test hypotheses regarding the physical and biological interactions and their impact on a global scale. New technologies for biological sensors in conjunction with *in situ* autonomous platforms for ocean observation (Lewis and Claustre, this volume) will surely play a significant role in the next decades to escape from an undersampled ocean, especially in its biological component. Therefore, one of the priorities for future research activities will be to transfer the new experimental findings obtained with these new tools into more realistic parameterizations of the mesoscale biological and physical dynamics for adoption in the numerical schemes for global studies.

4. WORKSHOP RECOMMENDATIONS

From the presentations and discussions held during the four days workshop, the participants highlighted some recommendations to research teams and institutions that can help improving the present and future activities on mesoscale research in the Mediterranean:

- develop the acquisition of time series with autonomous platforms/sensors;
- upgrade the existing system packages with new sensors for biological and chemical variables. Take into account specific Mediterranean problems, as biofouling and high corrosion;
- measure by default some JGOFS parameters (as database for climatic change studies) in all oceanographic field programs;
- ensure efficient and rapid preprocessing/tagging/standard formatting and archiving of all kinds of observational data collected in experimental surveys, to allow immediate and easy use to all involved researchers;
- adopt a common terminology for mesoscale structures, such as vortex, eddies, gyres, etc. for clarification and avoiding misunderstanding;
- organize an "operational analysis" of remote sensing data to compare with model outputs (validation purposes);
- promote the continuation of satellite altimetry missions, at present not guaranteed. There are similar concerns with respect to scatterometer winds and ocean color missions, and this could have devastating effects on mesoscale research;
- facilitate access to remote sensing data. All research teams should have rapid and easy access to a wide range of satellite products (at adequate spatial and temporal resolution for mesoscale studies, at adequate stage of processing, i.e. ready-to-use), with additional information on quality control/reliability;
- support monitoring programs at Mediterranean scale (such as CIESM Transmed http://www.ciesm.org/marine/programs/transmed.htm), as regular monitoring is essential for mesoscale studies;
- ensure the future operational effectiveness of existing relevant sampling programs (e.g. MedARGO, etc.) and data centers (e.g. MEDATLAS, etc.) beyond presently funded projects;
- examine the possibility that an international agreement forces all new ships (above a certain capacity) carry an environmental sampling package (at least a fully autonomous thermosalinometer, up to a "Ferry Box" more complete package);
- foster North-South cooperation to fill the monitoring gaps in the southern Mediterranean sub-basins (where mesoscale is crucial and data are scarce). Especially foster national programs dedicated to regular CTD transects (at least) across the current off southern coasts/slope, in order to get a good description of the variability at mesoscale. Typical period would be one month (2 weeks better), sampling interval ~5 miles, duration 1 year at least;
- organize a proposal to the European Union 6th Framework Program for a Research Training Network on mesoscale studies, to allow efficient cooperation between research teams in the Mediterranean countries.

The use of the satellite thermal imagery to track mesoscale features and infer circulation in the Mediterranean

Isabelle Taupier-Letage and Claude Millot

Laboratoire d'Océanographie et de Biogéochimie (LOB/CNRS), Antenne de Toulon, La Seyne, France

ABSTRACT

The overall functioning of the Mediterranean Sea, which transforms Atlantic Water (AW) into Mediterranean Waters (MWs), has been comprehended for decades now, and so is the process of dense water formation, which leads AW to sink in specific offshore northern zones of both basins. However, some circulation features are still being debated in the western basin, while a similar debate is currently being initiated in the eastern one.

One main reason for these debates lies in the fact that most studies do not take into account the large spatio-temporal variability induced by mesoscale dynamics, which is intense in the whole Mediterranean, especially in the southern parts of both basins. The flow of AW forms alongslope unstable currents that generate meanders and eddies along the Algerian and the Libyo-Egyptian subbasins (respectively). These eddies have diameters ranging from 50 to 150 km (up to 250 km), vertical extents from 100s to1000s of metres (down to the bottom: ~3000m), and lifetimes ranging from month to year (up to three years at least). These eddies propagate alongslope downstream (eastward) at a few km/day, can detach from the current to drift in the open sub-basin, and can have an impact on the general circulation. In order to interpret correctly the *in situ* observations, it is thus of the utmost importance to locate and track these mesoscale phenomena with a fine spatio-temporal interval. The medium-resolution satellite images (pixel ~ 1 km, ~1 pass/day) are an extremely efficient tool in this regard, the most-widely used being the thermal infrared (IR) images from NOAA/AVHRR (thermal resolution ~0.1°C). Provided some precautions are taken, IR images can be used indeed to infer surface currents. Mediterranean examples of the use of IR images to infer circulation features will be shown, from filaments to eddy tracking, up to the results of the analysis of a time series of images spanning ~4 years, from which we inferred a new schema of the surface circulation in the eastern basin. The use of IR imagery in near-real time will play a key-role in the sampling strategy of future cruises dedicated to test these hypotheses.

1. INTRODUCTION

The Mediterranean Sea is a domain where evaporation exceeds the water inputs by rivers and precipitations. As a result the Mediterranean sea level is lowered, and lighter (less salty) Atlantic Water (AW[1]) enters at Gibraltar at the surface. AW is made denser along its circuit in the western

1 See the water masses acronyms on http://www.ciesm.org/catalog/WaterMassAcronyms.pdf

and eastern basins through evaporation and mixing with resident Mediterranean Waters (MWs), all year long. During wintertime, cooling and intense mixing with deeper (saltier) MW in the northern parts of both basins lead to dense water formation processes. So that surface/lighter incoming AW is transformed into deeper/denser MWs, which will eventually exit at depth through the strait of Gibraltar (for a recent review of the circulation in the Mediterranean see Millot and Taupier-Letage, 2005a[2]). The agreement around this basic functioning of the Mediterranean is general. But when it comes to detail the circulation paths of the water masses, some features are still fiercely debated nowadays. It is all the more amazing when thinking that the first schema of the circulation (for both surface and intermediate layers) was issued nearly a century ago (Nielsen, 1912). He mainly considered the effect of the Coriolis force, and as a result the general circuit was mainly counter-clockwise around the basins. However some features raised questions: how to explain the "branching" of the AW circulation in the eastern part of the Algerian subbasin[3], one flowing "normally" eastward through the Channel of Sardinia, and the other flowing northward along the western slope of Sardinia? In the same way, some Levantine Intermediate Water (LIW) was found hardly modified at all in the central part of the Algerian subbasin: in addition to the vein flowing "normally" northward west of Sardinia, a vein of LIW was also drawn flowing westward across the subbasin at intermediate depth, in contradiction with the effect of the Coriolis force.

In the eastern basin this schema depicted a surface circulation around the basin in a counter-clockwise circuit. In the 1960s-1970s (Ovchinnikov, 1966; Lacombe and Tchernia, 1972) the diagrams still depicted a surface circulation around the basin in a counter-clockwise circuit, but in the southern part it was more widespread and included subbasin circulations. Between 1985 and 1990 intensive fieldwork was organized within the framework of the POEM experiment (Physical Oceanography of the Eastern Mediterranean, e.g. Robinson *et al*., 1991). The interpretation of this data set combined with modelling resulted in a schema (e.g. Robinson and Golnaraghi, 1993) showing a surface circulation crossing the basin with jets meandering offshore (among which the so-called "Mid Mediterranean Jet": MMJ), splitting in a complex system of swirls encircling mesoscale eddies and/or gyres, that were characterized as permanent, recurrent, and/or transient. Briefly stated, while the historical schemata represented a circulation mainly counter-clockwise "round-basin", the POEM schema switched to a circulation mainly "cross-basin", superseding the simple effect of the Coriolis force.

The satellite imagery, and especially the thermal NOAA/AVHRR (National Oceanic and Atmospheric Administration/ Advanced Very High Resolution Radiometer) imagery, provides since the late 1970s i) a synoptic view of the basin ii) at a spatio-temporal scale that allows to evidence the mesoscale phenomena, its ubiquity and its impact on the circulation of the water masses. Thus it offered the possibility to investigate and understand the high spatio-temporal variability of *in situ* observations, and to propose explanations and/or alternate interpretations to reconcile *in situ* observations and theory or basic principles, since numerical hence theoretical models can show cross-basin jets.

2. The use of satellite thermal images for circulation studies

a. Principle

The infrared signal remotely sensed only comes from the few upper microns of the surface (for the theory of thermal remote sensing see e.g. http://rst.gsfc.nasa.gov/Sect9/Sect9_1.html). Therefore the thermal signatures observed cannot be *a priori* related to the dynamics of the mixed layer. However very often the wind blows, so that the temperature of the surface is representative of a mixed layer that can reach a few 10s of metres due to the seasonal stratification, down to 1000s of metres where MWs are formed in winter.

In the Mediterranean, the surface circulation can be tracked most generally and in most places (see the following paragraph for restrictions) by tracking the higher temperatures, which correspond to the lower salinity water. Such conditions are optimum in winter, when the

2 Available on http://www.ifremer.fr/lobtln/OTHER/Millot_Taupier_handbook.pdf

3 See our terminology on http://www.ifremer.fr/lobtln/OTHER/Terminology.html

inflowing AW temperature is ~16°C and that of the MW ~13°C. Note that this can also be true independently of the latitude, as shown by the warmer current flowing along the northernmost parts of both basins in Figure 1a.

The medium-resolution satellite NOAA/AVHRR images are an extremely efficient tool to track mesoscale features. The Mediterranean basin-wide spatial coverage is provided by a swath wider than 2000 km. The fine temporal coverage is provided by two NOAA satellites flying simultaneously (for evolution see http://www.ipo.noaa.gov/), yielding at least four passes per day over the Mediterranean. The pixel is ~1 km, and the thermal resolution ~ 0.1°C (for more details see http://noaasis.noaa.gov/NOAASIS/ml/avhrr.html). The relatively weak cloudiness and the dimension of the Mediterranean thus let expect a coverage adequate at meso- spatial and temporal scales, even though possibly patchy (the whole sea is not cloud-free simultaneously, the same area cloud-free intermittently).

The sea surface temperature (SST) is derived from a linear combination of two (day) to three (night) channels (e.g. see http://www.ghrsst-pp.org/), which increases the noise in the resulting image. Although this is not a serious drawback, the preferred product to track the thermal signatures is the channel 4 image. The geophysical data are brightness temperatures, that are "relative temperatures", as opposed to SSTs, which are "absolute temperatures".

In order to optimise the visualisation of the thermal signatures it is necessary to use a colour table specifically adjusted for each image/area. This is required mainly because the marine thermal dynamics is usually very weak (few °C), so that a colour scale spanning temperatures lower than 10°C to more than 25°C results in a nearly colour-uniform image showing little, if any, dynamical information. This is also required because the temperature at the ocean-atmosphere interface can differ markedly between day and night, a temporal scale at which no significant variation occurs for the mesoscale phenomena. So if the temperatures cannot be compared from one image to the other, the evolution of the signature can be analysed. Following the conventions, the images will be presented with temperatures increasing from blue to red.

The tracking of mesoscale features from their thermal signature relies on the fact that there must be coherence between the temporal and the spatial scales. Indeed, the thermal signature that corresponds to a (small) shallow phenomenon will have a transient lifetime, of the order of day(s). Inversely, the (large) thermal signature that can be tracked for months up to years necessarily corresponds to a structure having a deep vertical extent, a condition required to maintain the signature over time, especially to survive winter mixing.

One image allows to deduce the current direction associated with the mesoscale eddies, since the isotherms always spiral inside, whether the eddies are cyclonic or anticyclonic. Most often the current is parallel to the isotherms because the latter are parallel to isohalines, hence isopycnals, so that geostrophic approximation is satisfied. Time series of images allow deducing a propagation speed from the successive positions of a feature such as an eddy, an upwelling cell, a front, or a filament. Isotherms are then generally perpendicular to the propagation direction. Most generally the inference of the currents is intuitive (cf meteorological scenes shown on TV), as one can verify considering the sub-scenes of Figure 1 (see legend for interpretation).

b. Precautions

First one must discriminate between marine signal and atmospheric contamination from water vapour and dust, in case the images are delivered without a cloud-mask. Most of the time it is fairly easy, since the atmospheric temperatures are much lower than the marine ones. In the case of light haze (when these temperatures can be in the same range), the atmospheric isotherms can be identified by their pattern, the fact that they cut the marine isotherms at any angle (see Figures 1f, i, k), and if there is any doubt, by looking at the signature on a previous or following image.

Then, in order to assign a thermal signature to an actual mesoscale dynamical structure, the presence and lifetime of the thermal pattern must be verified on several images, possibly using other satellite information too (e.g. visible images: cf Figure 1g, or altimetry).

Under calm wind conditions, the superficial microlayer can heat up due to solar heating. Then the "skin" temperature is higher (up to a few °C) than the "bulk" temperature, and the thermal

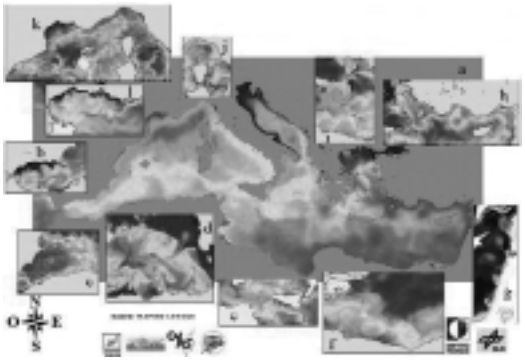

Fig. 1. (See page 108 for original color plate) Illustration of the mesoscale dynamics in the Mediterranean with thermal NOAA/AVHRR images from SATMOS/MétéoFrance and DLR (but **g**: ocean colour/chlorophyll content from SeaWiFS, from *ies*). Images have been selected at different dates. Temperature increases from blue to red, but all images have an independent colour scale. **a**: the monthly composite of January 1998 for the whole Mediterranean. **b**: the Alboran, in its classic situation of two gyres filling the sub-basin. **c**: the jet of AW on the western half of the eastern Alboran gyre reaches the algerian slope near 0° and continues as the Algerian Current, which can be seen (colder signature) propagating alongslope as far as ~4°E (south of Menorca), where it veers offshore (due to eddies interactions, not shown). An algerian eddy (warmer isotherms) can be seen south of Ibiza. **d**: Algerian eddies interacting strongly in the eastern part of the Algerian sub-basin, the accumulation zone ΣA_E. The strong shear between 2 close anticyclones creates small cyclonic shear eddies. Upwelling cells (dark blue tongues) are generated on the southwestern side of the AEs, where the current is directed offshoreward. **e**: the channel of Sardinia with an AE (blocked) at the entrance, and the channel of Sicily (the upwelling cells along the southern coast of Sicily are typical of summertime conditions). **f**: the western Levantine, with libyo-egyptian eddies (accumulation zone ΣL_W). **g**: the Middle-East, with coastal instabilities revealed by their chlorophyll content (SeaWiFS "ocean colour" image; situation not characteristic of the accumulation zone ΣL_E). **h**: the Northern Current off Turkey, showing sharp meanders and an eddy pinching off. **i**: most of the Northern Current is feeding the wind-induced Ierapetra eddy, east of Crete. **j**: the Ligurian subbasin, with a vortex dipole (mushroom-like structure) north of Corsica; the cold patch east of the strait of Bonifacio reveals the divergence induced by a strong (past) mistral wind event. **k**: the Liguro-Provencal subbasin: the Northern Current flows close to the coast since the slope is steep east of the gulf of Lions; there it skirts the continental shelf along the ~200m isobath, and thus crosses the gulf; the cold area off the gulf of Lions (and probably the one east of the strait of Bonifacio too) reveals the area where wintertime deep convection occurs, forming dense water (image typical of wintertime situation). **l**: upwelling cells in the gulf of Lions induced by strong Mistral events.

patterns are no longer representative of those of the mixed layer. Therefore it prevents, locally and temporally, any interpretation in terms of current. However such unfavourable conditions are easily detected thanks to their usual elliptic and concentric shape, and are circumvented by using nighttime images.

During cloudy periods the mesoscale structures can be tracked using the sea level anomaly (SLA) which they generate on altimetric tracks, and/or using composite thermal images (from weekly to monthly ones). However care must be taken when using composite images as the longer the time interval the smoother the signature of a propagating structure, up to potentially yielding a misleading picture. Indeed, the image resulting from the time-composition of eddies (thus inducing thermal gradients mainly cross-shore) propagating along a coast will present a smooth band parallel to the coast (thermal gradients mainly along-shore).

Besides cloudiness, specific meteorological conditions can also impair or even prevent tracking mesoscale features. This is especially frequent during summertime. In the Ionian especially the alternation of strong wind events and high warming calm periods in an orographically complex area leads to thermal patterns difficult to interpret. In the Aegean, possibly up to the Egyptian coast, the strong Etesian winds mix and cool the surface layer. The resulting strong gradients oriented north-south that delimit this cooler band will appear and supersedes thermal patterns linked to mesoscale dynamics in any automatic image processing. In the southeastern Levantine warming is such that a superficial warm layer usually caps the layer containing the dynamical information. Moreover, the dynamical features there tend to be of smaller size and to have a rapid evolution/propagation. Therefore statistical and climatological analyses of thermal images (e.g. Marullo *et al*., 1999a-b) do not provide adequate information on the mesoscale dynamics or on the general circulation. The visual analysis of (portions of) images remains, up to now, the unique way to make a detailed analysis and to track the eddies on the long term (years).

c. Validation

The use of thermal images to infer mesoscale dynamical structures and circulation features has been extensively validated in the western basin. In the eastern basin fewer observations are available yet, there is no objective reason to expect a different behaviour.

3. The results obtained on the mesoscale dynamics and the general circulation in the Mediterranean

A review of our present understanding of the circulation is presented in Millot and Taupier-Letage (2005a). The progressive steps that led to our current view of the surface circulation (Figure 2) are briefly described here below.

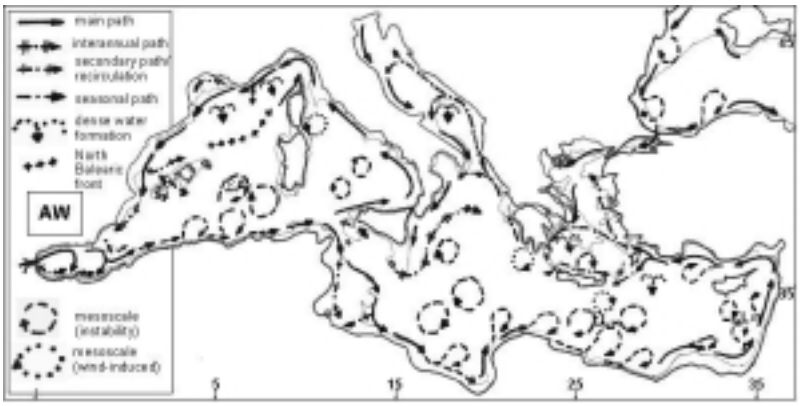

Fig. 2. The schema of the surface circulation (from Millot and Taupier-Letage, 2005a).

a. Definitive results in the western basin

The first analysis of thermal images (Millot, 1985) showed that the flow of recent AW along the Algerian slope -namely the Algerian Current (Figure 1c)- is unstable, giving rise to an intense mesoscale activity (Figure 1d). It generates meanders (width ~50km), which enclose a mesoscale anticyclonic eddy ~50 km in diameter. Meanders and enclosed eddies propagate downstream, i.e. eastward along the slope, at few km/day. The larger (diameter up to ~200km) and deeper (some can reach the bottom at ~3000m, see Ruiz *et al*., 2002, Millot and Taupier-Letage, 2005b) Algerian eddies (AEs) cannot go on eastward through the channel of Sardinia (Figure 1e), and are constrained to follow the Sardinian slope northward. This is illustrated by the trajectories of the drifters released upstream in a young AE and their various fates (see Salas *et al*., 2001, 2002). AEs generally follow a counter-clockwise circuit in the eastern part of the Algerian subbasin (Puillat *et al*., 2002; Isern-Fontanet *et al*., 2003), thus transporting recent AW offshore, which is released upon their decay (lifetimes can exceed three years). The AEs (enclosing AW), observed drifting in the open basin, provide the (simple) explanation to the AW branching in the eastern Algerian. Thus the Algerian subbasin acts as a buffer zone for AW, disconnecting the flux coming in at Gibraltar from the flux exiting the subbasin through the channel of Sardinia and along the southwestern coast of Corsica.

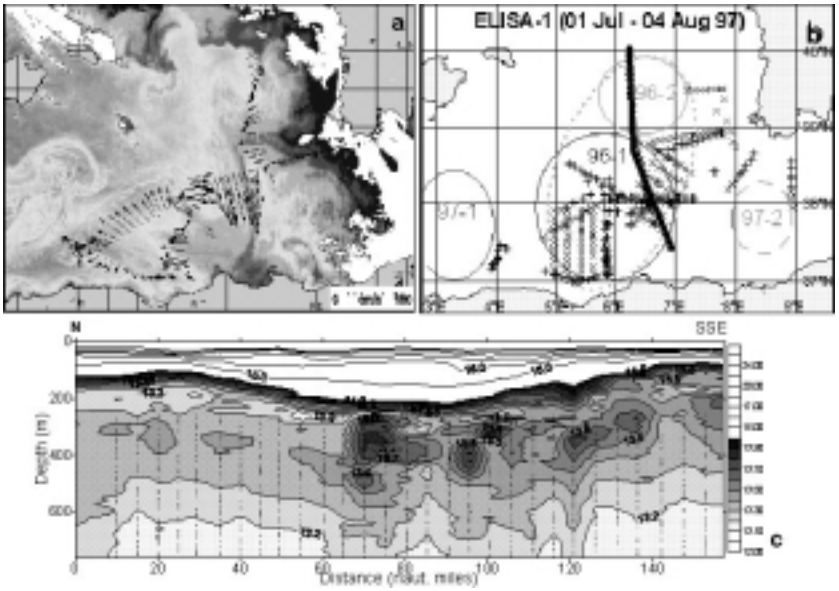

Fig. 3. The sampling at mesoscale during the ELISA-1 campaign. **a)** the associated surface ADCP current overlaid on a thermal infrared image of late July 1997. ; **b)** contours of the AEs and locations of the CTD and XBT casts; thick line: section detailed below; **c)** XBT transect showing several lenses of LIW trapped in 96-1.

It was then hypothesized that the AEs drifting along the Sardinian slope could catch lenses of LIW from the "normal northward flowing" vein, and transport it in the subbasin interior along their circuit (Millot, 1985). Thus there would be no vein of LIW flowing westward, but a patchy distribution of recent LIW in the subbasin, the most recent LIW values being related to AEs (as now shown in Millot and Taupier-Letage, 2005b).

Given the role assigned to the mesoscale phenomena in that region, the *in situ* sampling strategy had to be guided with satellite information in (near) real time, and required a fine (~ 10 km) sampling interval. Such a strategy has been successfully used in all our experiments, most recently in 1997-1998 during the experiment ELISA (Eddies and Leddies Interdisciplinary Study off Algeria, http://www.ifremer.fr/lobtln/ELISA). As an example of the data collected, the transects made across the southern part of AE 96-1 in summer 1997 (Figure 3) show that the LIW distribution is patchy, and restricted to the AE 96-1. Moreover, the LIW found close to the Algerian slope is related to the AE, since it has been shown that LIW progresses with the anticyclonic rotation (see Millot and Taupier-Letage, 2005b for detailed results).

A network of nine moorings was set in place for one year, equipped with ~ 40 currentmeters from the surface (~100m) to the bottom (~3000m). The time series (Figure 4) confirmed that the AEs can interact with the general circulation and modify it (e.g. Taupier-Letage and Millot, 1988), even revert it, locally and temporally, down to the deeper layer.

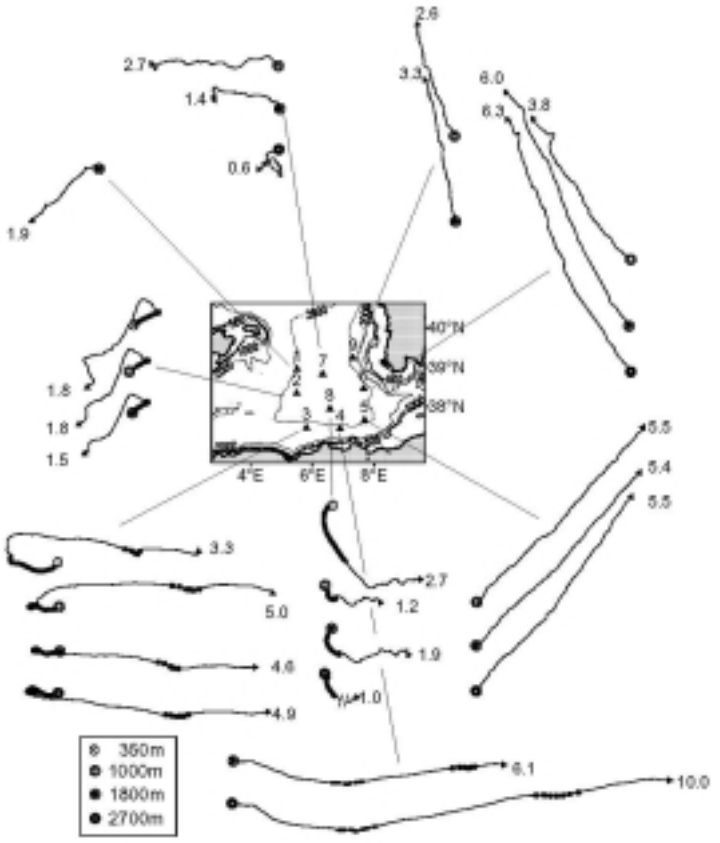

Fig. 4. The ELISA one-year progressive vectors diagrams at 350, 1000, 1800 and 2700 m together with the mean speed in cm/s. At the beginning of the record of mooring 3, at least, the circulation, normally eastward, has been reversed by the AE 96-1 on the whole water column (from Millot and Taupier-Letage, 2005b).

b. Recent results in the eastern basin

The dynamical phenomena in the eastern basin as seen on thermal images (see Le Vourch *et al*., 1992) do not differ markedly from their analogues in the western basin, and Millot (1992) disagreed with the main feature of the POEM schema (Robinson *et al*., 1991; Robinson and Golnaraghi, 1993) of an offshore cross-basin circulation with the MMJ. The eastern basin is an area where *in situ* data are scarce, especially in the southern part. The detailed analysis of ~1000 SST images spanning 1996-2000 (see details in Hamad *et al*., 2004, 2005a,b, available on www.ifremer.fr/lobtln/EGYPT) showed that the flow of AW along the Libyan and Egyptian slopes (the Libyo-Egyptian current) is unstable, and generates mesoscale anticyclonic eddies

(diameter ~100-200km, Figure 1f) that propagate downstream eastward alongslope, at 1-3 km/day, as illustrated by Figure 5. Each summer the Meltem generates, through the wind stress curl east of Crete and Peloponnese, two anticyclonic eddies: "Ierapetra" southeast of Crete, and "Pelops" southwest of Peloponnese. Based on our observations in the western basin, and on XBT data which show that eddies in the eastern basin are signed at least down to 700 m (Fusco *et al*., 2003), we hypothesise that some of these eddies have a deep extent (>3000m), and that they might be guided offshore by the bathymetry (the Herodotus trough). There (between ~27- 29°E) they would be trapped and accumulate, interacting up to merging and/or decaying. As a consequence there are always anticyclonic eddies in this area, which is where the POEM group observed a permanent/recurrent "Mersa-Matruh" gyre/eddy/anticyclone. To specify that the eddies observed at this location are not permanent, but that there are eddies permanently, we call this area ΣLw (for accumulation zone Levantine west). Along the Middle-East slope (Figure 1g) the mesoscale activity is also intense, although with smaller diameters and lifetimes (and thus probably shallower). In the easternmost part of the Levantine subbasin eddies also tend to accumulate, generally with a larger anticyclonic structure being fed by smaller ones (see Figures 14 and 15 of Hamad *et al*., 2005b). This area corresponds to that where the POEM group observed a permanent/recurrent/transient "Shikmonah" gyre/eddy/anticyclone. For the same reasons as mentioned earlier we name this area ΣL_E (for accumulation zone Levantine east). Overall, we infer from the images a circulation which is alongslope and counterclockwise at basin scale. And we hypothesise that what has (mis)led to conceive a Mid Mediterranean Jet are the facts that no *in situ* observations were made in the southernmost part of the basin, that no circulation was inferred there (although the historical schemes depicted one), and finally that sampling only on the northern edges of successive anticyclonic eddies does produce a meandering jet.

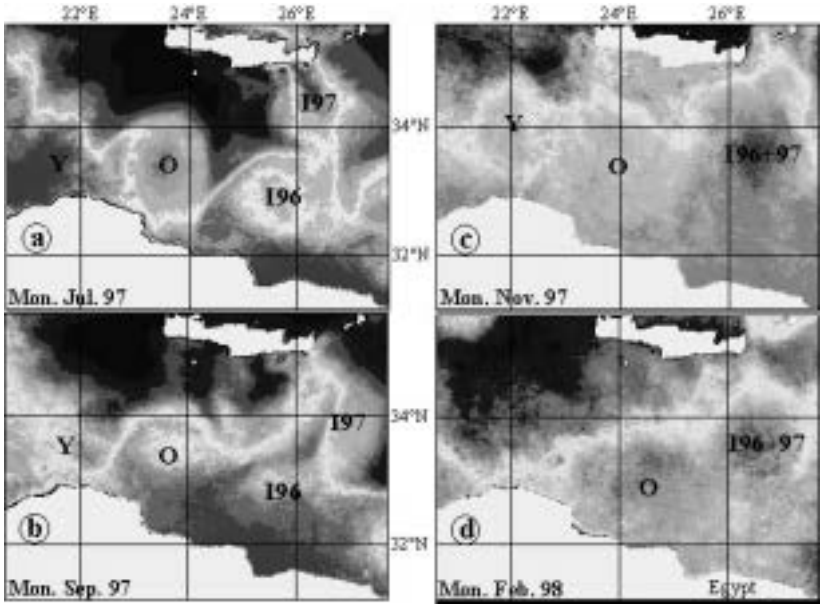

Fig. 5. A 8-month time series of monthly SST composites showing the eastward propagation of the libyo-egyptian eddies "O" and "Y", and the merging of the wind-induced anticyclones Ierapetra generated in 1996 (I96) and in 1997 (I97) (from Hamad *et al.*, 2005b).

4. CONCLUSION

On average we depict a surface circulation alongslope, following a counter-clockwise circuit in both basins. The situation is generally more complex in the south of the sea, where both the Algerian and the Libyo-Egyptian currents are unstable and generate mesoscale phenomena. It is thus of the utmost importance to sample with a knowledge of the actual eddy field (reception and analysis of images in (near) real-time), having a reasonably good knowledge of the space and time scales and movements characterising the mesoscale activity (possibly gained from a preliminary analysis of the time series of images).

This is also important when using data from climatological atlases. As an example, Figure 6 shows the result of a simple interpolation of all intermediate maxima of salinity and temperature (corresponding to the LIW signature) available from the MEDATLAS data base (see

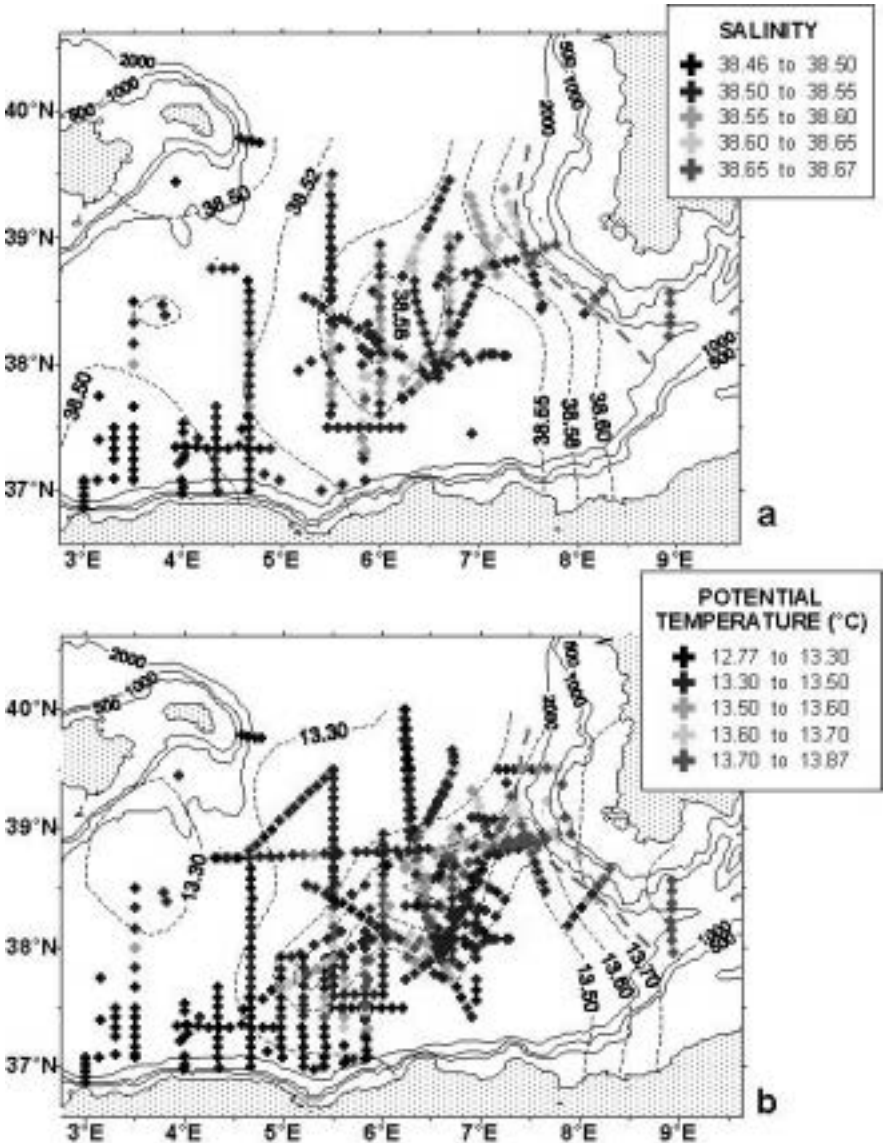

Fig. 6. Distribution of the salinity (**a**) and potential temperature (**b**) maxima associated with LIW from the MEDIPROD-5,6 and ELISA (CTD and XBT casts) in the eastern Algerian subbasin. Associated depths range from ~250 to ~650 m for salinity and from ~250 to ~550 m for temperature. The dashed black line would result from the unsupervised interpolation of this data set. The dashed red line figures the LIW vein external edge (from Millot and Taupier-Letage, 2005b).

www.ifremer.fr/sismer). Because CTD casts have been obtained at different times the data set is not coherent (AEs move), and the interpolation suggests a westward vein. But using individual data, campaign by campaign, and linking the hydrology to the AEs, we have concluded that this vein does not exist.

Now, the best would be to combine *in situ* and satellite information, in a multiplatform experiment. Whenever possible, several types of satellite observations should be used: altimetry and ocean colour efficiently complement the SST images. Combining time series from moored (Eulerian) and drifting (Lagrangian) instruments is especially efficient too, and must be confronted to the dynamical situation of their environment, using satellite images. Finally, an eddy-resolving sampling using a fine sampling interval (~10 km) must be adopted. Such an experiment (EGYPT: Eddies and GYres Path Tracking: www.ifremer.fr/lobtln/EGYPT) is currently being planned to investigate the southern Levantine at mesoscale, in order to possibly validate our hypotheses for the circulation there.

Tracking Meddies in the NE Atlantic

Isabel Ambar and Nuno Serra

Instituto de Oceanografia, Faculdade de Ciências da Universidade de Lisboa, Lisboa, Portugal

ABSTRACT

The North Atlantic hydrography is strongly influenced by the presence of the Mediterranean Water (MW) at intermediate levels and of the associated eddies. The role played by these eddies in the spreading of this water mass and in the physical processes relevant to the North Atlantic hydrography and to the global ocean circulation is presently considered an important issue. Project MEDTOP ("Mediterranean undercurrent - EDdies and TOPographic effects") was developed with the main objective of contributing to the understanding of the dynamical aspects of the eddies associated with the Mediterranean Undercurrent off south Portugal and of the role played by submarine canyons and capes in the current instabilities and eddy generation. The work programme included two main tasks: an observational task and a modelling task, leading to a final phase of integration of the respective results. The RAFOS floats that were deployed during the whole experiment have shown interesting aspects connected with the shedding of dipoles from the Mediterranean Undercurrent. Satellite remote sensing (sea surface temperature, chlorophyll concentration and surface altimetry) has proved to be an extremely valuable instrument for the detection of these deep eddies and dipoles through their imprint on the sea surface dynamics. An effort was recently started to further explore this identification of MW eddies by using artificial intelligence techniques for pattern recognition in satellite remote sensing images.

1. THE MEDITERRANEAN WATER IN THE ATLANTIC

The North Atlantic hydrology is strongly influenced by the presence of the Mediterranean Water (MW) at intermediate levels. This water mass flows through the Strait of Gibraltar and forms a warm and saline wedge extending southwestwards from off the Iberian Peninsula to the western side of the Atlantic. The Mediterranean Water intrusion is split into two cores (upper and lower) of distinct densities (γ_θ ~27.6 and 27.8 kg m^{-3}) centred respectively at 800 and 1200 m (Zenk, 1970, 1975; Ambar and Howe, 1979a, b). The upper core stays closer to the Iberian Peninsula whereas the lower core spreads in the North Atlantic.

Advection and diffusion were considered the only responsible processes for this water mass spreading (Needler and Heath, 1975; Richardson and Mooney, 1975) until the finding of a supposed MW eddy (meddy) off Bahamas (McDowell and Rossby, 1978) and the subsequent identification of isolated meddies in the NE Atlantic (e.g., Armi and Zenk, 1984; Armi *et al*., 1988, 1989; Richardson *et al*., 1989). The idea that these eddies could act as point sources of MW was then put forward (Armi and Zenk, 1984) and the role played by them in the spreading of this water mass is presently considered more important than the advection-diffusion processes. The comparison (Richardson *et al*., 2000) between the salinity anomaly associated with the presence

of MW at intermediate depths of the North Atlantic and the sites where isolated meddies have been found (Figure 1) gives some support to this hypothesis.

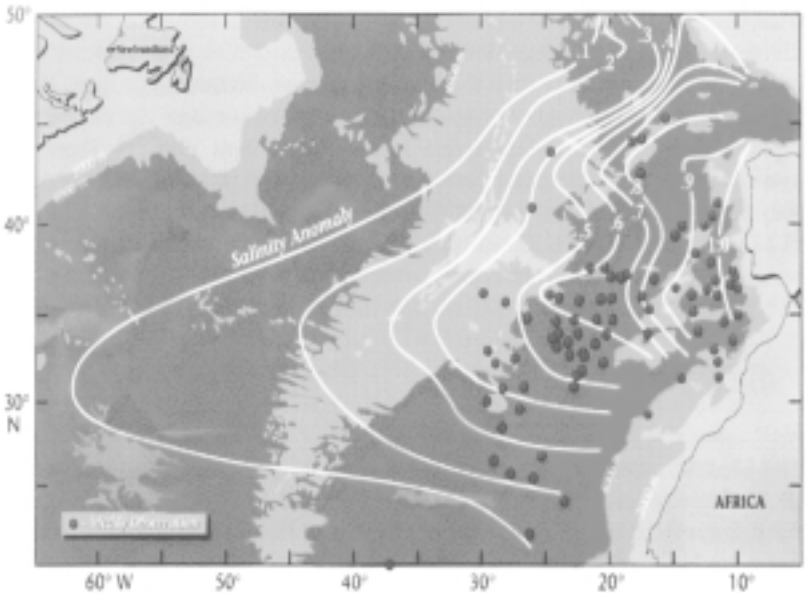

Fig. 1. Isolines of salinity anomaly at the MW levels and sites where meddies were found as reported in the literature (Richardson *et al*., 2000).

The lifetime of these coherent eddies can be longer than two years (Richardson *et al*., 1989) and distinct mechanisms contributing to their degradation have been identified, such as lateral mixing along their boundaries, impact due to bottom relief, erosion effects by double diffusion, etc.

Several processes responsible for the generation of the meddies have been suggested by different authors, such as diapycnal mixing followed by geostrophic adjustment (McWilliams, 1988; Hedstrom and Armi, 1988), baroclinic instabilities (Beckmann, 1988; Käse *et al*., 1989), separation processes (D'Asaro, 1988), etc.

Several projects aiming at the understanding of the generation and evolution of the meddies have used deep floats – RAFOS floats – for their tracking. Among them the AMUSE project (1993-1995) has identified the Cape St. Vincent and the Estremadura Promontory as sites of meddy generation (Bower *et al*., 1997), and later the CANIGO project (1996-1999) evidenced other sites like the Portimão Canyon and the Gorringe Bank (Serra and Ambar, 2002). The AMPOR project (1998-2000) joined together physical, chemical, geological and biological teams for the multidisciplinary characterization of the MW and specifically, of a meddy found at the eastern side of the Gulf of Cadiz (36ºN, 8.5ºW). An important aspect that was recognized in CANIGO and also in the French project SEMANE data was the existence of cyclones accompanying the meddies and thus forming dipoles (Carton *et al*., 2002; Serra *et al*., 2002; Serra and Ambar, 2002). It seems that these cyclones can only be detected close enough to the continental slope, the reason being their much shorter lifetime as compared with the anticyclones (meddies).

2. FOCUSING ON MEDDIES

The present interest on meddies is due to the increasing recognition of their role in several physical processes relevant to the North Atlantic hydrography and global ocean circulation:

(i) they contribute to the large scale spreading of the warm and saline MW in the NE Atlantic, thus contributing to the functioning of the thermohaline circulation (conveyor belt mechanism);

(ii) they transport water with low nutrients (Ambar *et al*., 1976, 2002), large concentrations of suspended sediments (Abrantes *et al*., 1994; Freitas and Abrantes, 2002) and, probably, heavy metals;

(iii) they carry with them biologic species (algae, fish larvae, etc.);

(iv) they interfere with the surface circulation, namely with the development of the coastal upwelling filaments off the Iberian Peninsula (Serra, 2004).

There are still some issues that should be clarified, such as estimating what fraction of the MW in the Atlantic meddies contribute to, the identification of the main mechanisms leading to the generation of dipoles, the formation of meddies with double core (upper and lower cores), etc.

3. THE MEDTOP EXPERIMENT

Project MEDTOP ("Mediterranean undercurrent - EDdies and TOPographic effects") was developed with the main objective of contributing to the understanding of the dynamical aspects of the eddies associated with the Mediterranean Undercurrent off south Portugal and of the role played by submarine canyons and capes in the current instabilities and eddy generation. The work programme included two main tasks: an observational task and a modelling task, leading to a final phase of integration of the respective results.

The observations took place in the region between 7.5ºW – 10.5ºW, 35.5ºN – 37.5ºN and were designed to study the effect of the Portimão Canyon and Cape St. Vincent on the Mediterranean Undercurrent and to describe the hydrographycal, chemical and dynamical fields of the vortices (cyclones or anticyclones) associated with this current. The project included high-resolution surveys using a CTD coupled to a rosette-sampler, in three different occasions along the year (see Figure 2), and the deployment of RAFOS floats within the Mediterranean Undercurrent along a section upstream of the Portimão Canyon. In case of detection of a meddy (or a cyclone) during one of these surveys, the dynamical and hydrographycal fields of that structure and of the layers above and below were object of intensive observations using expendable profiling instruments (XBTs and XCPs), RAFOS floats and surface drifters.

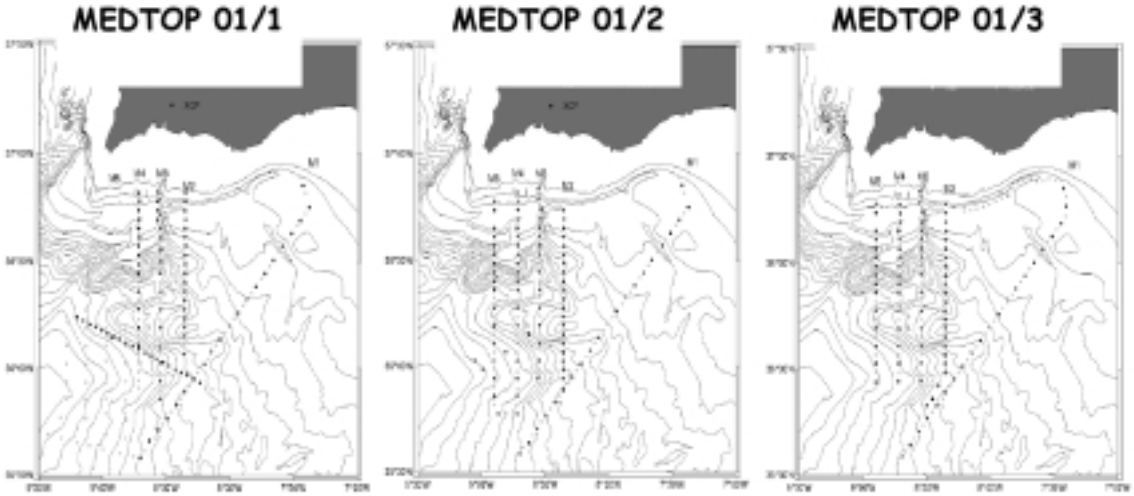

Fig. 2. MEDTOP surveys: location of CTD/XBT lines in MEDTOP 1 (January-February 2001), MEDTOP 2 (May 2001) and MEDTOP 3 (September 2001).

3.1. High-resolution surveys

The main objectives of the CTD surveys in the region of the Portimão Canyon off the south coast of Portugal were to evaluate the horizontal and vertical extension of the Mediterranean Undercurrent, to give the hydrological and chemical framework necessary to select the sites for the RAFOS deployments and to detect the presence of meddies and/or cyclones in the region. Along the CTD lines the spacing between stations was 5 to 10 miles. The surveys were repeated on three different occasions along the year (January/February, May and September) in order to evaluate any seasonal variation in the Mediterranean outflow properties (Ambar *et al.*, 1999). During two of these cruises (January/February and September), water samples were collected

(using a rosette-sampler coupled to the CTD) for chemical analyses (nutrients and dissolved oxygen).

3.2. Line of RAFOS deployment

The deployment of RAFOS floats along a section upstream of the Portimão Canyon aimed at following the main cores of the Mediterranean outflow along their paths within the region of the Canyon, allowing for detection of bathymetric constraints to the flow. The sampling time interval of the floats (and of the respective sound sources) was adjusted to 4 hours (instead of the more frequently used 8 hour-sampling) in order to get the required detail of the trajectories in the vicinity of the Canyon. This sampling rate (6 times per day) corresponds to a sampling space interval of about 7 km (assuming 50 cm/s as a reasonable value for the Undercurrent maximum velocities in the region). These floats were also intended to show the eventual shedding of eddies (cyclonic or anticyclonic) from the Mediterranean Undercurrent associated with the presence of the Canyon.

The RAFOS floats were deployed at two levels, namely the MW upper and the lower core levels, at three locations along a line upstream of the Portimão Canyon, where the Mediterranean outflow still constitutes a bottom current. This line was designed to cross the bathymetric contours at approximately right angles in order to intersect the outflow at its maximum transversal extension.

3.3. Intensive observations of eddies

The *in situ* observations had the support of near-real time satellite remote sensing (altimetry and sea surface temperature) data for meddy location. When the presence of a meddy and/or a cyclone was detected by remote sensing and confirmed during one of the high-resolution surveys, then the survey was interrupted and intensive observations of the structure started. Profiles of XBTs and XCPs (expendable current profilers) were made across the structure in two directions perpendicular to each other. The use of XCPs is very appropriate to estimate the shear above and below the eddy and the near bottom velocity, and as the flow is strongly cyclostrophic with a Rossby number of nearly 1, the hydrographic section will not resolve the bottom velocity and shear layer and will not give accurate determinations of velocity. Besides the profiling instruments, RAFOS floats were deployed at different levels (one above, one below and two within the structure) and surface drifters above the structure.

4. Some preliminary results

One of the intensive surveys of eddies allowed the characterization of a dipole, which was shed by the Mediterranean Undercurrent in the region of the Portimão Canyon.

The RAFOS floats that were deployed during the whole experiment (Figure 3a) have revealed some interesting aspects like a recirculation in the Gulf of Cadiz, a south and westward spreading tendency and the generation of meddies and dipoles (Figure 3b).

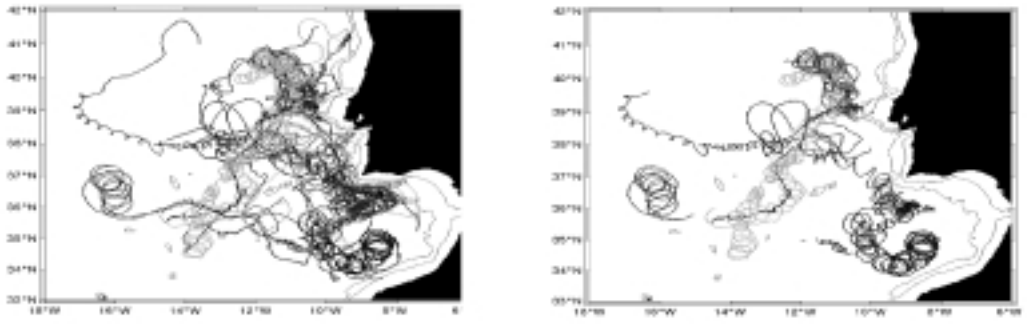

Fig. 3. RAFOS floats trajectories during the MEDTOP project: (**a**) the whole set of floats; (**b**) the floats caught in eddies.

Satellite remote sensing has proved to be an extremely valuable instrument for detection of the deep eddies imprint on the sea surface dynamics. Remote sensing images not only of sea surface temperature (Pingree, 1995; Oliveira *et al*., 2000; Serra, 2004) but also of chlorophyll concentration and surface altimetry (Serra, 2004) have been recently used for meddies and deep dipoles search. An example of this utilization is given in Figure 4, where the sea surface temperature patterns evidence the effect on the surface dynamics of a deep dipole tracked by floats during MEDTOP.

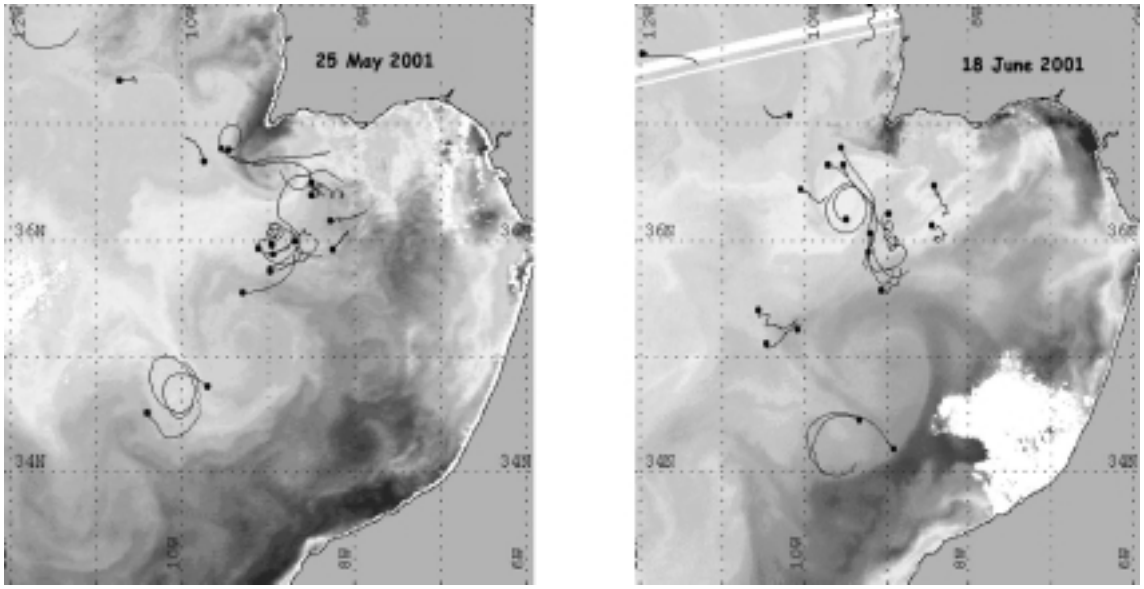

Fig. 4. Sea surface temperature images showing the surface signature of MW eddies and dipolar structures during MEDTOP project.

5. ONGOING WORK

A recent project, named RENA ("Remote Detection of Mediterranean Water Eddies in the Northeast Atlantic) and funded by the European Space Agency and the Fundação para a Ciência e a Tecnologia (Programa Dinamizador para as Ciências e Tecnologias do Espaço), further explores the identification of MW eddies using remote sensing data. The project includes the analysis of infrared, visible and microwave imagery, the development of a numerical model of the MW flow in the Northeast Atlantic (Serra *et al*., 2005) with data assimilation capabilities and the implementation of artificial intelligence techniques for pattern identification in remote sensing images.

Acknowledgements

The MEDTOP project was funded by the Fundação para a Ciência e a Tecnologia (FCT) in the frame of the Programa Dinamizador para as Ciências e Tecnologias do Mar (contract PDCTM/P/MAR/15301/1999). Financial support to NS was maintained by FCT in the frame of doctoral (BD/19535/99) and post-doctoral (SFRH/BPD/12472/2003) grants.

Eddy transport

John T. Allen

Southampton Oceanography Center, Institute of Oceanographic Science, Southampton, U.K.

ABSTRACT

Using observations and analyses familiar to the author, and references to similar work by others, a review is presented of ~ 20 years of discovery and understanding of the open ocean 'mesoscale'. The focus is on the three dimensional transports associated with baroclinic instability, from simple geometrical models of cross front eddy heat transport, to biological exploitation of the 'sub-mesoscale' vertical transport of nutrient replete deep waters.

PREFACE

In the last quarter of the 20th century, undertaking physical measurement of the ocean mesoscale rapidly accelerated from merely experimental to near-operational. Part of this resulted from the oceanographic technology race; oceanographic studies by satellite (Kuragano and Kamachi, 2000), the proliferation of the vessel mounted ADCP (Pollard and Read, 1989), the geographical positioning system (GPS) and ultra-short baseline navigation techniques, and the development of towed undulating vehicles (Pollard, 1986). Part of it resulted from the dramatic expansion in numerical computation and the development of a range of high resolution numerical models (Donners *et al*., 2004; Zodiatis *et al*., 2003; Lévy, 2003; Demirov and Pinardi, 2002), both for deliberate process studies and ocean circulation modelling. And in final part, it resulted from the application of fluid dynamic theory, developed in the middle of the 20th century during the early years of meteorological forecasting, to high resolution hydrography (Allen and Smeed, 1996; Fiekas *et al*., 1994; Pollard and Regier, 1992; Tintoré *et al*., 1991).

By the turn of the century, oceanographers from all disciplines were in a position to work together in an unprecedented way to begin to examine the marine ecosystem at the mesoscale (LeBlanc *et al*., 2004; Fielding *et al*., 2001; Prieur and Sournia, 1994; Strass, 1992). During the early 'naughties' observations began to support high resolution multidisciplinary model studies (Lévy *et al*., 2001), in showing that transport associated with baroclinic instability (sub-mesoscale, 1-10 km) provides a significant mechanism for increased new production and therefore atmospheric CO_2 drawdown by the biological pump (Allen *et al*., 2005). But how much of this is already included in bulk estimates? And how can global (or even basin scale) budgets be adjusted or re-calculated to incorporate the sub-mesoscale?

I will use some examples particularly familiar to me, to illustrate this development and I will conclude with pointers to current programmes and challenges that are going to stretch our knowledge further.

1. Eddies and Mixing at the Iceland Færœs Front (IFF)

At the western end of the Iceland Færœs Gap, there exists a very steep front the Iceland Færœs Front (IFF) between Nordic and Atlantic Waters (Smart, 1984). The front is unstable, creating meanders and eddies on a number of scales, and eventually further east the front becomes less well defined (Read and Pollard, 1992). During RRS *Charles Darwin* cruise 51 (July/August 1990), a large (~ 70km) warm intrusion north of the Front was observed and measurements of the density and velocity fields both indicated an anticyclonic circulation. On a smaller scale the IFF is perturbed by (15 - 30 km) cyclonic and anticyclonic eddies. In addition two double cored anticyclonic eddies were observed. The SeaSoar survey technique used for this cruise allowed the time development of a few of these structures to be observed. Estimates of cross front salt and heat transport due to eddy propagation were made using a simple model (Allen *et al*., 1994), whereby anticyclones lifted North Atlantic water up over cold, dense, Arctic and Nordic seas water masses and conversely cyclones transported Arctic and Nordic seas waters south across the front.

Using VM-ADCP velocity data in combination with SeaSoar hydrography, quasi-synoptic maps were produced of geostrophic velocity, vorticity and potential vorticity on isopycnal surfaces (Allen and Smeed, 1996). The data were also used to diagnose the vertical velocity field using the QG (quasi-geostrophic) omega equation. The results helped to elucidate the dynamical processes occurring at the front. Across the front there was a large change in potential vorticity on the density surfaces σt = 27.4 -27.6. Instability generated meanders which propagated eastwards along the front. A cyclonic vortex was observed to break off from a meander. Within the vortex the magnitude of the relative vorticity was large (~0.8 *f*), and the potential vorticity had high values similar to that of the water to the north of the front from which the vortex was derived. The eddy propagated north-eastwards relative to the underlying water resulting in large upward (downward) vertical velocities (in excess of 60 m/day) ahead of (behind) the vortex. We were beginning to observe baroclinic instability and the impact of the 'sub-mesoscale'.

Similar studies were progressing elsewhere; in the mid latitude Atlantic, Rudnick (1996) was looking at the dynamics of the Azores front region, whilst Shearman *et al*. (1999) were looking at mesoscale motion in the California current.

2. The eddy transport of Western Mediterranean Intermediate Waters (WIW) to the Alboran Sea

During the second cruise of the EU funded OMEGA project (December 1996) the towed CTD, SeaSoar, was deployed to survey the upper 350 m of the water column in the eastern Alboran Sea and extreme western Algerian basin (Allen *et al*., 2001b). The Almeria Oran front forms at the eastern boundary of the Alboran Sea gyre system, in the upper 150-200 m of the water column, and separates waters of predominantly Atlantic origin from those formed in the Western Mediterranean basin (Tintoré *et al*., 1988). Below these surface waters, but above the Levantine Intermediate Water, Western Mediterranean Intermediate Waters (WIW, formely known as Winter Intermediate Waters), believed to be formed to the north of the Balearic Sea (López-Jurado, 2002; Gasparini *et al*., 1999), are normally observed in this region. However, to our knowledge, this was the first time a discreet eddy of WIW, a "weddy", had been observed in the extreme western Algerian basin (Figure 1). Repeated surveys of the region allowed us to observe the evolution of the eddy over a period of 40 days.

A particularly cold temperature minimum layer water was observed in an anticyclonic eddy at around 36.6° N, 0.9° W. This had purer characteristics of WIW as described by Pinot and Ganachaud (1999), temperature < 13 °C and salinity 38.2 psu. The 'weddy' was observed in the first 6 of the 7 SeaSoar surveys of the Almeria-Oran frontal region (LSS1 and 2, and FSS1-5). By FSS5, the signature of the eddy had disappeared probably as a result of wind driven buoyancy loss and vertical mixing; the θ/S envelope for FSS5 showed a marked absence of a clear WIW signature and a significant cooling of surface waters.

Pinot *et al*. (2002) show that the size of the weddy is key to its passage from the Balearic Sea to the Algerian basin through the Ibiza Channel; those over 50 km in diameter will be significantly restricted by the narrow topography of the channel, and may block the normal mean circulation in the region. Interestingly, Viudez *et al*. (1998) may well have discovered a weddy at ~ 3° 20'W,

36° 00'N, in the centre of the Alboran Sea but resolved by just one CTD they were only able to offer conjecture as to the details of its structure and origin.

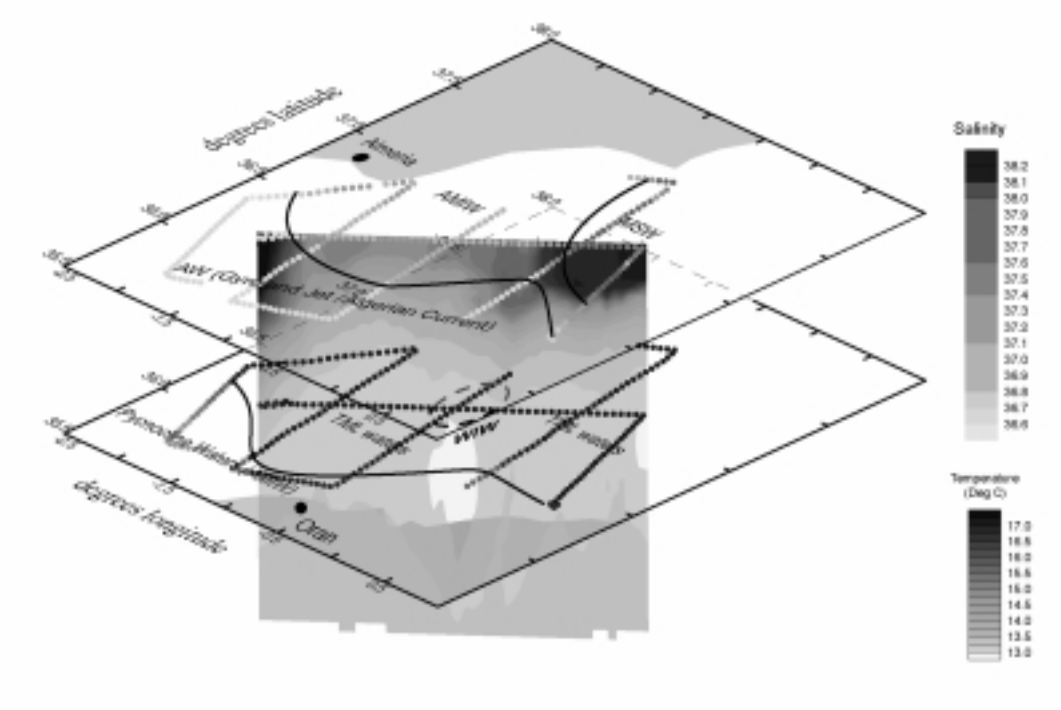

Fig. 1. Composite indicating the three dimensional structure of the upper 350 m of the water column during LSS2 of the OMEGA 2 cruise (Allen *et al.*, 2001b). The dotted cruise tracks show the horizontal salinity distribution at depths of 13 m and 157 m. The vertical contoured section shows temperature along the central leg of the cruise track, the vertical axis has been removed for clarity but the dotted tracks for this leg on the two horizontal slices are shown in the plane of the vertical section. Only the horizontal planes are annotated. The solid black cartoon lines on the horizontal planes indicate the boundaries between water types observed at the time of LSS2 *(redrawn from Allen et al., 2001b)*. Acronyms used are as follows, AW - Atlantic origin waters, WIW - Western Mediterranean Intermediate Waters, TML - temperature minimum layer, MSW - Mediterranean surface waters, and AMIW - Atlantic-Mediterranean interface waters.

3. MESOSCALE SUBDUCTION AT THE ALMERIA-ORAN FRONT

A detailed diagnostic analysis of hydrographic and current meter data from three, rapidly repeated, fine-scale surveys of the Almeria-Oran front showed that instability of the frontal boundary, between surface waters of Atlantic and Mediterranean origin, provides a mechanism for significant heat transfer from the surface layers to the deep ocean in winter (Allen *et al.*, 2001b). The high resolution hydrographic measurements traced the subduction of Mediterranean surface water across the Almeria-Oran front. Again this subduction was shown to result from a significant baroclinic component to the instability of the frontal jet. The QG omega equation was combined with a scale analysis to quantitatively diagnose vertical transport resulting from mesoscale ageostrophic circulation. The analyses were discussed with the support of satellite and airborne remotely sensed data; which provided the basis for a thorough and novel approach to the determination of observational error. Diagnosed vertical velocities, ~10 m/day were smaller than expected from the observed subduction of Mediterranean surface waters. However, new studies of the effects of asynopticity on dynamical data analyses (Allen *et al.*, 2001a) enabled us to explain the differences in the apparent magnitude of w. This error arises from the inherent time scale required to collect a set of measurements capable of resolving the mesoscale, which is similar to that in which the underlying distribution changes significantly. In this case, the necessary correction was large, doubling the diagnosed magnitude of to at least 20 m/day.

Traditionally, baroclinic instability is responsible for upwelling warm, light water and subducting cold, dense water as available potential energy is converted to kinetic energy and released across the front. During the winter months the surface waters of the western Mediterranean are made up of resident waters that have been heated and evaporated during the preceeding summer and modified Atlantic Waters (AW) inflowing from the Strait of Gibraltar and passing around the gyre system of the Alboran Sea. The Mediterranean surface waters are denser and subducted by the baroclinic instability at the Almeria-Oran front, but they are also warmer; the high density arising from the high salinity. Therefore these instabilities may result in a net heat loss from the surface layers to the deep ocean. Furthermore, we showed, this heat loss could locally exceed that lost to the atmosphere during the winter.

In multidisciplinary field experiment, we observed the biological impact of mesoscale frontal instability of the Almeria-Oran frontal jet. It was concluded that periodic vertical velocities of ~20 m/day, associated with the propagation of wave-like meanders along the front, have a significant effect on the vertical distribution of zooplankton across the front despite their ability to migrate at greater speeds (Fielding *et al*., 2001). As shown in Figure 2 a layer of fluorescence

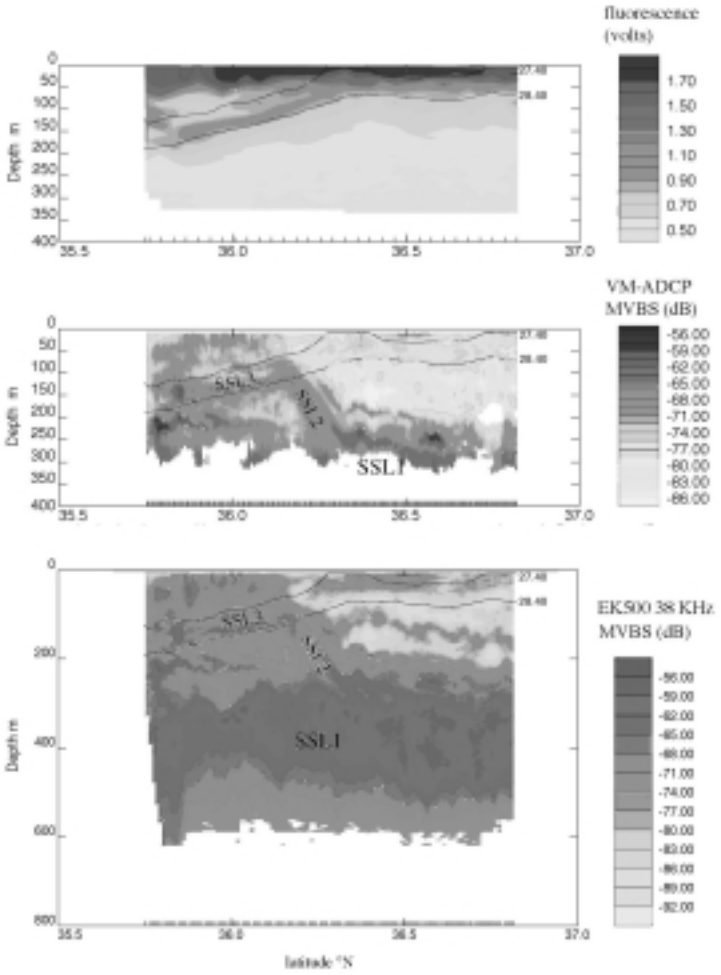

Fig. 2. Contoured sections of fluorescence yield (instrument volts - top), VM-ADCP acoustic backscatter amplitude (middle) and EK500 38 KHz acoustic backscatter amplitude (bottom), across the Almeria-Oran front for Leg g of FSS3 (Fielding *et al.*, 2001; Allen *et al.*, 2001b). The 27.4 and 28.4 sigma-0 isopycnals are over-layed for reference *(redrawn from Fielding et al., 2001)*. SSL stands for sound scattering layer and three layers are identified for continuity between the two acoustic datasets presented.

coincident with subducted surface waters indicates that phytoplankton cells were drawn down and along isopycnals, by cross front ageostrophic motion, to depths of 200 m. From the study of sound scattering layers identified in acoustic backscatter data, a layer of zooplankton was found coincident with the drawn down phytoplankton. This layer persisted during and despite diel vertical migration.

4. Diatoms and carbon export in the N. E. Atlantic

In May/June 2001, biological and physical data were collected in the vicinity of the IFF during two legs of the RRS *Discovery* cruise, FISHES (Færœs, Iceland, Scotland Hydrographic and Environmental Survey) (Brown *et al*., 2003). A sea surface chlorophyll (SeaWiFS) image of the region, on the 23 May 2001, showed a marked bloom along the meanders of the IFF (Figure 3). *In situ* fluorometers confirmed that the high chlorophyll concentrations (5-7.5 mg m^{-3}) were restricted to the frontal jet. Taxonomic analysis showed the frontal bloom was composed of typical bloom species diatoms, while phyto-flagellates dominated to the north and south. Surface $Si(OH)_4$ concentrations were limiting, however, baroclinic instability of the IFF was shown to be a supplier of new $Si(OH)_4$ sufficient to support the prolonged frontal bloom (Allen *et al*., 2005).

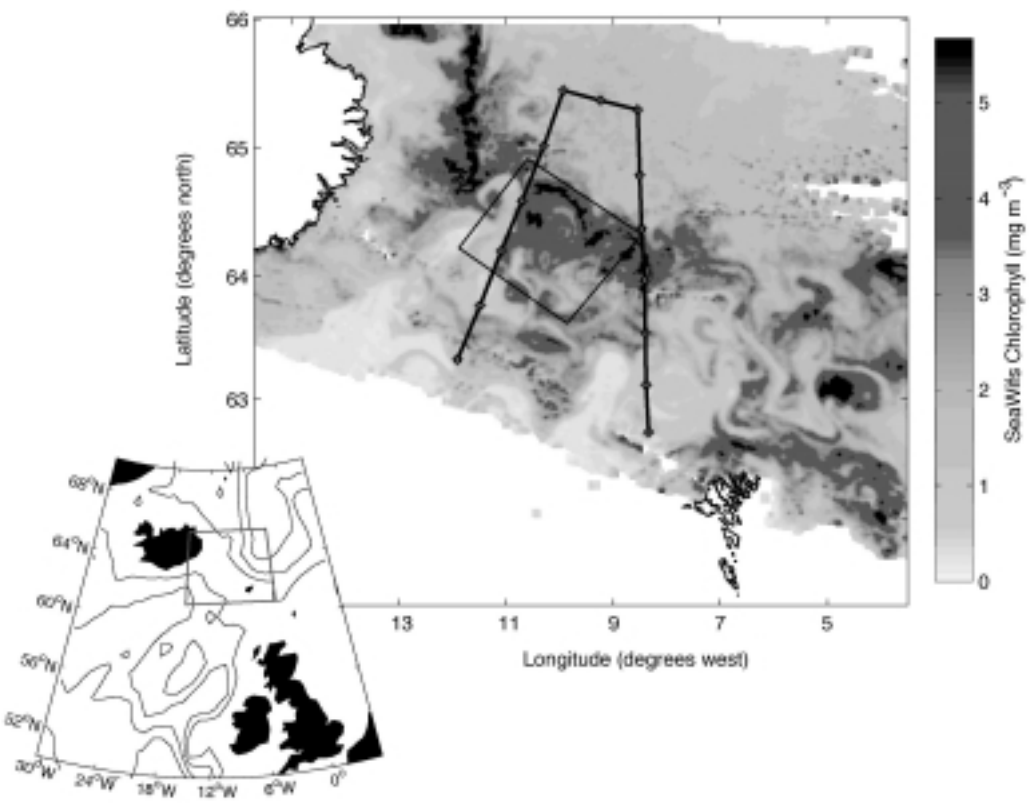

Fig. 3. Ocean colour image of the northern N. E. Atlantic (SeaWiFS) for the 23rd May 2001 (white areas are cloud and land). A marked phytoplankton bloom (dark greys) is associated with the meandering Iceland Færœs Front. The black lines on the image indicate part of the cruise track and an area chosen for high resolution sampling.

Understanding the detailed ecosystem exploitation of mesoscale and sub-mesoscale three dimensional physical flow requires observation of near-sufficiency, where supply and demand are closely matched: large, easily detected signals in nutrient concentrations or uptake rates should not be expected. This alone required a re-think of the traditional sampling strategies.

The FISHES experiment demonstrated responsive mode multi-disciplinary operational oceanography at the mesoscale. Rapid variations in zooplankton biomass were observed across an oceanic frontal region, associated with sharp changes in water mass characteristics. Ocean colour satellite images also indicated that a spring bloom existed in the vicinity of the front. Further, in general, satellite images also indicated that mesoscale meandering of the front was at least as pronounced in ocean colour as in infra-red images; suggesting that biological patchiness was dominated by physical processes.

In response, a SeaSoar survey region was determined from the satellite images and a regional multidisciplinary numerical model was initialised whilst steaming to begin the second leg of the cruise (Popova *et al*., 2002). The numerical model output indicated that the meandering eddy-like structures observed in the satellite images were the result of instability of the front and that an along front sampling interval of no coarser than 15 km would be necessary to resolve the dominant scale of instability. The first survey was therefore designed to have 15 km spacing between conventional cross-front parallel legs carried out in a downstream direction relative to the along front flow.

Data from the first SeaSoar survey were assimilated into the numerical model as quickly as they could be processed and roughly calibrated, minutes to a few hours. The model forecasts were then used to choose CTD and net sampling stations, within the time constraint of 24 hours between SeaSoar surveys.

The numerical model forecasts and satellite images confirmed that, in this case, the propagation speed of the wave like meanders and eddy structures along the front was much less than the effective along front sampling speed of the SeaSoar surveys: i.e. the survey was quasi-synoptic with regard to the mesoscale instability of the front (Allen *et al*., 2001a; Rixen et *al*., 2001). Optimising sampling according to the mapping error in horizontal temperature gradients, we were able to show that an upstream survey pattern would not increase sampling error. And indeed that a less conventional survey of more widely spaced parallel legs in line with the mean direction of the frontal jet could significantly reduce sampling error (Rixen *et al*., 2003a). Therefore, the second survey was designed as an upstream repeat of the first with an extra leg at the beginning, creating a little more time than anticipated.

Once again, data from this second survey were assimilated into the numerical model as quickly as they could be processed and roughly calibrated. And, the model forecasts were again used to choose CTD and net sampling stations. Optimised survey design continued to propose a survey of parallel legs in line with the front and therefore a third and final survey was determined objectively by this means.

By this time, the SeaSoar vehicle (Figure 4) was carrying an impressive array of instruments and recorded ~3000 km of high resolution data over the top 500 m of the water column. Once processed in near real time this was equivalent to ~750 CTD casts to 500 m at 4 km along track spacing in a period of less than 12 days. To our knowledge, this was the first time that primary productivity parameters from a Fast Repetition Rate Fluorometer were obtained in real time (Moore *et al*., 2005) and concurrent with a data set including temperature, salinity, pressure, fluorescence, and particle size and abundance from an optical particle counter (OPC).

5. THE FUTURE - MARINE ALGAE, STUDENTS OF ANGULAR MOMENTUM?

High resolution modelling studies have indicated that highly dynamic small scale flows associated with oceanic fronts and eddies are a dominant mechanism for the observed patchiness of marine algae (phytoplankton) blooms. In a most extensive modelling study Lévy *et al*. (2001) show that these 'sub-mesoscale' flows (~5-20 km scale) may provide both the fertilisation mechanism for nutrient depleted (oligotrophic) surface waters and a subduction mechanism for the rapid export of phytoplankton biomass to the deep ocean. We are now just beginning to observe these small scales for the first time, with multidisciplinary platforms making both physical and biological measurements at the same small temporal and spatial scales (Allen *et al*., 2005).

Fig. 4. (See page 109 for original color plate) The SeaSoar vehicle at the surface awaiting recovery. *Photograph courtesy of Prof. R.T. Pollard, National Oceanography Centre, Southampton, U.K.*

On the temporal scale of days and spatial scale of 1-100 km, we assume that phytoplankton can be considered passive with respect to the three dimensional fluid motions (Fielding *et al*., 2001), at least whilst in a healthy state. To a first order, at these scales, water particles move along surfaces of constant potential density (Allen *et al*., 2001), isopycnal surfaces, and therefore it has been instructive to look at chlorophyll fluorescence yield on isopycnal surfaces. Larger phytoplankton particles tend to appear more negatively buoyant as buoyancy becomes more important than viscosity. Nevertheless Rodríguez *et al*. (2001) showed that only small upward vertical motions in the water column (< 5 m/day) were sufficient to support the size range of the bulk of ocean phytoplankton cells. Large aggregated unhealthy diatom cells may sink considerably faster (Turner, 2002), more than 100 m/day perhaps, but such processes would clearly not line up with density surfaces or flow streamlines.

The FISHES data further confirm that mesoscale/sub-mesoscale transport mechanisms are constrained by the requirement to conserve angular momentum, expressed in a stratified water column as the conservation of potential vorticity. The 12 day evolution of the observed chlorophyll fluorescence on a 27.75 sigma-0 density surface echoes the filamentary structure in the vorticity field (Figure 5).

New programmes and those early in their analysis phases such as POMME (http://www.lodyc.jussieu.fr/POMME) and CROZEX (http://www.noc.soton.ac.uk/GDD/hydro/rtp/crozet) are well positioned to take our understanding yet further. The correct convolution of the biological datasets with derived three dimensional mesoscale/sub-mesoscale flow is not a straight-forward correlation. The observed patchiness will need to be associated with the evolution of the three-dimensional flow between the surveys; we will need to refer to model datasets in order to test our interpretations. However we have already noticed that potential vorticity (PV) may provide a valuable history for the biology as it indeed always has done for the hydrography; have we come full circle?

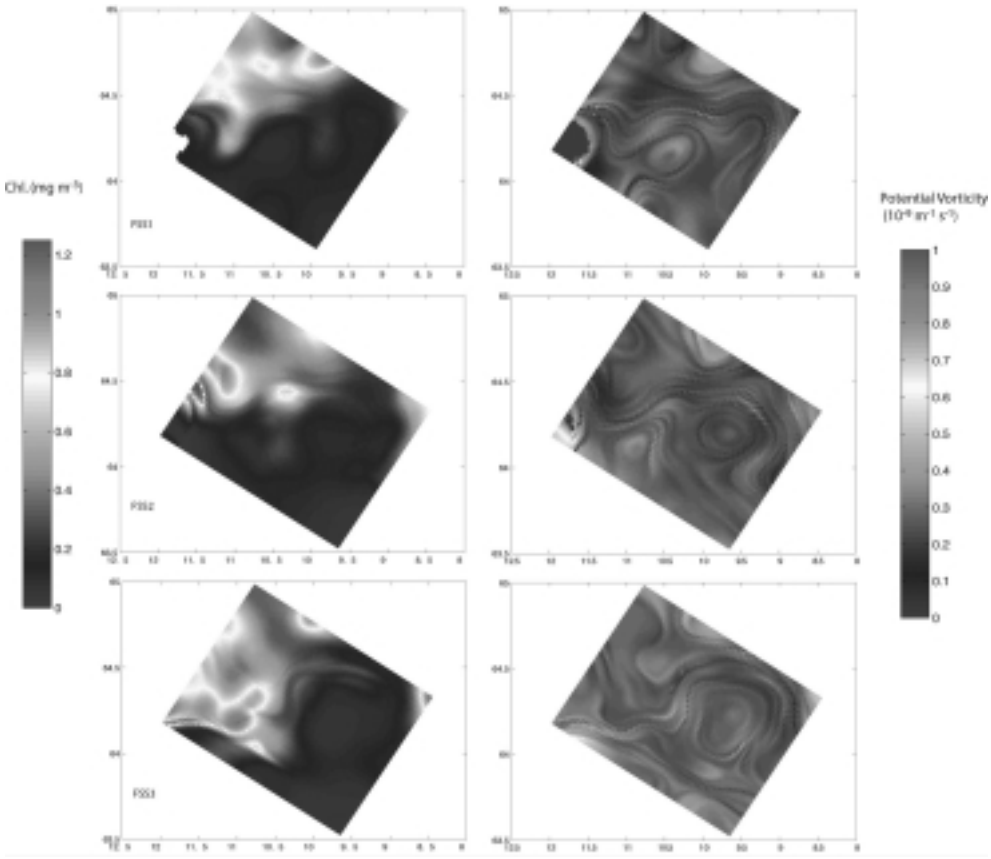

Fig. 5. Right, 12 day evolution of the diagnosed potential vorticity field (units in 10^{-9} $m^{-1}s^{-1}$): left, 12 day evolution of the observed chlorophyll fluorescence (units in mg m^{-3}). All presented on the 27.75 sigma-0 density surface. The sub-mesoscale filamentary structure in the vorticity field is clearly echoed in the chlorophyll fluorescence (Lévy *et al.*, 2001) wrapping round the anticyclonic eddy at ~ 64°15' N, 9°45'W. In looking for a close correlation we must remember that the advective boundaries of the vortices is where we expect high Froude numbers and strong mixing (Allen and Smeed, 1996), and that we are at the very limit of observational resolution.

Mesoscale variability of the Black Sea circulation as inferred from satellite data and model simulations

Temel Oguz

Institute of Marine Sciences, Middle East Technical University, Erdemli, Turkey

ABSTRACT

The Black Sea circulation involves a complex, eddy-dominated system with different types of structural organizations in which the eddies and the gyres of the interior cyclonic cell interact continuously among themselves and with meanders, and filaments of the Rim Current system. Taking the relatively narrow width of the basin into account, mesoscale processes can easily give rise to meridional transports from one coast to another. The circulation also possesses a distinct seasonal cycle whose major characteristic features repeat every year with some year-to-year variability. Recent *in situ* and satellite observations allow us to propose a revised schematic circulation picture of the major quasi-permanent and recurrent elements of the sea.

DISCUSSION

The Black Sea, located approximately between latitudes of 41° to 46°N and longitudes of 28° to 41.5°E, is an elongated and nearly-enclosed basin connected with the Bosphorus Strait to the Mediterranean Sea. The Black Sea, with a surface area of 423,000 km^2, is approximately one-fifth of the surface area of the Mediterranean. It has a total volume of 547,000 km^3, and a maximum depth of around 2200 m. It contains narrow shelves and very strong topographic variations around its periphery. The northwestern shelf (NWS), ~20% of the total area, is the only major shelf region with discharges from three of Europe's largest rivers: the Danube, Dniepr and Dniestr. In the north, the sea is connected to the shallow Sea of Azov by the Kerch Strait. At its southwestern end, it communicates with the Aegean basin of the Mediterranean Sea through the Bosphorus, Sea of Marmara and Dardanelles. The Black Sea has always been a basin with a positive water balance. The sum of fluxes due to precipitation (~300 km^3 yr) and runoff (~350 km^3 yr) exceeds that of evaporation (~350 km^3 yr). The freshwater excess of 300 km^3 yr is balanced by the net outflow through the Bosphorus, defined as the difference between the transports of its two layers. This particular net transport value agrees well with the estimates for 1980s and 1990s obtained by long-term hydrological-meteorological data (Peneva *et al*., 2001). It is also found to be consistent with the net Bosphorus transport computed independently by means of a two layer hydrodynamic Bosphorus model (Oguz *et al*., 1990).

The upper layer waters of the Black Sea are characterized by a predominantly cyclonic, strongly time-dependent and spatially-structured basinwide circulation. Many details of the circulation system have been explored using hydrographic and satellite (AVHRR, altimeter, CZCS, SeaWIFS) data, as reviewed recently by Oguz *et al*. (2005). These analyses reveal a complex, eddy-dominated circulation with different types of structural organizations within the interior

cyclonic cell, the Rim Current flowing along the abruptly varying continental slope and margin topography around the basin, and a series of anticyclonic eddies in the onshore side of the Rim Current. The interior circulation comprises several sub-basin scale gyres, each of them involving a series of cyclonic eddies. They evolve continuously by interactions among each other, as well as with meanders, and filaments of the Rim Current. The larger scale characteristics of the upper layer circulation system possess a distinct seasonal cycle, as suggested by objectively analyzed, optimally interpolated and dynamically assimilated sea level anomaly data provided by the Topex-Poseidon and ERS-1/2 altimeters period from 1 January 1993 to 31 December 1998 (Korotaev *et al*., 2003). As shown by the model-derived mean circulation patterns (Figure 1) for the middle of February, July and October, the interior cyclonic cell in winter months involves a two-gyre system surrounded by a rather strong and narrow peripheral jet without any appreciable lateral variations (Figure 1a). This system transforms into a multi-centered composite cyclonic cell surrounded by a broader and weaker Rim Current zone in summer (Figure 1b). The interior basin flow field further weakens and finally disintegrates into smaller scale cyclonic features in autumn (Figure 1c). A composite peripheral current system is hardly noticeable in this season. The turbulent flow field is, however, rapidly converted into a more intense and organized structure after November-December. The Rim Current structure is accompanied by coastal trapped waves with an embedded train of eddies and meanders propagating cyclonically around the basin (Sur *et al*., 1996; Oguz and Besiktepe, 1999; Ginsburg *et al*., 2002). Over the annual time scale, westward propogating Rossby waves further contribute to the complexity of the basinwide circulation system (Stanev and Rachev, 1999). According to the Acoustic Doppler Current Profiler measurements (Oguz and Besiktepe, 1999), the Rim Current jet has a speed of 50-100 cm/s within the upper layer, and about 10-20 cm/s within the 150-300 m depth range.

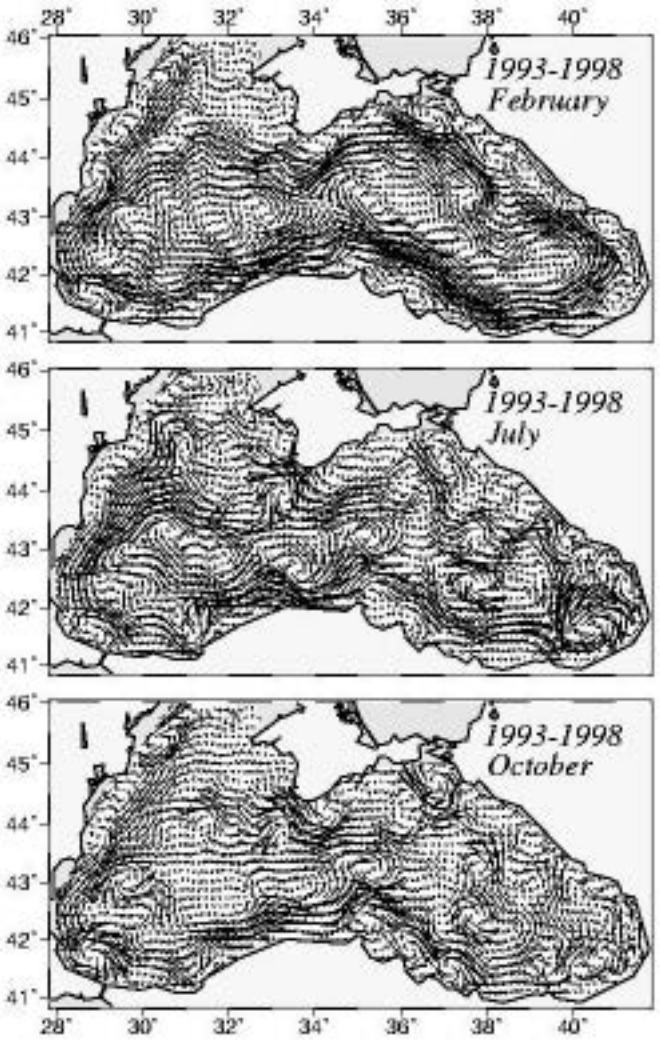

Fig. 1. The upper layer circulation maps for **(a)** mid-February, **(b)** mid-July, **(c)** mid-October, constructed by the six year averaging (1993-1998) of the daily circulation fields computed by assimilating the Topex-Poseidon and ERS-I,II altimeter data into a 1.5 layer reduced gravity model described by Korotaev *et al.* (2003).

The most notable quasi-persistent and/or recurrent features of the circulation system, as schematically presented in Figure 2, include (i) the meandering Rim Current system cyclonically encircling the basin, (ii) two cyclonic sub-basin scale gyres comprising four or more gyres within the interior, (iii) the Bosphorus, Sakarya, Sinop, Kizilirmak, Batumi, Suchumi, Caucasus, Kerch, Crimea, Sevastopol, Danube, Constantsa, and Kali-Akra anticyclonic eddies on the coastal side of the Rim Current zone, (iv) bifurcation of the Rim Current near the southern tip of the Crimea; one branch flowing southwestward along the topographic slope zone, the other deflecting first northwestward into the shelf and then contributing to the southerly inner shelf current system, (v) convergence of these two branches of the original Rim Current system near the southwestern coast, (vi) presence of a large anticyclonic eddy within the northern part of the northwestern shelf.

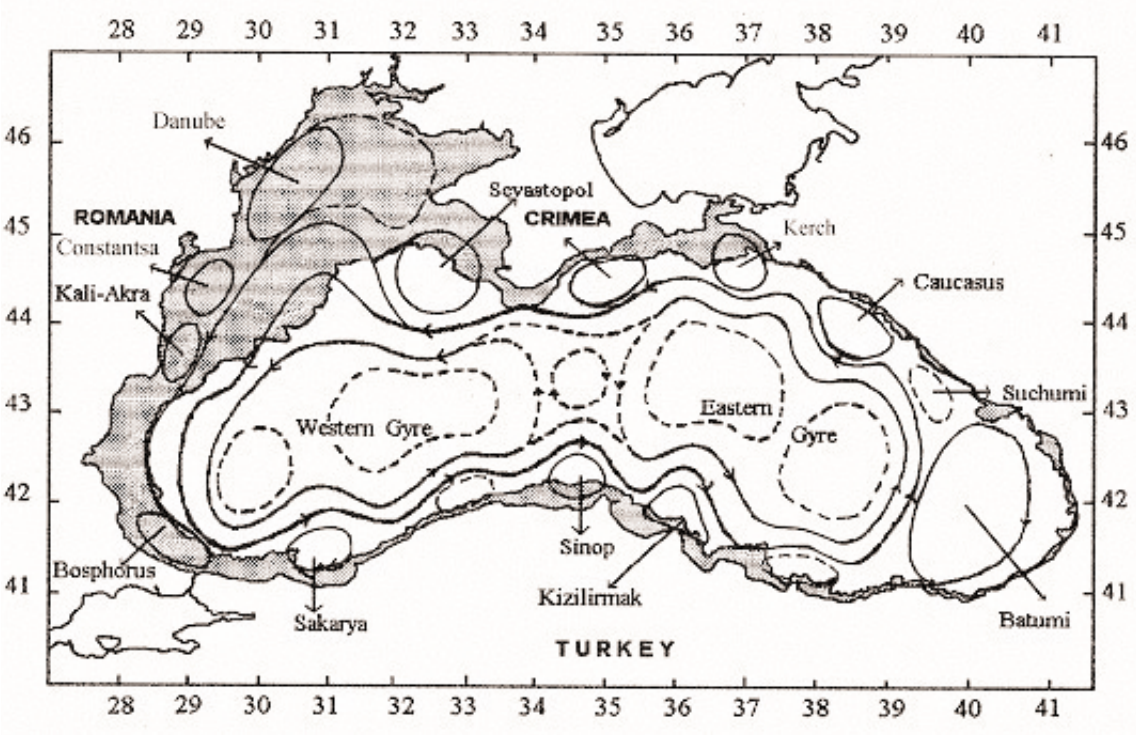

Fig. 2. Schematic diagram showing major quasi-permanent/recurrent features of the upper layer circulation in the Black Sea identified by synthesis of hydrographic studies and analysis of the Topex-Poseidon and ERS-I,II altimeter data (after Korotaev *et al.*, 2003).

An example of mesoscale evolution of the peripheral circulation system is depicted in Figure 3 by four snapshots of the flow field in the eastern part of the basin during January-April 1998. During 11 January 1998, the Rim Current system along the north Anatolian coast exhibits an offshore filament extending eastward along 42°N into the central part of the eastern basin (Figure 3a). Within a week, this feature is combined with an isolated anticyclonic eddy located within the interior to form a new filament which almost extends up to the Caucasian coast (Figure 3b). During the subsequent 10 day period, this filament is detached from its base at the south coast. The detached-eddy then merges with the meander of the Caucasus coast leading to the formation of a new offshore filament extending towards the interior from the northern coast (Figure 3c). Following its persistence for about two months, it is finally transformed into a pinched-off anticyclonic eddy occupying the central part of the eastern basin during late March and April 1998 (Figure 3d). Thus, the mesoscale features evolving along the periphery of the basin as part of the Rim Current dynamic structure provide a mechanism for two-way transports between nearshore and offshore regions. Taking the relatively narrow width of the basin into account, such mesoscale processes can easily give rise to meridional transports from one coast to another.

The basic mechanism which controls the flow structure in the surface layer of the northwestern shelf is the spreading of the Danube outflow. Wind stress and Rim Current structure along the

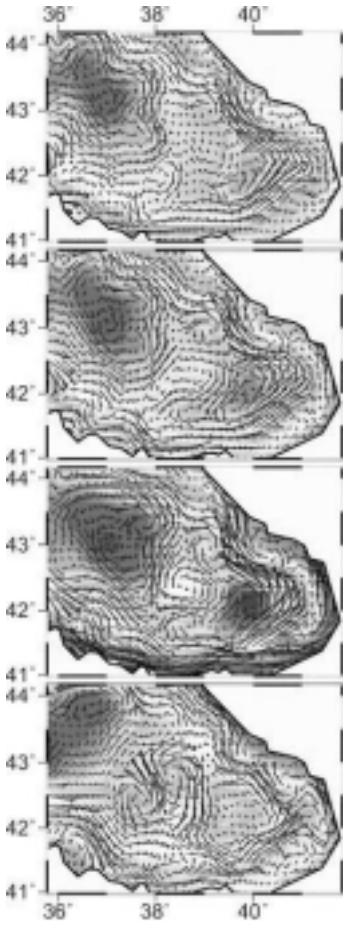

Fig. 3. Evolution of the flow field showing interaction between the Caucasus (northeastern) and Anatolian (southern) coasts of the eastern basin **(a)** during 11 January 1998, **(b)** 21 January 1998, **(c)** 31 January 1998, **(d)** 30 March 1998.

offshore side of the shelf are additional modifiers of this system. The freshwater discharge influences not only the circulation and mixing properties, but also the ecosystem of the entire shelf region along the western coast. The Danube plume generally forms an anticyclonic bulge confined within the upper 25 m layer. The leading edge of this plume protrudes southward (i.e. downstream) as a thin baroclinic boundary current along the western coastline. The coastal jet is separated from the interior waters by a well defined front with salinity differences of more than 3.0 over an approximately 50 km zone along the coast. It is often unstable, exhibits meanders and spawns filaments which extend across the wide topographic slope zone. The shelf and interior waters undergo cross-shelf exchanges as reported consistently in hydrographic surveys, satellite imagery, and altimeter data. An anticyclonic circulation system accompanied by small scale structures over the northwestern shelf has also been reproduced by modeling studies (e.g. Oguz *et al*., 1995; Staneva *et al*., 2001; Beckers, *et al*., 2002).

Mesoscale/sub-mesoscale variability of the Alboran Sea and the 3D circulation of Nador Lagoon (Morocco)

Hilmi K.[1], Orbi A.[1], Lakhdar J.I.[1] and M. Chagdali[2]

[1] *Institut National de Recherche Halieutique, Casablanca, Maroc*
[2] *Faculté des Sciences de Ben M'Sik, Casablanca, Maroc*

ABSTRACT

This study describes some aspects of the physical oceanography of Nador Lagoon (Eastern Morocco) and characterizes the circulation and the dispersion of Mediterranean water into this lagoon, using long recordings of wind, sea level and currents during spring 2001 and the HD/AD modules of the integrated MIKE 3 modeling system from DHI (Denmark). The surface of the lagoon is about 115 km^2 and its mean depth is 3-4 m, with a maximal depth in the center (6-7m). The M2 amplitude decreases from 13 cm outside the entrance channel to 3 cm inside the lagoon and its relative phase is retarded by about 3 hours as it enters the lagoon. This sets up tidal currents of about 1 m s^{-1} at the entrance which decrease progressively along both the south/north shores of the lagoon. Inside the lagoon, tidal currents remain very weak near the bottom (<0·02 m/s). Predominant winds, acting at time scales from two to ten days, blow from the north-west and from the east and produce down-wind coastal currents close to both the north and south shores of the lagoon. Close to the bottom, currents are directed up-wind. Mediterranean waters disperse inside the lagoon mainly along the northern banks reaching first both ends of the lagoon. The influence of the mesoscale/submesoscale hydrodynamics of the Alboran sea on the circulation/advection of Nador Lagoon is not well understood and needs the development of a coastal shelf model coupled with the HD/AD models.

1. INTRODUCTION

The Mediterranean Sea circulation is characterised by the presence of three different scales. At a large scale, the circulation is of thermohaline nature, due to the global dominance of evaporation over runoff and precipitation, and the compensating exchange through the strait of Gibraltar. At the regional scale, the different meteorological and topographic characteristics configure specific circulation patterns in the Mediterranean sub-basins (Font *et al*., 2004). The important mesoscale variability gives rise to the generation of meanders, eddies, filaments and other structures that can greatly influence the circulation in some areas (Millot, 1987). In the open sea, the mesoscale fluctuation spectrum spans length scales of the order 100 km, and time scales ranging between 10 and 100 days (Lewis, 2005). The Alboran Sea is the region of the western Mediterranean in contact with the Atlantic Ocean through the Strait of Gibraltar. A two layer exchange takes place with an inflow of fresh Atlantic water (S <36.5) in the upper layer (150-200m) and an outflow of saltier Mediterranean water (S< 38.4) below (Font *et al*., 2002). The incoming Atlantic water mixes with the surface water present in the region and gives rise to the modified Atlantic Waters (AW) (Gascard and Richez, 1985) that fills the southern Alboran Sea and then flows eastward to

the whole Mediterranean basin (Font *et al*., 2002). The surface inflow at Gibraltar occurs at a narrow northeastward jet (25-30 km wide) that latter forms a meandering front, usually coupled to one or two large anticyclonic gyres (100 km diameter): the Western Alboran Gyre (WAG) and the Eastern Alboran Gyre (EAG) (Figure 1). The Alboran Sea presents the most intense horizontal density gradients and current speeds in the Mediterranean basin. Most of the studies have revealed that the Alboran Sea large-scale structure presents high temporal variability. Mesoscale eddies are observed along the edges of the large gyres and are associated with intense vertical motion (Tintoré *et al*., 1991).

The coastal areas cannot be managed without a nowcasting/forecasting system that will allow the continuous assessment of system evolution (MFSTEP Monthly Bulletin). Such a system is at the base of the most urgent societal concerns for the protection and sustainable exploitation of resources in the open and coastal regions in the Mediterranean Sea (http://www.bo.ingv.it/mfstep/WP8/monthly). In the eastern mediterranean part of Morocco, Nador Lagoon is of great socio-economic importance to the surrounding region (Figure 1b). The surface of this lagoon is about 115 km^2 and its mean depth is 3-4 m, with a maximal depth in the center (6- 7m) (Figure 1c). Previous studies have focused on the hydrography, sedimentology and biological organization in

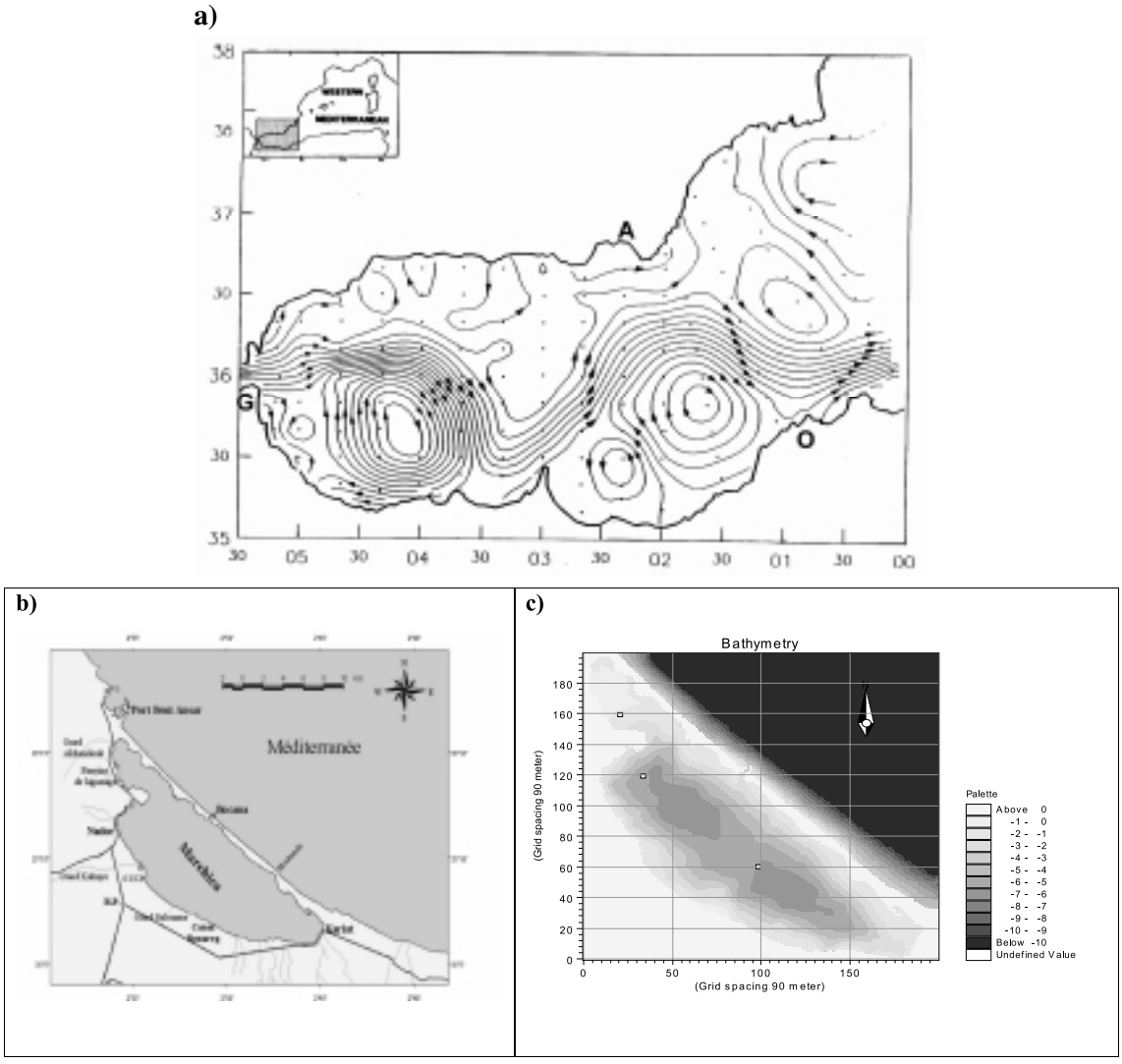

Fig. 1. **a)** The 10 dbar dynamic topography in the Alboran Sea derived from the 134 CTD profiles in September-October 1992 (*R/V Garcia del Cid*) shows the meandering front associated with the incoming jet of Atlantic water and the two big anticyclonic gyres. The reference level is 400 dbar (Font *et al*., 2002); **b)** Nador lagoon and its surrounding environment (from Boutaïeb and Madani, 2001) and **c)** its bathymetry and the location of currentmeters (•) inside the lagoon (Hilmi *et al.,* 2005).

the lagoon (Tesson, 1977; Brêthes and Tesson, 1978; Guelorget *et al*., 1987; Abouhala *et al*., 1995; Berraho *et al*., 1995; Lefebvre *et al*., 1997) and hydrodynamics studies are very few (Hilmi *et al*., 2005). This study aims to describe some aspects of the physical oceanography of Nador Lagoon and to characterize the circulation and the dispersion of Mediterranean water into the lagoon, using 47 days long recordings of wind, sea level and currents during spring 2001 and 3D models.

2. Material and methods

The models used in this study are the hydrodynamic (HD) and advection-dispersion (AD) modules of the integrated MIKE3 modeling system from DHI Water and Environment (DHI, 2000).The HD module simulates unsteady three dimensional flows, taking into account density variations, bathymetry and external forcing such as meteorology, tidal elevations, currents and other hydrographic conditions. The mathematical foundation includes the mass conservation equation, the Reynolds-averaged Navier-Stokes equations in three dimensions, including the effects of turbulence and variable density, together with the conservation equations for salinity and temperature (DHI, 2000). The Cartesian grid, developed for the lagoon, includes 200 cells in X (Eastern) and 200 cells in Y (Northern). Their horizontal dimensions are respectively 90m x 90m (Figure 1c). In the vertical dimension, the grid is divided into six layers of 1m thickness, except close to surface where the thickness is of 1.5 m. The advection-dispersion module was developed by Vested *et al*. (1992) and is normally used to determine the spreading of neutrally buoyant substances, such as organic compounds and heavy metals, in the marine environment. The HD model is forced at seaward side of the lagoon entrance by 47 days long sea level measurement (28 September to 16 November 2001) at Beni Ansar harbour (Figure 2b). Measurements from three currentmeters inside the lagoon (Figure 1c) are used to validate the model. Finally, hourly wind data (speed and direction), recorded by the National Meteorological Services (DMN) at Nador airport (approximately 15 km far away from the lagoon), are also used to force the 3D models (Hilmi *et al*., 2005).

3. Results

3.1. Wind

During spring 2001, predominant winds blow from the northwest and from the east (Figure 2a). Spectral analysis (Bendat and Piersol, 1986) reveals that they act from two to ten days in the low frequency band. Extreme atmospheric events, like storm surges acting at very high frequencies (less than 10h), have also been observed in sea level and current measurements during this period (Figure 2a).

3.2. Tides

Harmonical analysis of sea level (Pawlowicz *et al*., 2002) at Beni Ansar harbour (outside the lagoon) reveals that tides are mainly semi-diurnal (M2) (Table 1 and Figure 2). Their amplitude decreases from 13 cm outside the entrance channel to 3 cm inside the lagoon. Its relative phase is also retarded by about three hours as it enters the lagoon (Hilmi *et al*., 2005). This suggests that Nador Lagoon can be classified as a "choked" lagoon, by opposition to a "restricted" or "leaky" lagoon (Kjerfve and Magill, 1989).

Table 1. Harmonical analysis of sea level recorded at Beni Ansar harbour (Nador) from 28 September-15 November, 2001 (Hilmi *et al*., 2005).

Component	Frequency (cph)	Amplitude (m)	95% CI	Phase (Deg)	95% CI
O1	0.0387307	0.0215	0.005	123.25	12.66
K1	0.0417807	0.0219	0.005	141.13	14.68
N2	0.0789992	0.0266	0.003	47.19	5.77
M2	0.0805114	0.1300	0.003	68.33	1.31
S2	0.0833333	0.0459	0.002	87.26	3.18
K2	0.0835615	0.0125	0.003	109.66	14.18
M4	0.1610228	0.0145	0.003	177.57	10.75
MS4	0.1638447	0.0115	0.003	222.00	14.08

a)

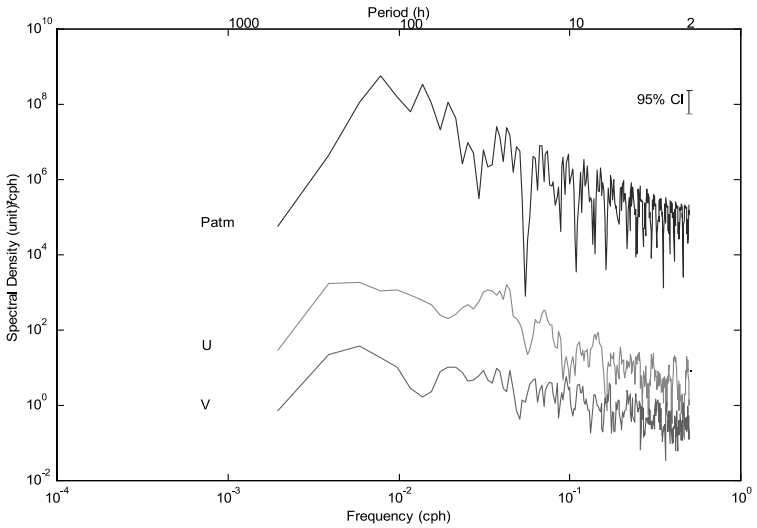

b)

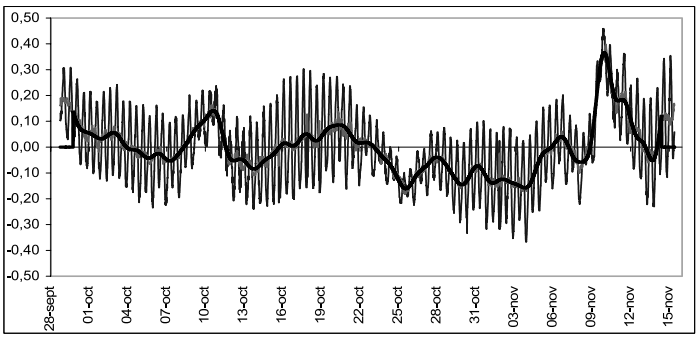

Fig. 2. **a)** Meteorological parameters (atmospheric pressure, U and V wind components) spectral analysis (right) from 28th September-15th November, 2001; the 95% CI is calculated for 8 degrees of freedom (Bendat and Piersol, 1986); **b)** Sea level recorded at Beni Ansar harbour and the low-pass filter, from 28th September-15th November, 2001 (Hilmi *et al*., 2005).

3.3. Circulation and advection of Mediterranean waters

Tidal gradients at the entrance set up tidal currents reaching about 1 m/s at the entrance which decrease progressively along the south/north shores of the lagoon. Inside the lagoon, they remain very weak relative to locally-wind induced currents (Figure 3a). Results of the hydrodynamic (HD) and advection-dispersion (AD) models are presented for two predominant and intense meteorological situations for the observed period (Hilmi *et al*., 2005). Figure 3a shows surface (0-1.5m) and bottom (4.5-5.5m) currents induced by northwesterly winds while Figure 3b shows the same information for easterly winds. In both cases, predominant winds produce down-wind coastal currents close to both the north and south shores of the lagoon and their speeds reach 0.1 to 0.2 m.s-1 at times. At the center of the lagoon, currents at the surface are weaker and are slightly deviated towards the south shore. As a result, downwelling occurs at the downwind end of the lagoon and upwelling at the up-wind end. Close to the bottom, currents are directed against the wind or up-wind. These three-dimensional wind-induced currents result from the balance between wind stress at the surface and pressure gradients set up by winds along the lagoon axis (Koutitonsky, 2004). Water renewal in the lagoon results from onshore (or off-shore) Ekman transports during nortwesterly (or easterly) winds outside the lagoon. Sea levels outside are set-up (set-down) and large volume fluxes at the entrance contribute to the water renewal inside the

lagoon. Therefore, water renewal in the lagoon occurs during extreme atmospheric events such as storms surges. Once inside the lagoon, Mediterranean waters are found to disperse mainly along the northern banks and they reach the lateral ends of the lagoon (Figure 3c).

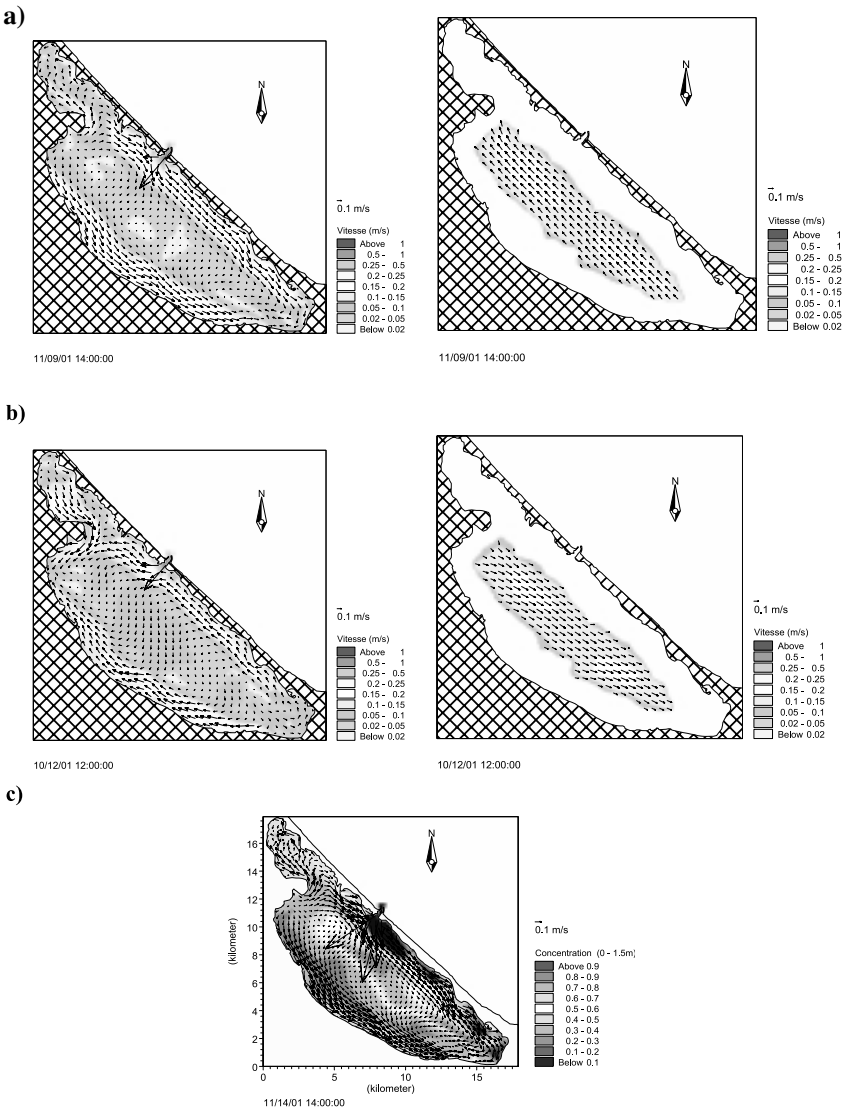

Fig. 3. Examples of surface and bottom circulation resulting from **a)** Northwestly wind (11/09 at 14:00); **b)** Easterly wind (10/12/01 at 12:00) and **c)** Dispersion of Mediterranean waters inside the lagoon (11/14 at 14:00 for example) (Hilmi *et al.*, 2005).

4. CONCLUSION

For several decades, Nador Lagoon has supported various fishing and aquaculture activities. A rational exploitation of these ressources, their protection against harmful effects of increasing urbanization and associated marine pollution requires the implementation of an integrated management plan. In turn, such a plan requires scientific results from various disciplines. The Mediterranean sea is a surrounded by land and the coastal influence should be taken into consideration when investigating mesoscale processes (Gorsky *et al*., 2002). Therefore, a coastal shelf model coupling with HD/AD models is needed to be developed in Nador area. The outstanding question is the mechanism(s) by which variations in the physical dynamics at the mesocale (and sub-mesoscale) translate into variabily in biological processes.

Acknowledgments

The authors thank V. Koutitonsky (ISMER, Canada) and A. Srour from Centre Régional de l'INRH à Nador and A. Abouhala from MAROST (Atalayoune-Nador) and their staff for their contributing help during the 2001 campaign. They also thank M.M.Y. Azaoui, R. Boutaïeb, S. Charib, M. Hassoune and Z. Massik from INRH for their contributing work during this campaign. The 3D circulation study of Nador Lagoon was carried out within the framework of research activities of the Oceanography Department of INRH (Morocco) and a collaborative research agreement with ISMER (Canada).

Extrapolating baroclinic signals from surface data to deeper layers: application to different datasets

Bruno Buongiorno Nardelli

Istituto di Scienze dell'Atmosfera e del Clima, Sezione di Roma, CNR, Roma, Italy

ABSTRACT

A short discussion on the problem of extrapolating vertical profiles from surface and integrated measurements is presented. Two new statistical methodologies to reconstruct the profiles of temperature, steric heights and/or salinity are briefly introduced and some examples of their application are shown. A simple extension of these techniques to infer the chlorophyll concentration along the water column from satellite data is also presented.

1. MOTIVATION AND BACKGROUND

In the last twenty years, different methods have been developed to infer the vertical structure of the sea from surface and/or integrated measurements through remotely sensed and/or inverted echo sounders (IES) data. All of them aim at improving our understanding of the ocean dynamics, from large to mesoscale processes, and at getting better forecasts through data assimilation in operational models. These studies take advantage of the high accuracy measurements of sea surface elevation obtained by satellite altimeters as Topex/Poseidon, ERS-1/-2, Jason and Envisat, and of the round trip acoustic travel time with moored IES.

Actually, many approaches are based on the statistical or empirical analysis of the observed data (e.g. Hurlburt, 1984; Thacker and Long, 1988; Hurlburt *et al*., 1990; Carnes *et al*., 1990; Carnes *et al*., 1994; Gavart and De Mey, 1997; Pascual and Gomis, 2003; Buongiorno Nardelli and Santoleri, 2004, 2005; Meinen and Watts, 2000; Watts *et al*., 2001; Mitchell *et al*., 2004), while more complicated schemes assimilate the observations into realistic numerical models (e.g. Fukumori *et al*., 1993; Chin *et al*., 2002; Vossepoel *et al*., 2002; Parent *et al*., 2003).

In practice, observational methods are often very similar to simple assimilation schemes (such as optimal interpolation), where the first guess (i.e. the 'background' analysis) is given by an average of the observations instead of being estimated with a numerical model. The error associated to this background is exactly the signal we want to determine, and the background error covariance, in turn, is the observed covariance. Most of the vertical profiles extrapolation statistical methods are effectively based on the analysis of the covariance and of the principal modes associated to a set of profiles. However, it has been found that the accuracy of the techniques depends significantly on the variables included in the state vector and on the degrees of freedom that are absorbed by the method (e.g. Buongiorno Nardelli and Santoleri, 2005). Different performances have also been found, depending on the observations and on the dynamics of the area studied, or, from the other way round, on the validity of the stationarity hypothesis and accuracy of the estimated mean field and covariance of the signal.

Quite basic techniques correlate each parameter sub-surface values to surface and integrated parameters, without separating the different modes that drive the observed variability (e.g. Guinehut *et al*., 2004). At one step further, univariate methods as the single Empirical Orthogonal Function Reconstruction (sEOF-R) proposed by Carnes *et al*. (1994) separately analyze the covariance of each hydrographic parameter time series, and hypothesize a nonlinear relation between the amplitude of EOF modes and a combination of surface parameters (obviously including the steric height). These techniques, applied to DYFAMED and HOT time series led only to slight improvements (if any was found) with respect to climatological (monthly) estimates (Buongiorno Nardelli and Santoleri, 2004).

2. NEW METHODOLOGIES

Recently proposed Coupled Pattern Reconstruction (CPR) and multivariate Empirical Orthogonal Function Reconstruction (mEOF-R) directly couple steric height, temperature and/or salinity profiles (Buongiorno Nardelli and Santoleri, 2004). The methods are based on the coupled pattern/multivariate EOF decomposition of the two/three parameters' vertical profiles present in a learning dataset, and on the assumption that only few modes are needed to explain most of the covariance of the fields. The stationarity of the statistics of the parameters is also assumed. With these assumptions, limiting the expansions to the first two/three modes, the vertical profiles can be extrapolated from any independent measurement of the surface values solving a simple algebraic linear system. In practice, these techniques differ little from a simplified reduced-space multivariate Optimal Interpolation (OI) scheme, mainly for the fact that they assume the surface inputs to be fully uncorrelated and the observations used to train the model to be error-free (an interesting discussion about OI is found in Kaplan *et al*. (2003). The true novelty of CPR and mEOF-R methods, however, is the choice of the state vector used to characterize the covariance of the system. In fact, they include a proxy of the geopotential streamfunction at each pressure level (the whole steric height profile). In this way, they search a relation between the variability of the conservative water properties and the dynamics. In fact, it must be noted that, while EOF decomposition is just a statistical technique not necessarily tied to dynamical processes, it may also be able to identify and discriminate physically meaningful processes (e.g. Buongiorno Nardelli and Santoleri, 2005).

Compared to other univariate and empirical techniques (such as the Gravest Empirical Mode determination), mEOF-R and CPR generally give reliable estimates even when introducing errors in the surface input and also training the methods from limited datasets (Buongiorno Nardelli and Santoleri, 2004, 2005). However, CPR seems not adequate if both (uncorrelated) salinity and temperature variations lead to significant steric signals. On the other hand, mEOF-R assumes that the sea surface salinity can be used as an additional input. The two techniques have been first applied to time series of *in situ* measurements at fixed locations, and successively tested in an area of fundamental importance for the Mediterranean Sea dynamics as the Sicily Channel (Cavalieri *et al*., 2005). This last task implied the extension of the methods to a 3D problem. This was done computing the 'multi'-covariance with respect to a space-time average of all available profiles, meaning that a single 'background profile' (per parameter) and a unique set of mEOF modes for the whole area have been considered. Hindcast analyses of the CPR and mEOF-R performances demonstrated that the information on the salinity is fundamental to get reasonable estimates, and consequently only the mEOF-R method was effectively applied to altimeter data, using MEDATLAS data as training dataset, and SYMPLEX surveys measurements (that include CTD profiles along a T/P track simultaneous to the satellite pass) as hydrological surface input and validation profiles.

3. INFORMATION EXTRACTION FROM ALTIMETER DATA

All the methodologies cited are based on an estimate of the steric elevation from *in situ* data (equivalently called steric or dynamic height). This estimate is limited to the upper layers baroclinic contributions, while altimeters measure also the variation associated to barotropic signals and to residual deep steric variations. As a matter of fact, sea level variations are caused by the volume (steric) variations, due to the heat and salt exchanges between the atmosphere and ocean and to the internal ocean dynamics (baroclinic signals), and by the variation of the total

mass (eustatic change) associated to barotropic signals, such as tidal currents, atmospheric pressure load adjustments, barotropic wave propagation, etc.

As most of the tidal contribution can be filtered with a proper processing, and an isostatic inverse barometer correction can sort out the response to atmospheric pressure variations, the residual altimeter signal is mainly a measure of the volume occupied by the water column plus a generally low residual barotropic contribution. However, altimeter measurements are referred to the reference ellipsoid which does not coincide with the geopotential surface (geoid). The geoid slope contamination is thus filtered out averaging over a sufficiently long time period. Nevertheless, Sea Level Anomalies (SLA) obviously neglect both the baroclinic and barotropic mean component of the flow.

These considerations must be taken into account when applying any reconstruction method to altimeter data, as the methods are not necessarily trained with anomalies, and in general they need an absolute level estimate. Consequently, we also quantified the impact of the adjustment of altimeter data with a synthetic mean dynamic topography computed from drifter and altimeter data (Rio *et al*., 2004) in the extrapolation of the geostrophic velocity transects along a TP track crossing the Sicily Channel (Figure 1). In this context, the Sicily Channel represents a perfect test area, as it is characterized by an intense mesoscale activity (relatively to the Mediterranean Sea), but also by a strong mean current system associated to the exchange of surface and intermediate waters between the western and eastern Mediterranean basins. In fact, as a consequence of numerous oceanographic surveys, the Channel of Sicily general circulation and hydrology are relatively well known. Moreover, some studies on the upper layer circulation have been conducted also through a combined analysis of infrared and/or altimeter satellite data and *in situ* measurements (Buongiorno Nardelli *et al*., 1999). The results of the reconstruction of a geostrophic velocity transect from Topex/Poseidon data are presented in Figure 1.

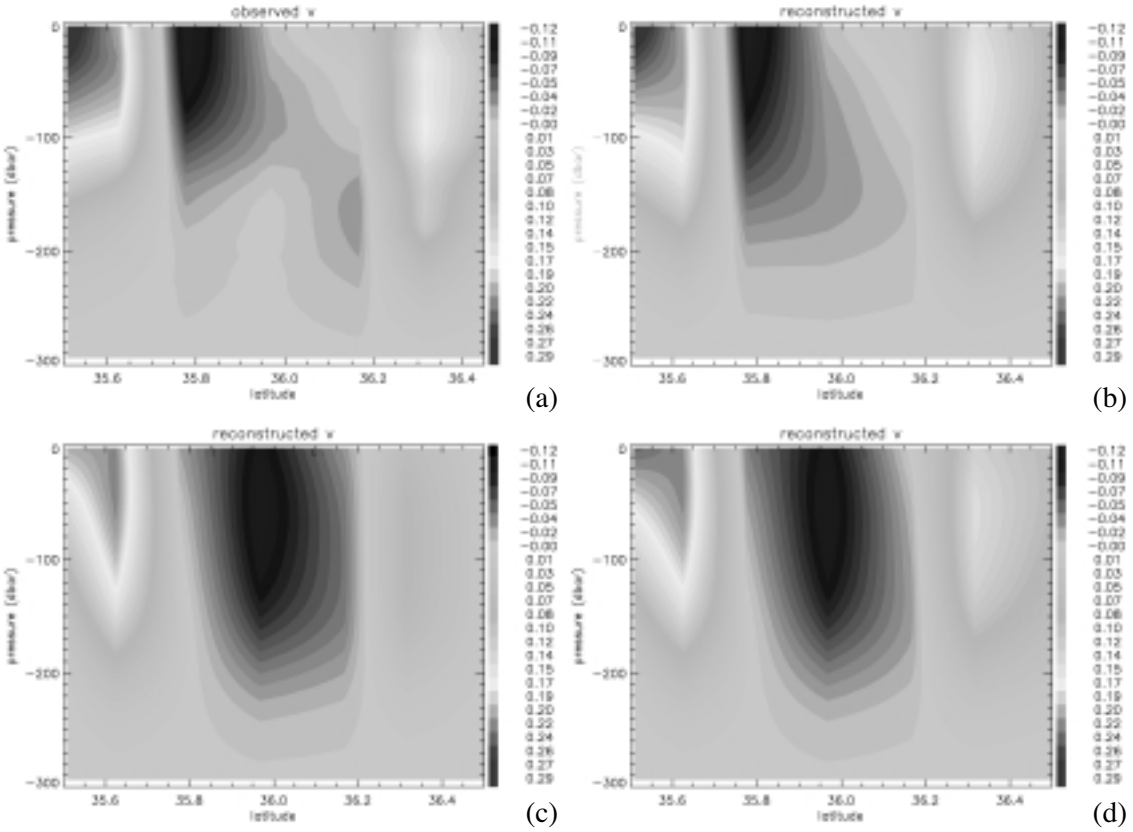

Fig. 1. (**a**) Geostrophic velocity (m/s) section along the Topex Poseidon track 059 (on April 16th 1996) computed from CTD data using a no-motion level of 300 dbar. (**b**) Velocity section along the same transect, applying the mEOF-R method to *in situ* surface T, S and SH data. (**c**)Velocity section reconstructed applying the mEOF-R method to *in situ* surface temperature and salinity data and SLA. (**d**) Section reconstructed applying the same method to *in situ* surface temperature and salinity data and SL.

4. APPLICATION TO CHLOROPHYLL

A slightly modified mEOF-R method aiming at extrapolating chlorophyll-a profiles from ocean colour measurements has also been developed. In the discussion presented here, only the temperature (T), steric height (SH) and chlorophyll-a (Chl) profiles are considered, even if the method can clearly be extended to include also salinity. The *learning* series of the three parameters (after normalization) are decomposed through the mEOF:

$$\begin{aligned} T(z,t) &= \sum_{k=1}^{n} a_k(t) L_k(z) \\ SH(z,t) &= \sum_{k=1}^{n} a_k(t) M_k(z) \\ Chl(z,t) &= \sum_{k=1}^{n} a_k(t) N_k(z) \end{aligned} \tag{4.1}$$

where a_k represent the amplitudes of the modes (indicated with L_k, M_k, N_k)

The modified technique assumes that, besides the surface steric elevation and the surface temperature, also the chlorophyll integrated to the first optical depth (which is the equivalent of what observed by the satellite) and the penetration depth of the sunlight (that can also be estimated from satellite data) are known. Actually, the concentration of chlorophyll measured by a satellite sensor can be computed from *in situ* data as the integral (Gordon and Clark, 1980):

$$C_{sat} = \frac{\int_0^{z_{pd}} Chl(z) e^{-2kz} dz}{\int_0^{z_{pd}} e^{-2kz} dz} \tag{4.2}$$

where k is the attenuation coefficient of light, $Chl(z)$ is the *in situ* chlorophyll-a profile, z_{pd} is the sunlight penetration depth ($z_{pd}=1/k$). The penetration depth z_{pd} can be estimated as $z_e/4.6$, where z_e is the depth of the euphotic zone. This last is defined as the depth where the PAR (Photosynthetic Available Radiation) is reduced to 1% of its surface value (Gordon and McCluney, 1975).

z_e can be computed through recursive methods from the *in situ* profiles of chlorophyll concentration or through statistical regressions when only satellite measurements of C_{sat} are available (Morel and Berthon, 1989). Truncating the series (4.1) to the first three terms, and assuming known C_{sat} and z_{pd}, a simple linear system is found (4.3), that can be easily solved to obtain the amplitude of the first three modes (a_1, a_2 and a_3), and, in turn, the vertical profiles of chlorophyll concentration:

$$\begin{cases} a_1(t)L_1(0) + a_2(t)L_2(0) + a_3(t)L_3(0) = T(0,t) \\ a_1(t)M_1(0) + a_2(t)M_2(0) + a_3(t)M_3(0) = SH(0,t) \\ a_1(t)\int_0^{z_{pd}} N_1(z)e^{-2kz}dz + a_2(t)\int_0^{z_{pd}} N_2(z)e^{-2kz}dz + a_3(t)\int_0^{z_{pd}} N_3(z)e^{-2kz}dz = \int_0^{z_{pd}} Chl(z,t)e^{-2kz}dz \end{cases} \tag{4.3}$$

5. CONCLUSIONS

Different approaches can be followed to extract as much information as possible from sea surface and vertically integrated measurements, potentially allowing infer vertical profiles from sea surface level or acoustic round trip travel time measurements coupled to other remotely sensed data. Among these, data assimilation in numerical models is obviously crucial in order to obtain accurate analyses and forecasts, but its results are also strongly dependent on the models' assumptions and characteristics. On the other hand, the approach explored here, namely the direct analysis of the sole observations and of their covariances, can help to identify what is the real information content of the data, how this can be extracted more efficiently, and also what measurements are needed operatively to optimize an observational network. The most relevant results of these analyses are summarized below.

First of all, the addition of a proxy of the geostrophic streamfunction profile in the state vector describing the system improved the estimates obtained through multivariate vertical reconstruction methods as the CPR and mEOF-R, when applied to different test datasets (Buongiorno Nardelli and Santoleri, 2004). In many cases, however, all methods (including residual GEM and sEOF-R) failed to give reliable results using only SST and surface steric heights as input, as salinity variations not directly correlated to temperature can significantly contribute to observed baroclinic signals and related sea level variations. Surface salinity thus appears as a crucial parameter, and its extended measurement through Voluntary Observing Ships programs such as FerryBox, or including conductivity sensors on surface drifters, should be strongly encouraged and supported, also considering their potential in the calibration/validation of future satellite missions as SMOS (Soil Moisture and Ocean Salinity), scheduled for launch by ESA in early 2006, and Aquarius/SAC-D, that has been recently approved for launch by NASA.

The use of Lagrangian autonomous instruments to sample the mesoscale circulation in the Mediterranean Sea

P.M. Poulain

Istituto Nazionale di Oceanografia e di Geofisica Sperimentale (OGS), Sgonico (Trieste), Italy

ABSTRACT

The use of Lagrangian autonomous instruments, such as satellite-tracked drifters and profiling floats, to study the mesoscale variability of the Mediterranean circulation is reviewed. Examples are given for the near-surface circulation in the Adriatic and southern Ionian Seas. The MEDARGO global Mediterranean profiling float program is also presented.

Key-words: Drifters, subsurface floats, Mediterranean Sea

INTRODUCTION

As part of various international and national programs, satellite-tracked drifters have been released in the Mediterranean Sea since the 1980s to monitor near-surface currents and sea surface temperature (SST). These drifter data have been processed (data reduction, editing, interpolation and filtering) and archived in a common database (Poulain *et al*., 2004) to allow studying the basin-scale and mesoscale dynamics in various basins and sub-basins of the Mediterranean with high-quality and copious Lagrangian data.

Satellite-tracked profiling floats have been used from the late 1990s to measure profiles of water properties (temperature and salinity, TS) throughout the Mediterranean. In particular, in the framework of the EU-sponsored MFS/MEDARGO project (Pinardi *et al*., 2003), profiling floats have been deployed starting in late summer 2004 to provide TS data in near-real time to forecasting models of the Mediterranean.

NEAR-SURFACE MEDITERRANEAN CIRCULATION DERIVED FROM DRIFTERS

Most of the drifters operated in the Mediterranean are CODE designs (Figure 1) manufactured by Technocean, Cape Coral,

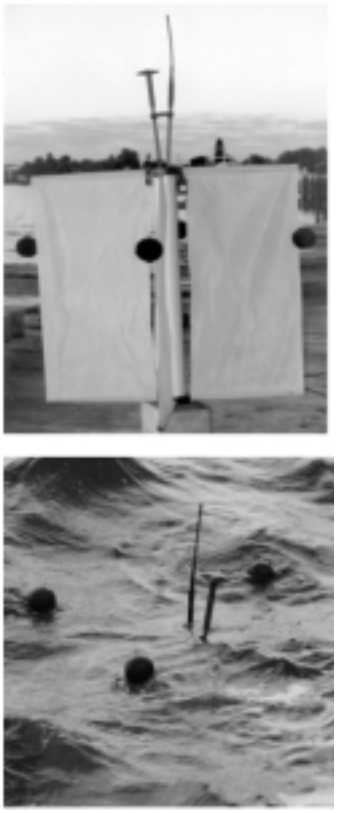

Fig. 1. (Top) Photograph of a CODE drifter showing the GPS (left) and Argos (right) antennas at the top, and the main structure of the drifter with 1-m height sails. (Bottom) CODE drifter floating at the sea surface.

Florida, USA. They consist of a slender, vertical, 1-m-long negatively buoyant tube with four drag-producing vanes extending radially from the tube over its entire length and four small spherical surface floats attached to the upper extremities of the vanes to provide buoyancy (Poulain, 1999). All drifters were tracked by the Argos Data Location and Collection System (DCLS) carried by the NOAA polar-orbiting satellites.

The drifter data spanning 1986-1999 have been used to compute maps of pseudo-Eulerian statistics, that is, maps of mean circulation and of variance ellipses (Figure 2). Energetic currents are mainly found in the Algerian Current, in the vicinity of the Strait of Sicilya (in the Atlantic Ionian Stream, and its extension in the northern Ionian), and in some areas of the Levantine basin (e.g., near Rhodes and Ierapetra Gyres). The circulation dynamics in the Adriatic Sea and in the Strait of Sicily, the two regions with the highest data density, is well resolved by the drifters.

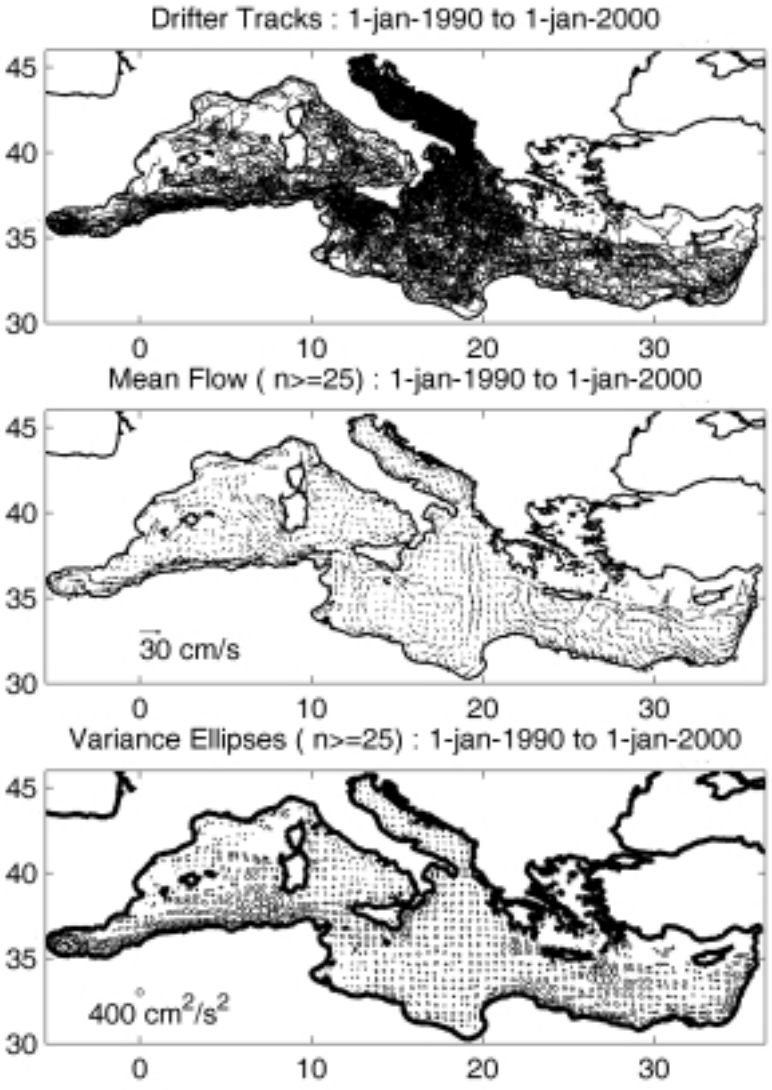

Fig. 2. Pseudo-Eulerian statistics computed from the drifter data spanning 1986-1999 in the Mediterranean Sea using 40-km radius bins: 6-hourly drifter positions (top), mean circulation (middle) and velocity variance ellipses (bottom).

Drifter data are also used in concert with satellite images to describe the spatial structure and temporal evolution of the mesoscale circulation and associated TS distribution. Ocean color (chlorophyll concentration from SeaWiFS and MODIS) and infrared (SST from AVHRR) are usually very useful to track mesoscale features (Mauri and Poulain, 2001). Drifter tracks overlaid on the images provide information of the velocity of the water masses. An example is shown in Figure 3 in the northern Adriatic Sea.

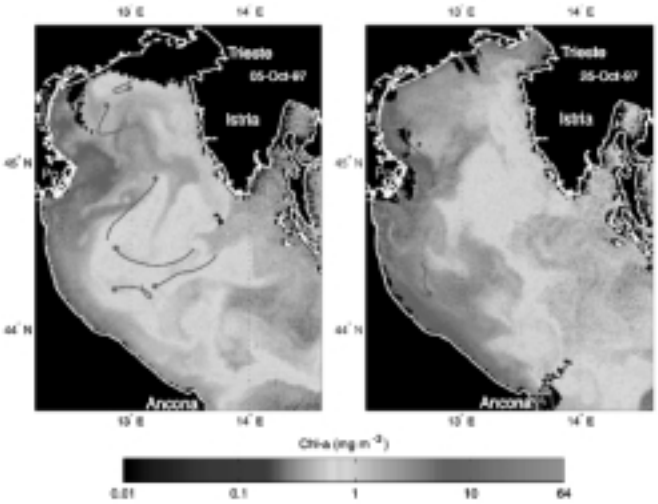

Fig. 3. SeaWiFS images of surface chlorophyll-a concentration for 5 October (left) and 25 October (right) 1997. Drifter trajectories are superimposed in green for a period of three days preceding the satellite pass. The "worm head" represents the drifter location at the time of the image.

SUB-SURFACE CURRENTS AND TEMPERATURE-SALINITY PROFILES FROM MEDARGO FLOATS

Two types of profiling floats were operated, one called APEX (manufactured by Webb Research Corporation, USA) the other one PROVOR (produced by Martec, France). The APEX is the successor of the ALACE (Davis *et al*., 1992) whereas the PROVOR is based on the MARVOR technology (Loaec *et al*., 1998). All floats were equipped with Sea-Bird CTD sensors (model 41 pumped MicroCAT). They were programmed in the "Park and Profile" configuration with a total cycle length of five days, a neutral parking depth of 350 m (near the salinity maximum of the Levantine Intermediate Water - LIW) and a maximum profiling depth of 700 m (2000 m every ten cycles, Figure 4). When at surface, the floats are located by, and transmit data to, the Argos system onboard the NOAA satellites. The data are processed and archived in near-real time at the CORIOLIS Data Center (IFREMER, Brest, France) and are disseminated on the GTS following the standards of the international ARGO program.

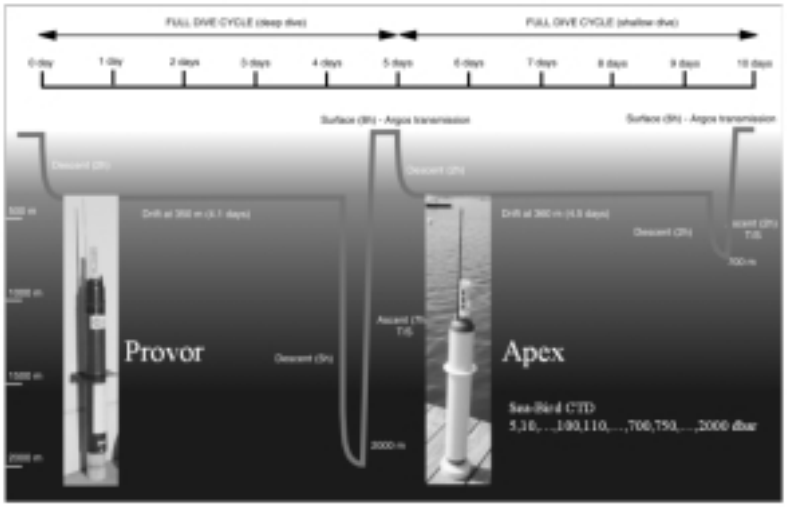

Fig. 4. Cycling and sampling characteristics of the MEDARGO floats.

The MEDARGO floats were deployed from VOS ships and research vessels starting in late June 2004. As of April 2005, fourteen MEDARGO floats were operational, providing TS profiles in most areas of the Mediterranean. The tracks (and positions on 22 April 2005) of the MEDARGO and other (U.S. Navy, Spain-Argo, Greece) floats are shown in Figure 5 in a map downloaded from the CORIOLIS web site.

Fig. 5. Tracks and position on 22 April 2005 of the MEDARGO, U.S. Navy, Spain-Argo and Greek profiling floats, as downloaded from the CORIOLIS web site.

The TS seasonality and mesoscale variability along a float track in the Algerian Current system are depicted in Figure 6. The cooling and erosion of the thermocline are evident in the fall, before the water column becomes thermally homogeneous in the winter and early spring. Structures are striking in the salinity contour plot with a time scale of about one month. They most likely correspond to instability features of the Algerian Current and related vortices (Millot, 1999; Salas *et al*., 2001).

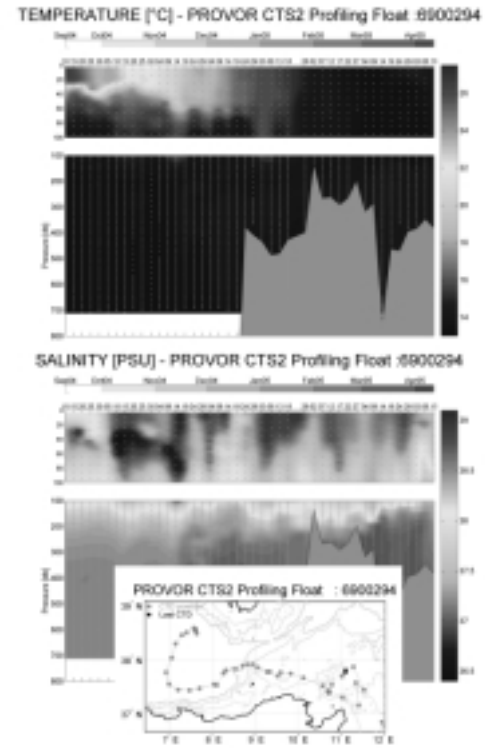

Fig. 6. Contour plots of temperature (top) and salinity (bottom) following a PROVOR float in the Algerian Current between September 2004 and April 2005.

Examples of TS profiles are shown in Figure 7, together with MEDAR/MEDATLAS II annual climatology for the Tyrrhenian and south Ionian Seas. The TS observations are significantly larger than the climatology values in the Western Mediterranean. In contrast, this trend is not apparent in the Eastern Mediterranean.

The float displacements at their neutral depths, near 350 m depth, are used to map the sub-surface currents and provide information on the main pathways of the LIW in the Mediterranean.

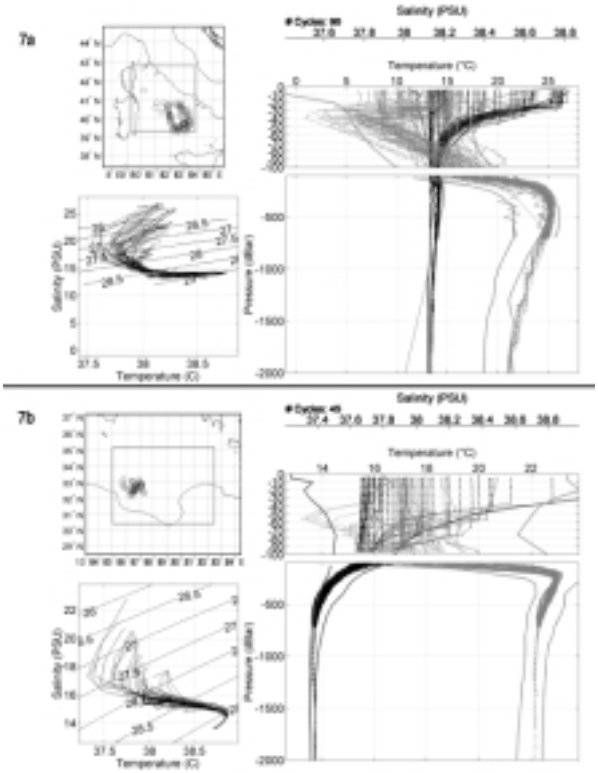

Fig. 7a) and b). TS profiles and diagrams from the MEDARGO floats in the Tyrrhenian (top) and southern Ionian (bottom) Seas. The annual MEDAR MEDATLAS II climatology ranges (mean ± three standard deviations) are depicted on the left side of the Figures with dark (temperature) and grey (salinity)

Merging multiple satellite altimetric missions to monitor the mesoscale circulation in the Mediterranean Sea

Ananda Pascual, Gilles Larnicol and Pierre-Yves Le Traon

CLS, Space Oceanography Division, Toulouse, France

ABSTRACT

Two years of four satellite altimeter missions [Jason-1, ERS-2/ENVISAT, TOPEX/POSEIDON interleaved with Jason-1 (T/P) and Geosat Follow-On (GFO)] are intercalibrated and merged in an objective analysis scheme with the aim of improving the estimation of mesoscale surface ocean circulation in the Mediterranean Sea.

1. INTRODUCTION

Satellite altimetry is a useful tool as it provides surface dynamic topography measurements, which constitute a strong constraint to estimate and forecast the three-dimensional ocean state through data assimilation. One requirement for satellite altimetry is that at least two altimeter missions are needed to resolve the main space and time scales of the ocean (Koblinsky *et al*., 1992). For instance, in the Mediterranean, the combination of T/P + ERS-1/2 has allowed a characterization of the major changes in the Mediterranean Sea level variability for the 1993-1999 period (Larnicol *et al*., 2002). However, several theoretical studies (e.g. Le Traon and Dibarboure, 1999) found that a combination of three satellites can actually provide an important reduction of the velocity mean mapping error with respect to one or two satellites at the mesoscale. But these papers were based on simulated data, not on real data.

Fortunately, since mid-September 2002, four altimetric missions have been flying simultaneously providing complementary data with an increased spatial and temporal resolution: Jason-1, ERS-2 (replaced by ENVISAT after June 2003), Geosat Follow-On (GFO) and TOPEX/POSEIDON interlaced (T/P). In fact, in September 2002 the orbit of T/P was modified in such a way that it now flies between two adjacent Jason-1 ground-tracks. This has resulted in a track separation which is half that of the T/P mission, offering a much improved sampling for the study of mesoscale variability.

In this work we present results of merging real data in the Mediterranean Sea from these four altimeters, with the aim of obtaining high resolution maps capable of monitoring the mesoscale variability. We use two complete years of data (from October 2002 to October 2004). For that purpose, the ENVISAT mission has been intercalibrated to be included in the data set replacing ERS-2 after June 2003. On the other hand, several new geophysical corrections have been applied to the altimetric data in order to improve the sea level anomalies (SLA) along track estimations. Furthermore, some comparisons with CTD data coming from an intensive oceanographic cruise have been performed.

2. Datasets and Data Processing

Two years of Jason-1, ERS-2/ENVISAT, Topex/Poseidon interleaved (T/P) and Geosat Follow-On (GFO) delayed time data are used for this study. The data span from the beginning of the T/P inverleaved mission (October 2002) to October 2004. ERS-2 is used since October 2002 until June 2003, when it is replaced by ENVISAT.

For all datasets, the best geophysical corrections available at the moment (April 2005) have been applied (wet and dry tropospheric, ionospheric, electromagnetic, the FES-2004 tides, and MOG2D to correct the ocean response to short-period atmospheric forcing including pressure and wind effects). The major improvement, regarding the corrections for the Mediterranean is with no doubt the inclusion of the MOG2D model (Carrere and Lyard, 2003) replacing the inverted barometer correction which is classically unsatisfactory especially for semi-closed basins like the Mediterranean. To extract the SLA for the different missions, a mean profile <SSH> from the individual SSH measurements (SLA=SSH - <SSH>) has been removed.

SLA maps combining different altimeter missions (Jason-1, Jason-1+ERS-2, Jason-1+ERS-2+T/P, Jason-1+ERS-2+T/P+GFO) and covering the entire Mediterranean Sea are produced every week on a regular 1/8° grid using a suboptimal space/time objective analysis (Bretherton *et al*., 1976). The method takes into account the long wavelength correlated errors (Le Traon and Ogor, 1998) that remain from the orbit errors and from the atmospheric pressure effects (e.g. large-scale high-frequency barotropic signals). For more details on the specific processing in the Mediterranean, (Pascual *et al*., 2005).

3. Results

In this study we will analyse the following configurations (Figure 1):

a) One altimeter (C1): Jason-1;

b) Two altimeters (C2):
Jason-1 + ERS-2/ENVISAT;

c) Three altimeters (C3):
Jason-1 + ERS-2/ENVISAT + T/P;

d) Four altimeters (C4):
Jason-1 + ERS-2/ENVISAT + T/P + GFO.

The reason for the selection of these configurations is somehow historical. The first altimetric studies in the Mediterranean used T/P (same orbit as Jason-1) or ERS-1 data independently (Larnicol *et al*., 1995; Vignudelli, 1997a; Iudicone *et al*., 1998). Posterior works combined T/P and ERS-2 (Vignudelli, 1997b; Ayoub *et al*., 1998; Larnicol *et al*., 2002). No study before Pascual *et al*. (2005) has analyzed either the three or four altimeter configurations specifically in the Mediterranean.

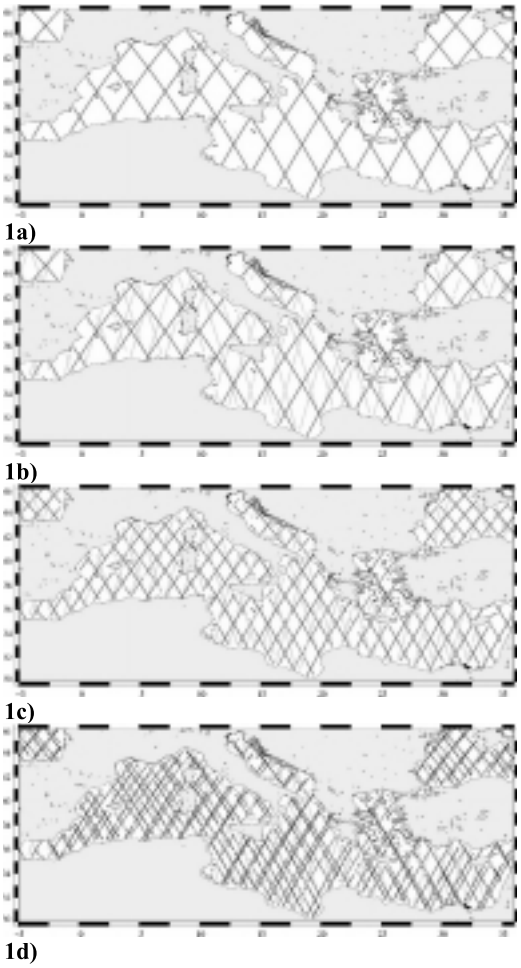

Fig. 1. The study area (the Mediterranean Sea) with the different satellite configurations considered in this work: **a)** Jason-1 (C1), **b)** Jason-1 + ERS-2/ENVISAT (C2), **c)** Jason-1 + ERS-2/ENVISAT + T/P (C3), **d)** Jason-1 + ERS-2/ENVISAT + T/P + GFO (C4). [Jason-1 is in red, ERS-2/ENVISAT is in green, T/P is in purple and GFO is in blue]. The figure shows all the along-track data that are taken into account to compute a gridded SLA field of a particular day (12 November 2002) for the different altimeter configurations.

An interesting variable for monitoring the mesoscale is the Eddy Kinetic Energy (EKE), which is a measure of the degree of variability and may identify regions with highly variable phenomena such as eddies, current meanders, fronts or filaments. Figure 2 shows the mean EKE (i.e. $\frac{1}{2}(u^2+v^2)$, where u and v are the zonal and meridional velocities computed through finite differences from SLA) averaged over two years (October 2002 - October 2004) for the different altimeter configurations analyzed in this paper, putting in evidence the impact of merging several missions. Jason-1 alone (Figure 2a) depicts some areas of intense variability such as in the Alboran Sea (associated with the Western Alboran Gyre), the southern Tyrrhenian eddy, some in the Algerian basin and very clearly the Ierapetra eddy. However it is evident that the intense signals are only located along the Jason-1 tracks and that the sampling is unsatisfactory.

A clear improvement is obtained with the mean EKE for Jason-1+ERS-2/ENVISAT configuration (Figure 2b). In essence, there is a more clear continuity in all the features of EKE. However, Figure 2b still presents some deficiencies. For instance, along the Libyan coast, just south of Ierapetra, there is a gap in an energetic area identified as the Mersa-Matruth gyre. The combination of three satellites (Jason-1+ERS-2+T/P, Figure 2c) confirms that this area (between 26°E and 27.5°E) is characterized by an intense variability. Some energy is also added in the Alboran Sea, Algerian basin (between 6°E and 8°E), and an eddy in the Central Ionian, as well as the signature of the Shikmona gyre.

Finally, the differences between three- and four- altimeters configurations are not very large but not negligible. Essentially, the fourth altimeter (GFO) contributes to the intensification of all the structures. In average, the merged Jason-1 + ERS-2 + T/P + GFO maps yield EKE levels 15% higher than Jason-1 + ERS-2 (Pascual *et al.*, 2005).

The combination of several altimeters has not introduced noise in areas of low variability, such as the North-Western Mediterranean where the variability remains weak for all the configurations. On the contrary, the EKE has been only gained in zones that are known to be energetic, suggesting that the merging has been successful.

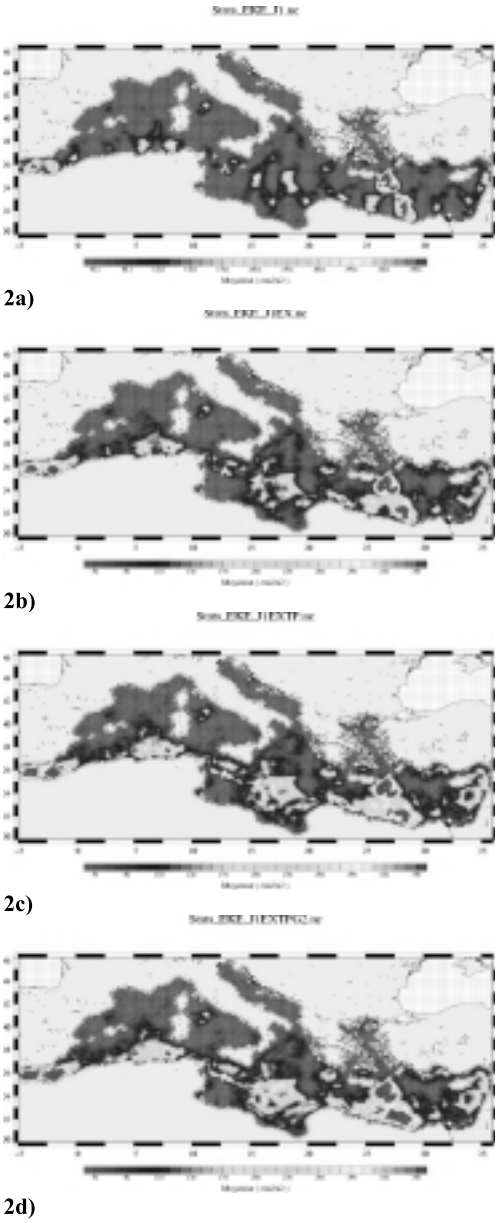

2a)

2b)

2c)

2d)

Fig. 2. Mean EKE averaged over the period of study (October 2002- October 2004) for the different satellite configurations as marked in Figure 1. Units are cm^2/s^3.

A validation with independent altimetric data (Pascual *et al*., 2005) shows that, with the combination of three altimeters, in regions of large mesoscale variability the sea level and velocity can be mapped with a relative accuracy of about 6% and 23%, respectively. This is a factor of 2.2 less than the results derived from Jason-1 alone, and a factor of about 1.5 less than the results obtained from Jason-1 + ERS-2. Furthermore, the consistency between altimetry and Sea Surface Temperature, drifting buoys and tide gauges, is significantly improved when four satellites are merged compared to the results derived from the two satellites configuration (not shown, Pascual *et al*., 2005).

Satellite altimetry can also be compared with *in situ* CTD data. For instance, we present here a case of a migration of the Western Alboran Gyre. The BIOMEGA oceanographic cruise (Figure 3a), that took place from 9 to 17 October 2003, reported the first field evidences of such migration, since the Western Alboran Gyre was located about 100 km to the east of its usual position (Figure 3b and in Flexas *et al*., 2005). The SLA field simultaneous to the cruise and obtained with the combination of four altimeters (Figure 3c) is in good agreement with the dynamic height field at surface (computed with a reference level of 300 m), which shows again that four altimetric missions are useful to detect and monitor anomalous mesoscale features.

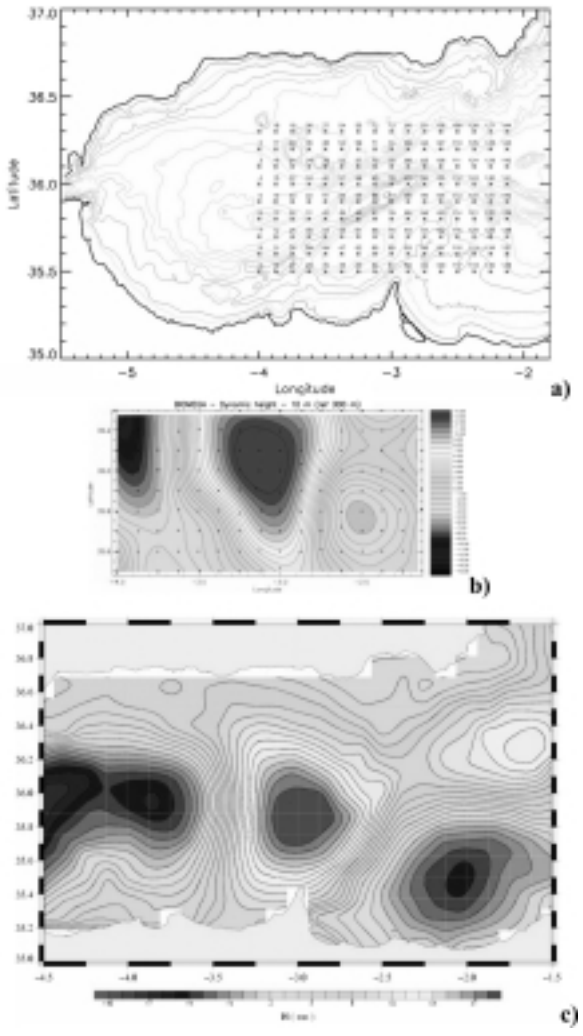

Fig. 3. **a)** CTD stations positions carried out during the BIOMEGA cruise in the Alboran Sea. **b)** Surface dynamic height field obtained from the BIOMEGA cruise (9-17 October 2003), with a reference level of 300 m. **c)** SLA from the four altimeters configuration on 15 October 2003.

4. CONCLUSIONS AND RECOMMENDATIONS

Based on the results presented here, at the very least two, but preferably three or even four altimeters, are needed for a correct monitoring of the mesoscale circulation in the Mediterranean Sea. Our results are in good agreement with those obtained in theoretical studies (Le Traon and Dibarboure, 1999; Le Traon *et al*., 2001; Le Traon and Dibarboure, 2002) in the sense that the contribution of a third and a fourth altimeter is less critical than just a second one. However, we have shown that in the Mediterranean the impact of the third and fourth altimeters would be higher than in other parts of the ocean, probably due to the typical size of the structures that are not correctly sampled by the Jason-1 + ENVISAT configuration.

Unfortunately, the future of satellite altimetry is uncertain. At the moment, only one altimeter mission (Jason-2) is planned and approved to ensure the continuity of the actual altimeter configuration. Therefore, the most urgent requirements are:

1. to fly a post ENVISAT altimeter mission;
2. to have a high resolution altimeter system consisting of a constellation of three optimized altimeters in addition to the Jason series. In a long term, the concept of swath altimetry should be explored, which is an attractive possibility for improving the spatial/temporal coverage but a demonstration of its capabilities prior to enter into an operational status is required.

The Atlantic water mesoscale hydrodynamics in the Levantine Basin

George Zodiatis[1], Panos Drakopoulos[2], Isaac Gertman[3], Steve Brenner[4] and Daniel Hayes[1]

[1] *Oceanography Centre, University of Cyprus, Nicosia, Cyprus*
[2] *Technological Educational Institute of Athens, Greece*
[3] *Israel Oceanographic and Limnological Research, Haifa, Israel*
[4] *Department of Geography, Bar Ilan University, Ramat Gan, Israel*

ABSTRACT

The spatial and temporal variability of the Atlantic Water (AW) and the mid-Mediterranean jet (MMJ) in the Eastern Mediterranean Levantine basin is investigated using *in-situ* data sets collected between 1995 and 2005. The data provide insight on the mesoscale spatial variability, the seasonal and even the hourly variability of the AW in the area of interest. Synoptic and high frequency *in-situ* data from hydrological surveys and an open sea observatory indicate the MMJ meanders eastward, between the southern shore of Cyprus and the northern periphery of the Cyprus warm core eddy or the Shikmona gyre. The MMJ is documented to transfer eastward the AW, both at surface and subsurface layers. The results confirm that the MMJ, as an offshore cross-basin jet, is indeed the major driving force responsible for the eastward spreading of the main volume of the AW in the SE Levantine basin, while *in-situ* data closer to Egypt provide evidence of a westward recirculation offshore Egypt.

INTRODUCTION

The most variable water mass of the Levantine basin (Figure 1) is the relatively low salinity Atlantic Water (AW). The inflow of the AW in the Mediterranean compensates for the high rates of the sea water evaporation in the Levantine basin and of the outflow of the Levantine Intermediate water (LIW) into the North Atlantic (Ovchinnikov *et al*., 1976). The estimated AW inflow through the Strait of Gibraltar (1.01 Sv) exceeds the total mean outflow fluxes (0.97 Sv) of the Mediterranean waters (Astraldi *et al*., 1999). The AW, after its entry into the Mediterranean through the Strait of Gibraltar, with salinity as low as 36.3 psu, follows a complicated pathway eastwards, as far as the Levantine basin (Figure 1). There the AW is most often well-pronounced as a subsurface layer with minimum salinity, spanning 40 to 80 meters, with salinity as low as 38.60-38.95 psu (Ovchinnikov *et al*., 1976; Hecht *et al*., 1988; Ozsoy *et al*., 1991). However, periodically surface AW has also been found in the western part of the Levantine with similar salinity values.

The high rates of heating and evaporation, which revail over the Levantine basin during summer, are able to transform the surface layer of the AW to the warmest and most saline (up to 29 deg. C

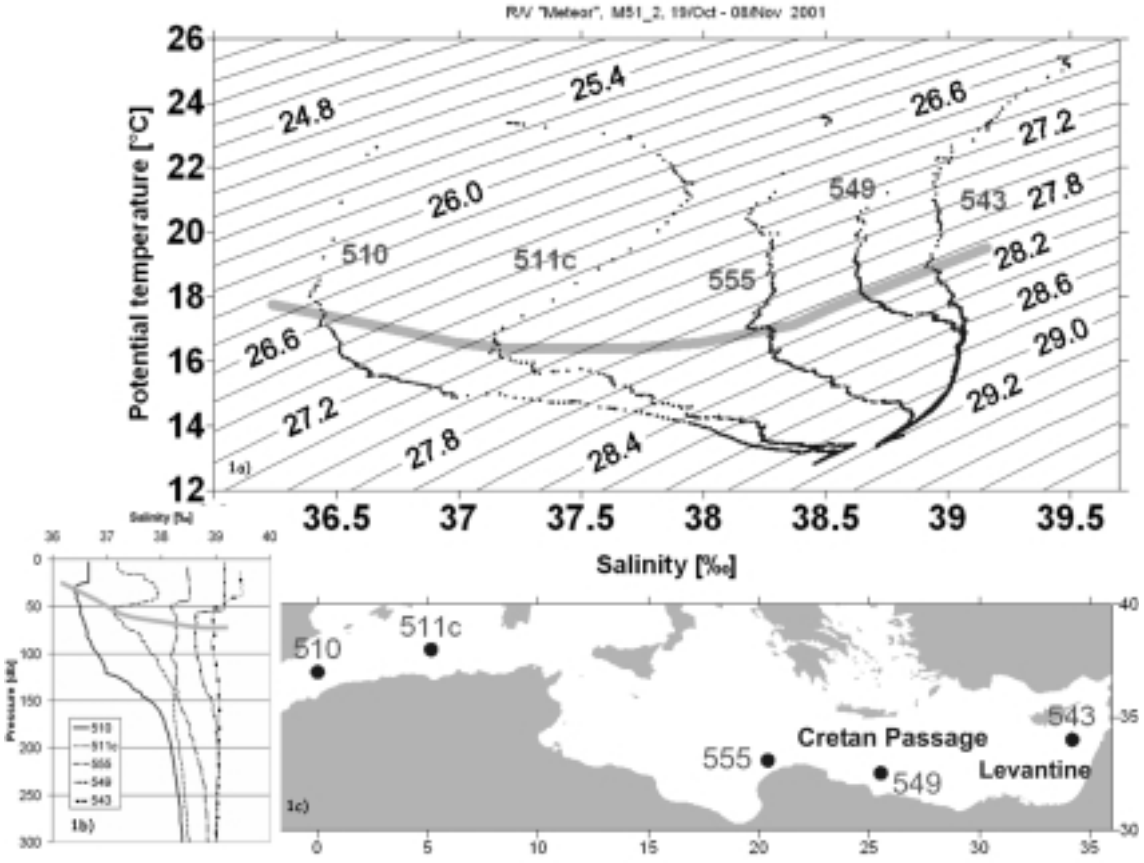

Fig. 1. **a)** T/S diagrams across the Mediterranean showing the transformation of the AW (obtained during a cruise of the R/V METEOR, between Oct.-Nov. 2001). **b)** Associated salinity profiles at selected stations across the Mediterranean. **c)** Associated station locations.

and 39.6 psu) surface waters in the Mediterranean, as observed during the summer 2003 CYBO cruise (Zodiatis *et al*., 2004). In winter, convection mixing processes in the SE Levantine usually initiate the homogenization of the water column from the surface down to subsurface and intermediate layers, in some cases even down to 200-350 m (Zodiatis *et al*., 2001). Consequently, the salinity of the mixed water mass at the typical depths of the AW increases, and the AW is not evident. The spatial variability of the MMJ (mid-Mediterranean jet) in the Levantine basin is also influenced by the local surface processes (summertime evaporation, winter mixing) and by the fluctuations of the local flow dynamics dominating the area (Ozsoy *et al*., 1991).

The general circulation in the Eastern Mediterranean as inferred in the 1960s and 1970s (Ovchinnikov *et al*., 1976) shows an anticlockwise flow with sub-basin features in the Levantine basin (Figure 2a). In the 1980s, the POEM (Physical Oceanography of the Eastern Mediterranean) mesoscale field experiments (Ozsoy *et al*., 1991; POEM Group, 1992), showed that the AW is transferred within the Levantine by the MMJ (Figure 2b). This offshore cross-basin jet is generated as a result of the interaction between the mesoscale cyclonic (Rhodos gyre) and anti-cyclonic (Mersa Matruh and Shikmona gyres) flow features during the eastward spreading of the surface and subsurface waters of Atlantic origin, after passing the Cretan passage.

The use of satellite sea level anomaly (SLA) nowadays is documented to provide a true background of the sea surface circulation. This is the main reason that these remote sensing data are assimilated into the numerical models producing the operational flow forecasts in the Mediterranean Sea (MFSTEP) and elsewhere. It should be noted that remotely-sensed sea surface temperature (SST) is not generally assimilated in numerical models, but is used to relax the heat

fluxes used at the surface boundaries of the models. Recently, the use of a series of SLA patterns of the Mediterranean Sea has made possible the direct estimation of the general sea surface circulation (Pascual *et al*., 2005). This SLA-derived circulation has been used for simulating the pathways of passive tracers in the Mediterranean: particles released in the Western Mediterranean spread after traversing the Cretan Passage, diverging from the south-western coast of the Levantine basin, from where they crossed the Levantine basin, more or less in a similar way as that followed by the MMJ crossing the basin during the POEM experiments in the 1980s.

The present work makes use of new *in-situ* data sets obtained from different observing platforms (synoptic oceanographic surveys and continuous records from an open sea observatory) and provide the most recent evidence of the presence of AW and MMJ in the SE Levantine basin. This supports the earlier schema of the MMJ as an offshore cross-basin flow, depicted in the 1980s within the framework of the POEM experiment.

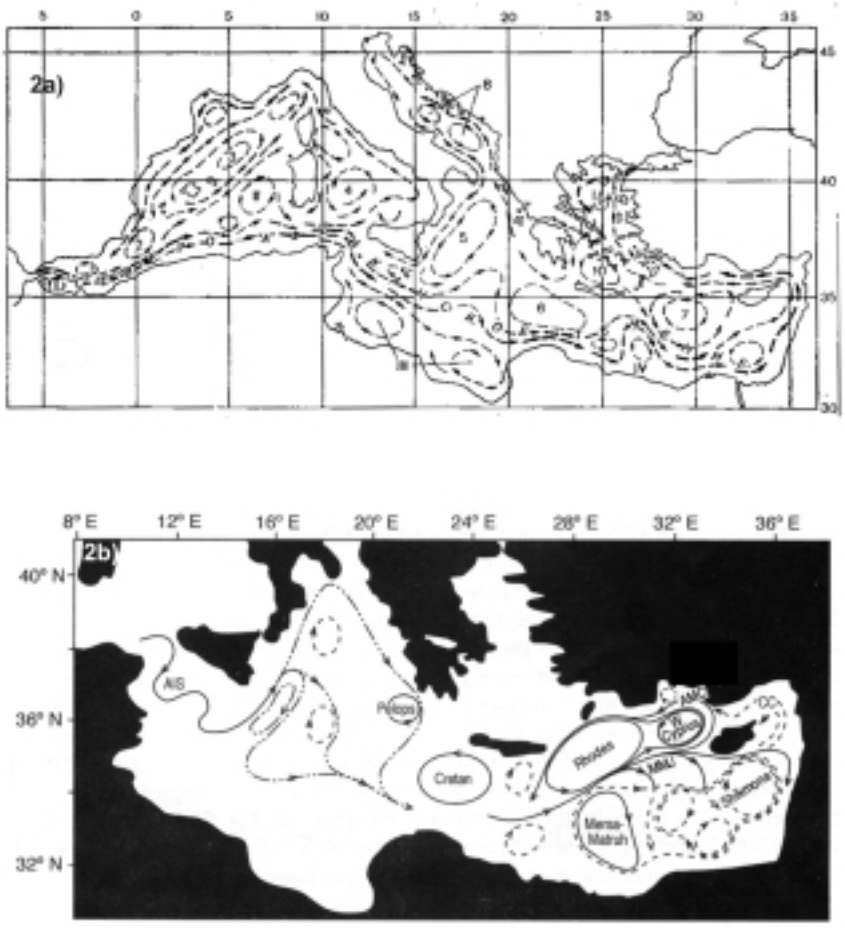

Fig. 2. **a)** The general circulation as depicted during the 1960s and early '70s by Ovchinnikov *et al.* (1976). The prominent feature in the Levantine basin is the Rhodos gyre, labeled "7". **b)** The SE Levantine dynamics during the 1980s consisted of a mesoscale flow structure with anticyclonic eddy activity south of Cyprus and the MMJ meandering eastward transferring the AW (POEM Group,1992).

Data and Methods

The existence of the AW and of the MMJ in the SE Levantine are documented on the basis of *in-situ* data collected seasonally from more than 20 quasi-synoptic oceanographic cruises. The cruises usually lasted not more than 10 days each and were carried out in winter or late winter-early spring and in summer periods from 1995 to 2005. The *in-situ* data for the CYBO (Cyprus basin oceanography), CYCLOPS (Cycling of phosphorous in the Mediterranean) and HaiSec (Long-term Haifa section) projects were gathered from a telescopic grid of stations (with a grid

station spacing from 30 nautical miles in the open sea to 5 nautical miles closer to the coastal zone), using Sea Bird Electronics (SBE 911plus) profilers. An SBE 19plus profiler was used for the CYCO (Cyprus coastal oceanography) cruises. The measurements were sampled at a rate of 24 Hz for the 911plus and 4 Hz for the 19plus, and they were averaged *in-situ* over 1 s intervals. The CTD sensors were calibrated annually, prior to the winter cruises, by Sea Bird Electronics.

Continuous measurements of temperature, conductivity and pressure at five subsurface water layers (at 17, 22, 27, 33, 38 m depths) were obtained at a half-hour interval for the period June 2004 to June 2005, from the SBE 16 CT and SBE 16 CTD profilers of the ocean observatory of the Cyprus coastal ocean forecasting and observing system (CYCOFOS). The ocean observatory is located at the open deep sea area of the SE Levantine, west of Eratosthenes seamount, at the location 33° 41'N and 32° 07.5'E, at about 70 nautical miles southwest of Cyprus. The area of the deployment of the CYCOFOS ocean observatory is considered a passage for the MMJ, during its offshore crossing from the southern part of the western Levantine basin.

In order to complement the hydrodynamic patterns obtained from the above *in-situ* data sets, a corresponding time series of daily remote sensing satellite SST images of the Levantine and of the Eastern Mediterranean, with a spatial and thermal resolution of about 1 km and 0.1 ºC, respectively, were utilised. The single night passage thermal infrared (IR) satellite images, obtained from NOAA-AVHRR were received and processed by the HRPT receiving station operated at the Oceanography Centre, University of Cyprus.

Results and Discussion

The renewed investigations of the SE Levantine, from 1995 to 2005, within the framework of CYBO, CYCO, CYCLOPS, and HaiSec projects, provided strong evidence about the existence, the spatial and temporal fluctuation of the MMJ, the AW, and of the dominating flow features of the area. The current analyses of the *in-situ* data confirm earlier works (Ozsoy *et al*., 1991; POEM Group, 1992) that the MMJ, which carries the AW in the area, enters the study area from the southwest, at surface and subsurface layers, after crossing the basin from the southwest part of the Levantine and then meanders mainly eastward. The present work confirms that the jet meanders between Cyprus and the northern periphery of the Cyprus warm core eddy (Zodiatis *et al*., 1998). The latter is revealed as the dominant flow feature of the study area. Periodically the MMJ bifurcates southwest of Cyprus, generating a secondary branch flowing northward along the western coast of Cyprus. The Cyprus warm core eddy and Shikmona gyre (when present), as well as smaller-scale cyclonic and anticyclonic eddies, increase the complexity of the flow path of the MMJ and subsequently of the AW transport in the SE Levantine (Ozsoy *et al*., 1991; POEM Group, 1992). Throughout the period of study the fluctuation of the MMJ was found to be connected with the Cyprus warm core eddy. The latter undergoes strong seasonal variability, for example the westward shift of the Cyprus warm core eddy during the period 2000-2001 and the re-establishment of the Shikmona gyre during the period summer 2001-2003 (Zodiatis *et al*., 2005).

During summer 1998, as in all summer cruises from 1995 to 2004, the composite T/S diagram of the area shows the well know "S" shape of the temperature and salinity relationship (Figure 3a). The minimum subsurface salinity was quite well defined at a depth below the thermocline (about 40-50 m) with salinity as low as 38.65-38.75 psu. North-south and west-east salinity sections, south of Cyprus, such as those carried out in summer 2003, show the AW in the form of less saline subsurface lenses with salinity as low as 38.67 psu. These water lenses were attributed to the stream of the MMJ that transferred the AW eastward (Figures 4a,b).

During severe winter weather conditions the presence of the AW is difficult to detect, often being eradicated by winter mixing processes, as shown in the composite T/S during winter 2002 (Figure 3b). However, in milder winter conditions, such as in January 1999 and in early spring, as in May 2000, the AW has been found very well pronounced with salinity values comparable to those observed during summer periods. Periodically the AW has been found at the south-western part of the study area, from the surface down to 100 meters.

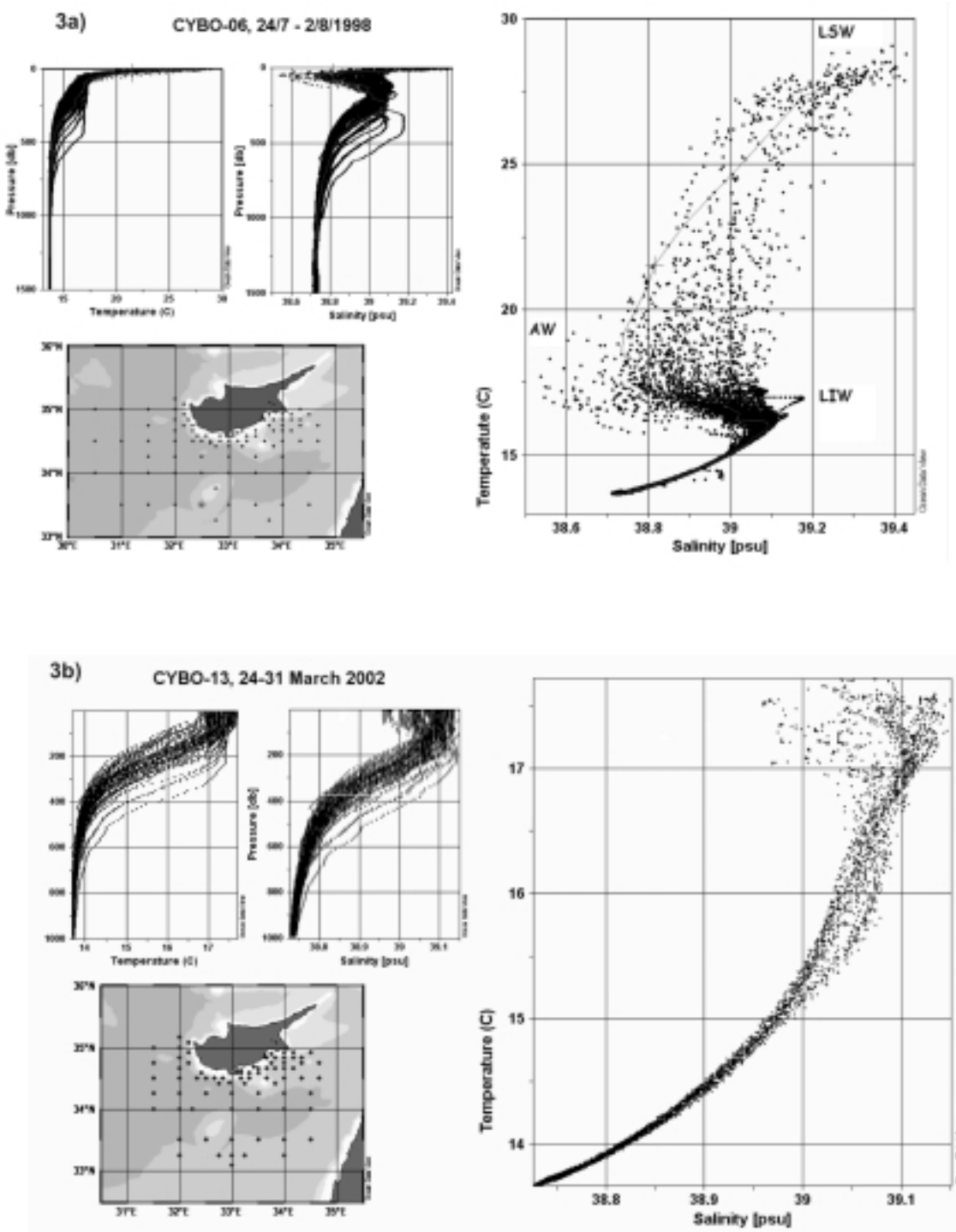

Fig. 3. **a)** *In-situ* data from Cyprus basin Oceanography cruise CYBO-06 in July and August 1998 (all stations are indicated in the location map), showing temperature and salinity profiles, as well as the T-S diagram. **b)** *In-situ* data from Cyprus basin Oceanography cruise CYBO-13 during March 2002 (all stations are shown in the location map), showing temperature and salinity profiles, as well as the T-S diagram. Note the absence of Atlantic Water as a subsurface layer (due to strong vertical mixing).

In early spring 2000 the north-south salinity section south of Cyprus, which crossed the eastward pathway of the MMJ, showed a very well pronounced lens of AW origin (Figure 5). The lens was found to extend from the surface down to the depth of 90 m and from north to south for about 40

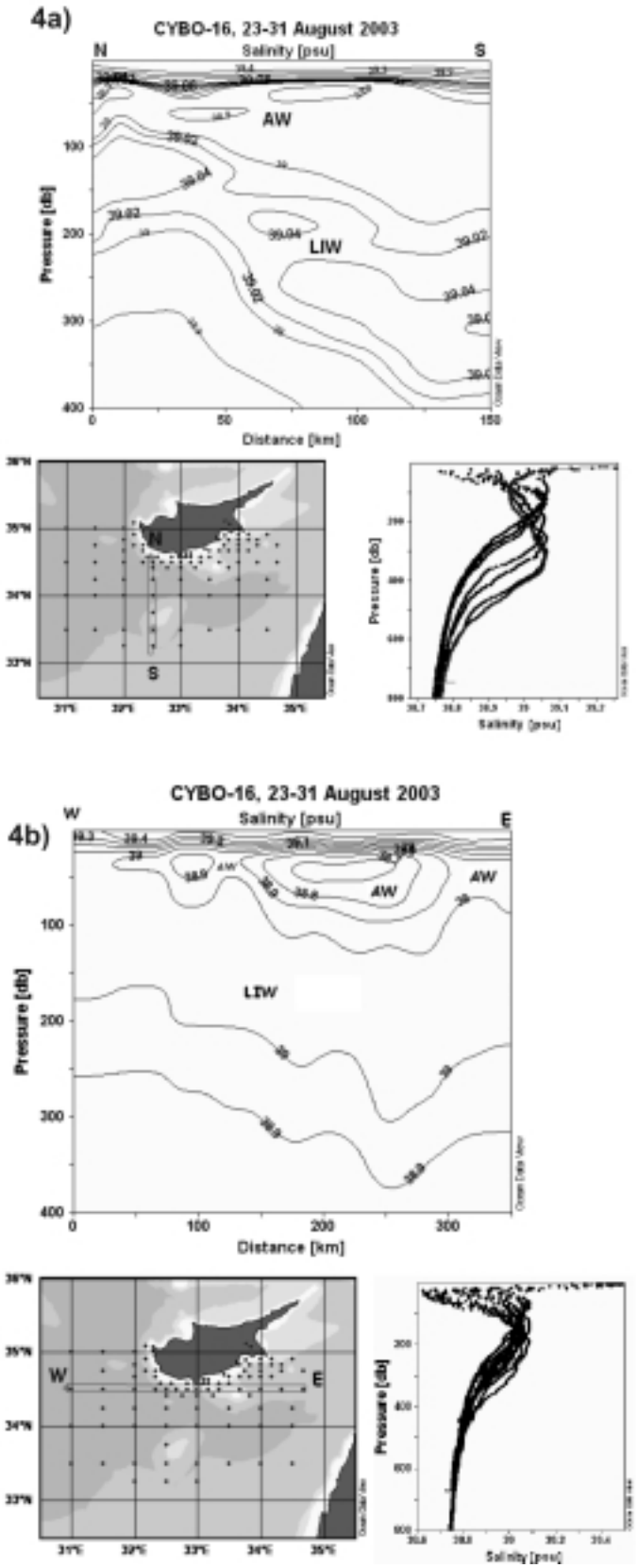

Fig. 4. **a)** *In-situ* data from Cyprus basin Oceanography cruise CYBO-16 in August 2003 (all stations are shown in the location map), showing salinity profiles for a meridional section south of Cyprus, as well as the vertical section (top 400 m only). Atlantic Water (AW) and Levantine Intermediate Water (LIW) are indicated. **b)** As in Figure 4a, but for a zonal section south of Cyprus.

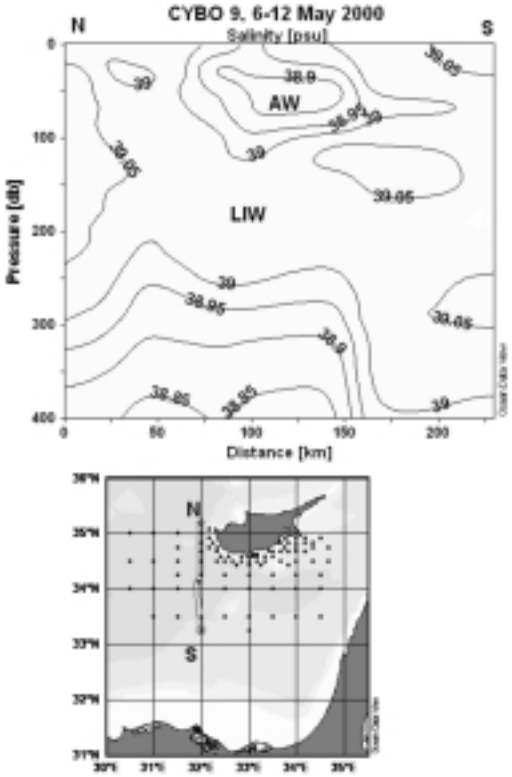

Fig. 5. As in Figure 4a, but for CYBO-09 in May 2000. The core of the AW extended from the surface down to 100 meters and spanned up to 75 km horizontally. Vertical profiles are not shown.

nautical miles, with salinity between 38.85-38.95 psu. The lens is attributed to the MMJ. In this region eastward geostrophic velocities of 30-35 cm/s were observed, transferring the AW through the saline waters of the Levantine basin.

During the CYBO and CYCLOPS experiments carried out in 2001 and 2002, it was found that the significant seasonal spatial displacement of the Cyprus warm core eddy to the west (about 60-80 nautical miles from its original position, Zodiatis *et al*., 2001, 2005) caused an even more complicated flow path for the MMJ. In particular, in April-May 2001 the northward extent of the Cyprus eddy caused for a short period the restriction of the eastward transfer of the AW. The main flow path of the MMJ became northward offshore west Cyprus, as opposed to its usual eastward direction offshore south Cyprus. In August 2001, the southern relaxation of the Cyprus warm core eddy for about 20 nm and a secondary new anticyclonic eddy, between southeast of Cyprus and offshore Lebanon, resulted in the re-establishment of the eastward MMJ flow, with velocities up to 45 cm/s, along the northern peripheries of these two warm core eddies. The co-existence of these two warm anticyclones until summer 2003, contributed to the re-appearance of the well known Shikmona gyre (Zodiatis *et al*., 2005). During this period the AW was observed also below the secondary anticyclone, at greater depth than usual, down to 200 m. The latter suggests that the AW after its eastward advection along the Cyprus eddy was then picked up by the new (secondary) anticyclone, which was more intense at the upper surface layers comparable to the Cyprus eddy.

The spatial and temporal variations of the dominating dynamic flow features of the SE Levantine are illustrated in the three circulation diagrams (Figures 6a,b,c), characterizing the periods: a) 1995-1999, b.) 2000-2001, c) summer 2001-2003. Figure 6a shows the Cyprus warm core eddy to be located east of the meridian of 33 00.E, while Figure 6b shows the significant westward shift (about 60-80 nm) of the Cyprus eddy at the end of 2000-early 2001. Finally, Figure 6c shows the re-establishment of the Shikmona gyre that constituted from warm core eddies, similar to

those found during the 1980s. A detailed description of the circulation during the CYCLOPS experiments will be found in Zodiatis *et al*. (2005).

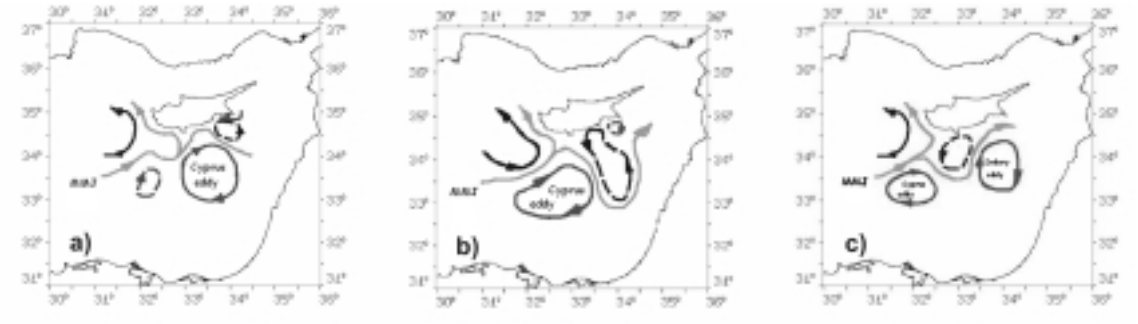

Fig. 6. Diagrams of the prevailing general circulation in the SE Levantine, based on CYBO and CYCLOPS cruises. **a)** For the period 1995-1999; **b)** for the period 2000-2001; **c)** for the period summer 2001-2003.

In summer 2004, the north-south salinity section, between south Cyprus and offshore Egypt, shows the AW to be transferred within the pathway of the MMJ, with salinity as low as 38.8 psu, between the depths 30-100 m (Figure 7). The geostrophic flow at the same section indicated that the MMJ flowed eastward along the northern periphery of the well- established Cyprus warm core eddy, transferring the AW. Moreover, the current intensity of the eastward flow in general was greater, particularly at the most northern part of the section, comparable to the westward flow in the southern part of the section (offshore Egypt). These results give additional evidence that during summer 2004 there was no significant eastward current offshore Egypt. On the contrary, the AW is mainly transferred eastward by the MMJ, flowing between south offshore Cyprus and the northern periphery of the Cyprus warm core eddy, after crossing the basin from the south-western part of the Levantine basin.

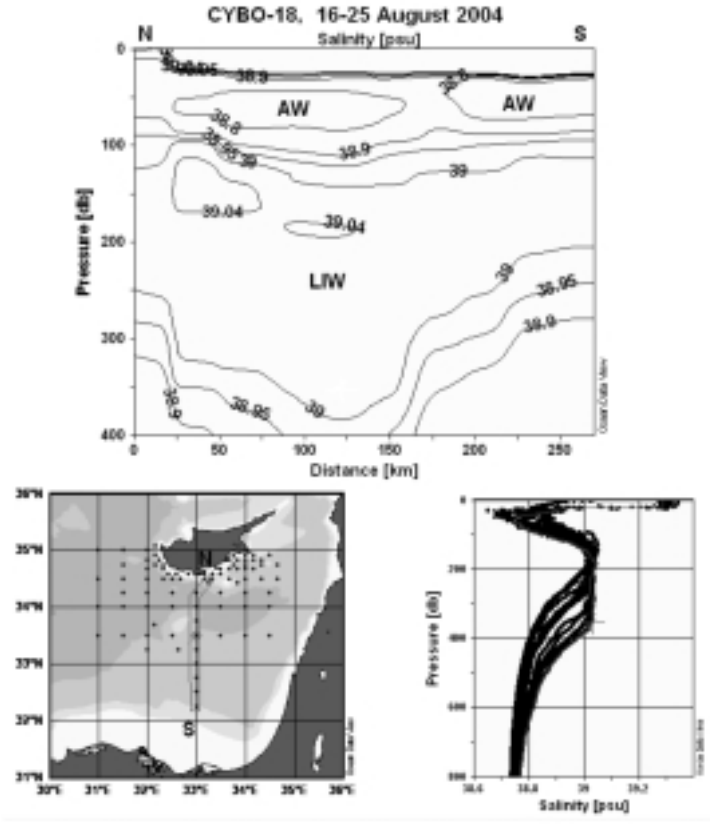

Fig. 7. *In-situ* data from Cyprus basin Oceanography cruise CYBO-18 in August 2004 (all stations are shown in the location map), showing salinity profiles for a meridional section from Cyprus as far south as offshore Egypt.

A series of daily single passage satellite SST images were used to complement our knowledge on the daily variability of the general flow dynamics of the broader Levantine region during the synoptic oceanographic surveys discussed here. It was possible to define the main flow features of the broader area of interest using the remote sensing IR images, but the AW pathways could not be identified without the use in parallel of *in-situ* data. The main reason is that the AW usually appears as a subsurface salinity minimum in the Levantine basin. However, in cases when the transferred AW by the MMJ was cooler than the surrounding surface waters of the Levantine, then the pathway of the MMJ appeared in SST images. As an example the geostrophic flow pattern derived from *in-situ* density profiles in the SE Levantine during the CYBO experiment, in March 2002, two months prior to CYCLOPS (Figure 8) indicated a jet flowing along the periphery of the Cyprus warm core eddy and of the secondary anticyclone offshore eddy that was located between SE Cyprus and Lebanon.

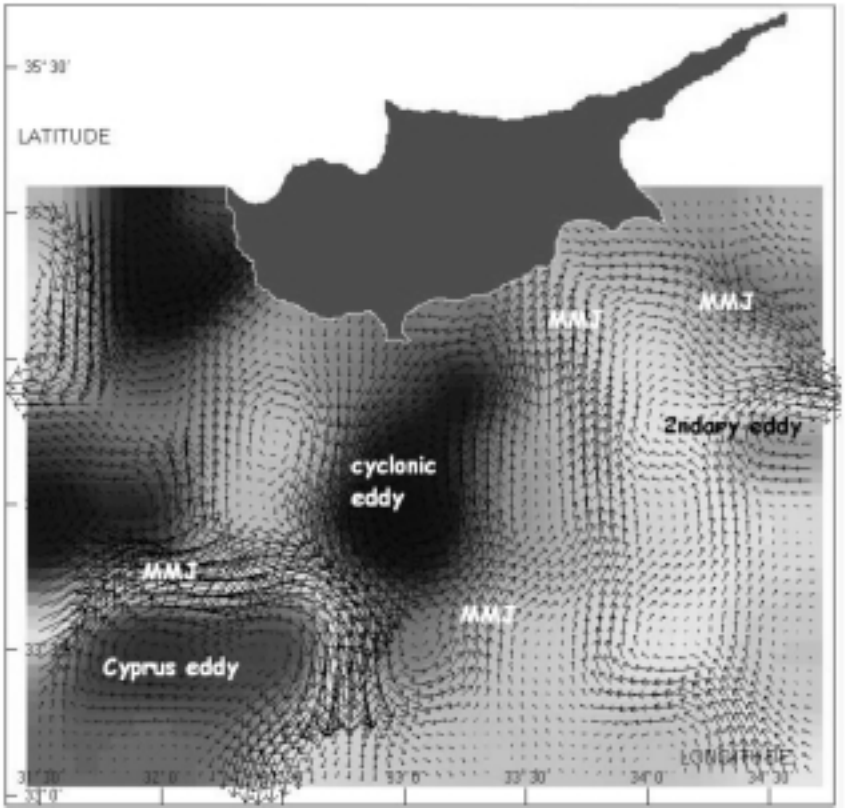

Fig. 8. The general geostrophic circulation pattern estimated using *in-situ* data obtained during the CYBO experiment, late March 2002, in order to support the forthcoming CYCLOPS experiment in May 2002.

High frequency *in-situ* data from the CYCOFOS ocean observatory, located at the open deep sea southwest of Cyprus, provide unique evidence for the half-hourly variability of AW in this particular area, which is considered a passage of the MMJ. From June through October 2004, the 38 m sensors indicated the presence of AW. The salinity at 38 m was nearly always below 38.8 psu and temperatures were 3-6 C° lower than the 17 m values where salinity was above 39 psu. In winter 2004-2005, the mixed layer extended deeper than the deepest (38 m) ocean observatory sensor (Figures 9a,b). Salinities in the mixed layer were greater than 39 psu. From May to June 2005 the salinity at 38 m showed again the intrusion of the AW with salinity to be fluctuating between 38.8-38.98 psu. The sensors at the depth of 17 m showed the salinity to increase gradually during the same period, with values above 39 psu.

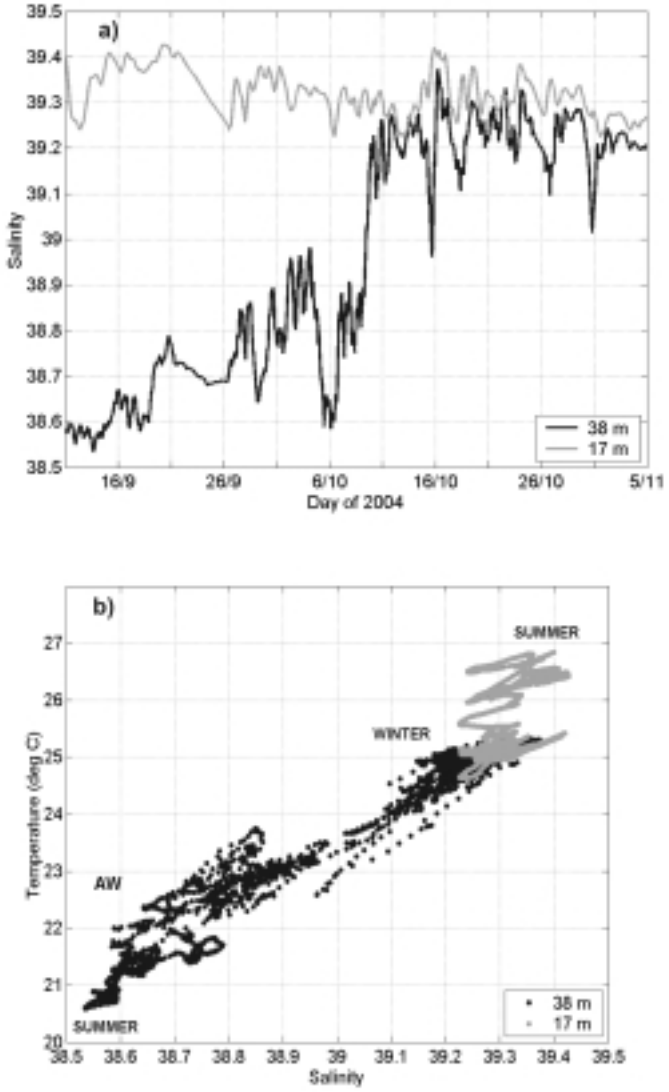

Fig. 9. Data from MedGOOS-3 Buoy, part of the Cyprus Coastal Observing and Forecasting System (CYCOFOS). **a)** Salinity time series at two of the five observed depth levels (17 m and 38 m) for the late-summer period September to November 2004 showing transition to well-mixed conditions in early October 2004. **b)** Temperature-Salinity diagram for the same period and same two depths showing the presence of Atlantic Water (AW) at 38 m during the summer stratified period but not at 17 m.

CONCLUSIONS

The analyses of *in-situ* data sets collected over a ten-year period from two different observing platforms, with different sampling time and spatial scale, provide strong evidence that the MMJ transfers the main volume of the AW in the SE Levantine basin. These *in-situ* data confirm that the MMJ, after crossing the basin from the offshore southwest part of the Levantine, meanders eastward between offshore Cyprus and the northern periphery of the Cyprus warm core eddy or the Shikmona gyre (when present). Moreover, at a certain period *in-situ* data closer to Egypt provide evidence of a westward re-circulation offshore Egypt.

Bio-optical Sensors of mesoscale variability on Autonomous Floats and Gliders

Marlon R. Lewis[1] and Hervé Claustre[2]

[1] *Department of Oceanography, Dalhousie University, Halifax, Nova Scotia, Canada*

[2] *Observatoire Océanologique de Villefranche, Lab. d'Océanographie de Villefranche, Villefranche-sur-mer, France*

1. Introduction

A view has emerged over the past decade of an open and coastal ocean rich in a wide spectrum of variability in both time and space, particularly at the so-called "mesoscale". This variability must be either explicitly resolved, or sensibly parameterized, to even begin to address the ocean's role in future climate, and the larger scale evolution of the oceanic carbon cycle. New modelling approaches which resolve or permit mesoscale eddy scales (e.g. McGillicuddy and Robinson, 1997; Pinardi *et al*., 2004; Guinehut *et al*., 2004; Levy and Klein, 2004), the routine availability of satellite observations of physical (e.g. altimetry) and biological (e.g. ocean color) processes, long term continuous moored and drifting buoy observations (e.g. Twardowski *et al*., 2004; Dickey *et al*., 2005), and advanced data assimilation schemes which tie the models and data together (e.g. Doney, 1999), have all contributed significantly towards bringing this new view of the open ocean into widespread acceptance (Lewis, 2002).

The Mediterranean Sea is not immune from the influence of mesoscale variability. New perspectives on previously known structures such as the Alboran gyre have emerged from satellite observations and high resolution models (e.g. Font *et al*., 2002). The impact of such variability on forecasting skill can be significant; it is however extremely difficult to characterize from traditional sampling platforms, particularly in a way that would generate near-to-real time data for assimilation into nowcast and forecast models of the ocean environment. This is particularly true for observations relevant to biogeochemical processes.

Here we examine a few autonomous mobile ocean sampling platforms which have sufficient duration and range to be able to provide near-real-time three-dimensional views of mesoscale variability in both physical and biological processes.

2. Background and scales of variability

The mesoscale fluctuation spectrum in the ocean spans length scales order 100 km, and time scales order 5 - 100 days. These scales dominate the frequency-wavenumber spectra of eddy kinetic energy as seen in both moored instrumentation (e.g. Wyrtki *et al*., 1976; Dickey *et al*., 1998), and satellite observations (e.g. Le Traon, 1991; Stammer, 1997). Processes that dominate the mesoscale as well are associated with (and perhaps are responsible for) variability at the sub-mesoscale, with significant implications for biogeochemical fluxes (e.g. Levy *et al*., 2001).

The mesoscale eddy kinetic energy distributions are in general aligned in time and space with the low-frequency (mean) baroclinic flow and are highly correlated with the primary mode internal Rossby radius of deformation. For example, high levels of mesoscale energy are found along boundary currents at mid-latitudes, and along frontal structures and current systems (e.g. Stammer and Wunsch, 1999). Minima are found in the interior of the ocean gyres.

The surface kinetic energy distributions are dominated by the first baroclinic mode, and hence the variance in the sea-surface height observed by altimetry should directly reflect the vertical displacements of isopycnals in the ocean interior (Gill, 1982). Siegel *et al*. (1999) have analyzed a combined TOPEX/POSEIDON -ERS altimeter data set on sea level height anomalies, and related these to subsurface displacement of isopycnals in cyclonic eddies found in the northwestern Sargasso Sea. Turk *et al*. (2001) have examined inter-annual variability in sea surface height anomalies in the Equatorial region from TOPEX/POSEIDON altimetry, and also related this to anomalies in the displacement of the subsurface isopycnal surface characterized by the 20° isotherm. The importance of this lies in the fact that, below depths of significant photosynthetic activity, isopycnal surfaces relate to surfaces of constant nutrients, and by examining the displacements associated with mesoscale activity one may be able to infer an effective nutrient flux into the well-lit surface waters.

Mesoscale variations are also clearly seen in the distribution of the scalar chlorophyll a fields. An outstanding question concerns the mechanism (s) by which variations in the physical dynamics at the mesoscale (and sub-mesoscale) translate into variability in biological processes. In turn, variability in the concentration of phytoplankton in the upper ocean alters the rate of absorption of solar energy, and hence the vertical distribution in the irradiance divergence that governs local heating. Given that a primary source of variability in primary production and chlorophyll biomass is due to variations in nutrient input, then the focus becomes the role of mesoscale eddies and processes in moderating the nutrient flux into the upper well-lit euphotic zone. As this represents a "new" source of nutrients (*sensu* Eppley and Peterson, 1979) it is relevant to estimate the export of organic carbon to the deep sea removed from contact with the atmosphere.

Mesoscale processes potentially contribute to nutrient enrichment in a number of ways. These include the uplift of isopycnals with high nutrient concentrations into the euphotic zone ("eddy pumping"), enhanced shear and vertical mixing associated with eddy dynamics, and ageostrophic circulation associated to frontal and jet processes that input new nutrients into potentially productive surface waters, both vertically and in the horizontal. To address the role of mesoscale eddies in the variance of new production will require a combination of high resolution models and multidisciplinary data fields which can be used for both initialization and assimilation of observations into models run in a nowcast and forecast sense.

3. PLATFORMS AND SENSORS

Autonomous LaGrangian Profiling Floats

Surface Drifters. Surface drifting buoys have been successfully used to measure the optical characteristics of the upper ocean, which for the open ocean are largely dependent on the concentration and activity of phytoplankton. The first of such floats, based on an air-launched design, was deployed in the Equatorial Pacific, and measured the upwelling radiance just below the sea surface (Foley *et al*., 1997; Landry *et al*., 1997). When normalized to a measurement of surface downwelling irradiance, quantitative measures of the color of the ocean can be made, and from this, the concentration of chlorophyll and the nature of biological processes can be inferred in near-to-real time. Subsequent deployments using WOCE standard Surface Velocity buoys have been successfully made in many oceans, and in addition to the analysis of ocean color, the fluorescence of phytoplankton induced by absorption of solar energy has been used to characterize the photosynthetic process in the upper ocean (see Abbott *et al*., 1990; Abbott and Letelier, 1998; Abbott *et al*., 2000), and a set of consensus protocols developed for further applications (Kuwahara *et al*., 2004).

Profiling Floats. More recently, profiling floats, which use buoyancy changes to move vertically, have provided real-time hydrological data throughout the water column collected during their rise

and descent at 10-day intervals to 1500 or 2000 m depths (e.g. Wilson, 2000; ARGO Science Team, 2001). Large numbers (>1800) of these floats have now been deployed, with the data telemetered via satellite after surfacing briefly at pre-specified times. The baseline ARGO floats are built by several manufacturers (e.g. SIO, University of Washington, Webb Research, MARTEC); these generally carry a CTD as a primary payload and have mission durations of up to five years.

Such floats hold promise as well for the measurement of properties other than temperature and conductivity. Some investigators are already testing and using profiling floats adapted for bio-optical and biogeochemical measurements and observations. For example, Mitchell *et al*. (2000) have instrumented a Sounding Oceanographic Lagrangian Observer (SOLO; Davis *et al*., 2001) profiling float to measure the diffuse attenuation coefficient at three wavelengths in the Sea of Japan/East Sea. The floats were able to capture mesoscale features in the distribution of phytoplankton through their influence on the attenuation coefficient of visible light in the upper ocean. Other optical instruments for determining particulate organic carbon (POC) and particulate inorganic carbon (PIC) have been used on C-Argo floats (specially programmed to cycle three times per day in the upper ~200m) by Bishop *et al*. (2002) in a study of carbon enhancement by dust storms in the North Pacific and in another case, in a study of the consequences of deliberate introduction of iron to the Southern Ocean (Bishop *et al*., 2004). These sensors rely largely on the scattering of light by particles in the sea. Unlike the sensors used for the estimation of the diffuse attenuation coefficient, which depend on the irradiance from the sun, the sensors used for POC and PIC have an active source of light and can profile throughout the water column in both day and night (Figure 1). Active light sources are also used for fluorometers, which measure the light emitted by phytoplankton (or with different wavelength sets, Chromophoric Dissolved Organic Matter, CDOM) after absorption at a different (shorter) wavelength. Finally, new fluorescence-based optical sensors for the measurement of oxygen concentration have recently provided unique insight into the seasonal "breathing" of the upper ocean (Körtzinger *et al*., 2004), and have now been deployed with fluorometers for examination of the biogeochemical oxygen cycle in the Labrador Sea (Boss, pers. comm., 2005; Figure 1).

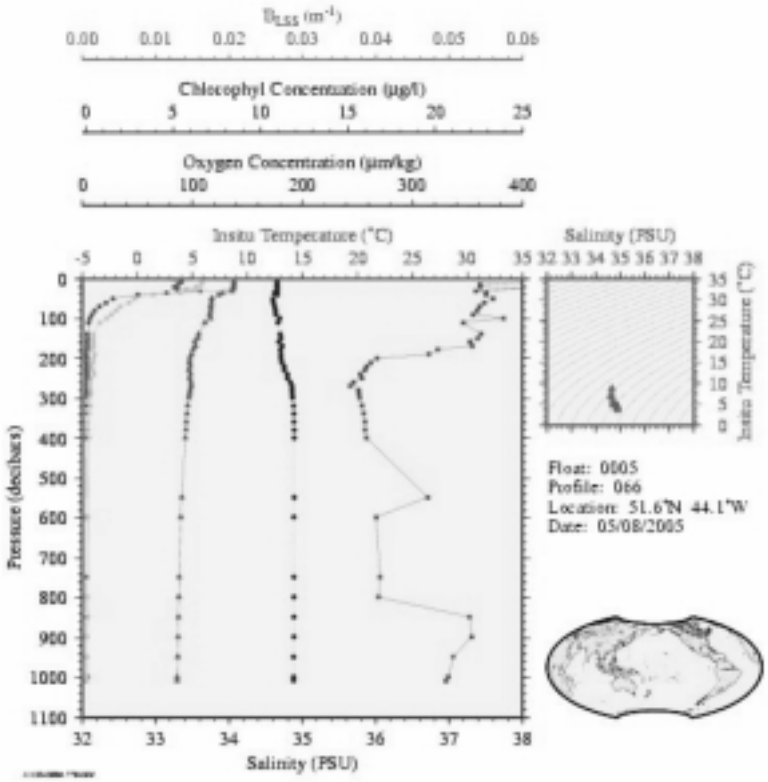

Fig. 1. Profile from bio-optical profiling float deployed in the Labrador Sea (8 May, 2005; Boss, pers. comm.).

Several other sensors are in development, including those for the measurement of micro-second fluorescence dynamics (which provide an estimate of photosynthetic performance, see Gorbunov and Falkowski, 2004) and nitrate (e.g. Johnson and Coletti, 2002). The routine deployment of optical sensors on floats faces several obstacles, e.g., modification of float design (or sensors) to accommodate new sensors with regards to ballast, drag, power and communication bandwidth requirements, biofouling issues, data calibration and validation, and potential sampling regimen conflicts (e.g., diurnal versus 10-day profiling scheme), etc. These are currently being successfully addressed.

Fig. 2. SatRover, a new bio-optical sensor for profiling float deployments. A three channel irradiance sensor (Satlantic Inc) is at the top, and the bottom open area is a transmissometer (WetLabs Inc.).

Gliders

Gliders are relatively new vehicles which, like the profiling floats, rely on buoyancy changes to alter their vertical position. In addition they can actively alter their horizontal position through aerodynamic control surfaces (see Figure 3). Gliders are therefore able to observe the ocean in three dimensions autonomously.

Fig. 3. (See page 109 for original color plate) Slocum glider (Webb Research).

Gliders are manufactured largely by the same groups involved in profiling sensors (Webb, SIO, UW). Their saw-toothed sinking and ascending trajectories result in horizontal displacements of ~ 25-30 km per day with an horizontal resolution of 2-5 km and with typical mission durations of approximately 30 days. Because their horizontal movements can be controlled, rendezvous and recovery of the vehicle is possible at the end of the mission, something not usually done with drifting buoys.

Gliders can accommodate similar bio-optical and biogeochemical payloads as profiling floats (Rudnick and Perry, 2003; Rudnick *et al*., 2004), although the constraints are more stringent with respect to size, power, and interference with vehicle drag. To date, only a limited subset of sensors other than CTDs have been deployed, including oxygen sensors, active fluorometers, turbulent velocity shear probes, optical scattering sensors, and a long-pathlength capillary waveguide absorption sensor (Rudnick *et al*., 2004; Scholfield *et al*., 2004).

4. Potential observation strategies for the Mediterranean

Autonomous profiling floats and gliders, when suitably equipped with a broad range of sensors, can play a useful role in an observational strategy focused on the mesoscale, and can complement observations of the surface from satellite and focused, process-oriented, shipboard campaigns. The relatively low cost permits deployments of many units in a coordinated fashion. Fleets of gliders for example have been shown to resolve temporal variations of two days and spatial variations of 20 km in the coastal zone (Rudnick *et al*., 2004), which are relevant for the mesoscale problem in the Mediterranean Sea. New sensor developments will open doors to new observational strategies, firmly coupled to clever inversion models and with active assimilation of near-to-real time data into nowcast and forecast models of ocean biogeochemical dynamics (e.g. Pinardi *et al*., 2003).

Satellite chlorophyll as a tracer for upward velocities in the surface ocean

Javier Ruiz and Gabriel Navarro

Instituto de Ciencias Marinas de Andalucía (ICMAN),
Consejo Superior de Investigaciones Científicas (CSIC), Cádiz, Spain

ABSTRACT

Cold waters poor in chlorophyll are quite unusual during spring-summer at the surface of the subtropical latitudes where the Mediterranean is located. They result from very intense dynamic processes that lift deep water of different properties to surface. Detection of these waters by radiometers in orbit can be used as a satellite tracer for the areas where these processes occur. In such areas, the chlorophyll detected by satellites depends on the vertical velocities bringing deep-waters properties towards the surface layer, which can be estimated through the information derived from radiometers like AVHRR, SeaWiFS or MODIS.

DISCUSSION

At subtropical latitudes, radiometers in orbit usually detect high chlorophyll concentrations associated to cold surface waters. The occurrence of these features is the consequence of a nutrient limitation that is broken by the input of cold waters from deeper layers. The light regime of the mixed layer in the Mediterranean is sufficient in spring-summer to trigger exponential phytoplankton growth when nutrients are lifted to the surface. This rapid response by phytoplankton underlies the strong correlation between high chlorophyll levels and low temperature values. Therefore, surface waters characterised by both low chlorophyll and temperature are quite scarce during the spring-summer period in the Mediterranean. Their presence is associated to very recent events of upward transport to the surface before phytoplankton develops, a phenomenon that allows to use these waters as an indicator of spots with intense upwelling. As an example, Figure 1 shows the probability to find these upwelling

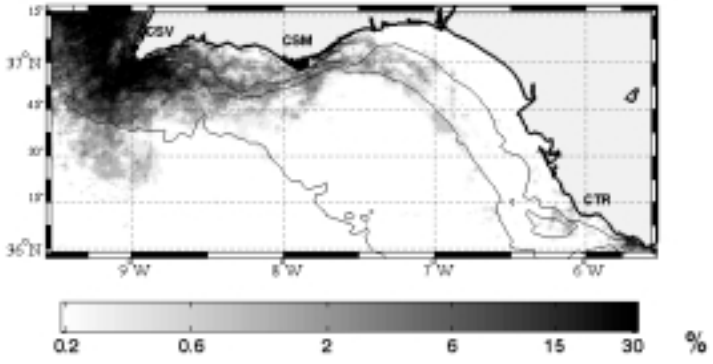

Fig. 1. Probability (%) to find upwelling spots (water temperature and chlorophyll concentration below 17ºC and 1 mg/L respectively) in the Gulf of Cádiz. The map is based on daily images from 1998 to 2002 between April to September. CSV, CSM and CTR stand for Cape San Vicente, Santa Maria and Trafalgar respectively. Black lines represent 50, 200 and 1000 isopleths (in metres).

spots in the Gulf of Cádiz when the water column is stratified in the area. High probabilities concentrate at Capes San Vicente and Santa María where intense dynamic events occur. Despite the large number of images analyzed, the majority of the basin does not exhibit a single occurrence of cold waters poor in chlorophyll at the surface.

The location of waters characterised by both low temperature and chlorophyll can be considered not only a tracer for intense dynamic processes that inject deep water properties into the surface but also a finding that sheds light on the nature of the process. Thus, Figure 2 shows temperature and chlorophyll monthly climatologies for the same period illustrated in Figure 1. In the graph, Cape Trafalgar displays low temperature and high chlorophyll climatological values. At first sight, this observation might lead to the conclusion that this is an area of significant vertical advective input of nutrients. However, and contrary to Capes San Vicente and Santa María where climatological low temperature and high chlorophyll also occur, Cape Trafalgar has low probabilities. This difference results from the vertical advection associated to Ekman pumping under upwelling favourable conditions in Capes San Vicente and Santa María (Navarro and Ruiz, submitted). Near both capes, the wind forces deep and cold water to reach the surface before phytoplankton burst. However, the forcing at Cape Trafalgar is the consequence of tidal mixing associated with an abrupt bathymetric change. It constitutes a diffusive input that does not permit the neat transfer of deep water properties into the surface as the advective Ekman pumping does in Capes San Vicente and Santa María. The presence of cold waters poor in chlorophyll in the region only indicates the existence of areas with intense vertical advection.

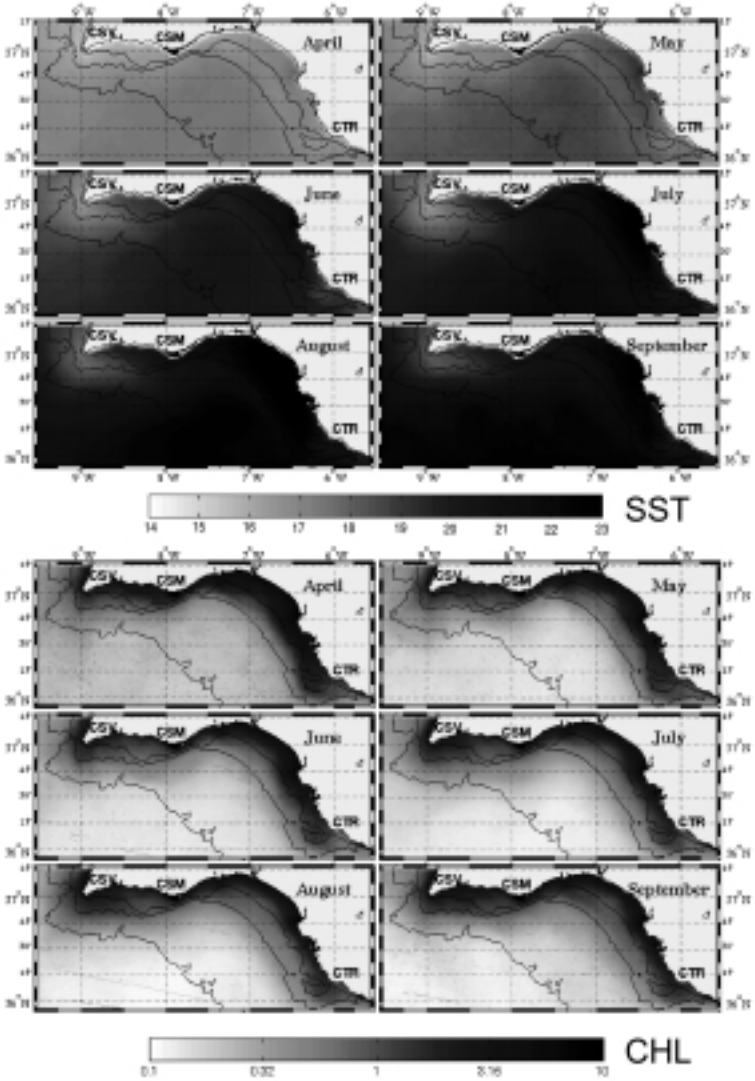

Fig. 2. Monthly climatologies of SST (ºC) and satellite chlorophyll (mg/L) in the Gulf of Cádiz between 1998 and 2002.

These upward velocities lead to different patterns of phytoplankton growth in the water column (Zakardjian and Prieur, 1998). If the question is analysed from a vertical Lagrangian perspective, phytoplankton immersed in a parcel of water ascending from the deep starts growing once it reaches the photic zone, before the water parcel arrives completely at the surface. During an upwelling event of low intensity, an ascending parcel of water would spend a long period of time in the photic zone and, under these conditions, phytoplankton would be able to grow rapidly before reaching the surface. On the other hand, during an intense upwelling event, the water would approach the surface at a higher velocity and phytoplankton would not stay at the photic zone the time necessary to support a significant growth. Therefore, for areas under upwelling conditions, surface chlorophyll can be a tracer for the transfer velocity of waters from the bottom layers to the surface. The formulation of the Lagrangian phytoplankton growth allows an explicit derivation of this velocity (w):

$$w \approx \frac{V_m \left(1 + \frac{\bar{I}_0}{I_k}\right)}{K_d \log\left(C_0 / C_{z^*}\right)} \qquad \text{[equation 1]}$$

where V_m is the maximum phytoplankton growth rate (Brush *et al*., 2002), $\bar{I}_0$ is the average daily incoming PAR radiation at the ocean surface, I_k is the saturating onset parameter (O'Brien *et al*., 2003), C_{z^*} is the residual chlorophyll concentration, K_d is the coefficient for PAR attenuation and C_o is the satellite chlorophyll concentration at the surface.

When applied to the Gulf of Cádiz, this approach provides climatological maps that are in agreement with Figure 1 and consistent with the meteorological forcing in the area, which expects upwelling conditions under westerlies for Capes San Vicente and Santa María. In addition, the calculated vertical velocities are consistent with independent estimates of vertical velocities such as those resulting from nitrogen demand to hold new production in the zone (Figure 3). When applied to the Alborán Sea (Figure 4), the approach also generates vertical velocities coherent with the meteorological forcing as well as with the mesoscale dynamics and eddy kinetic energy diagnosed previously in the area (Gomis *et al*., 2001).

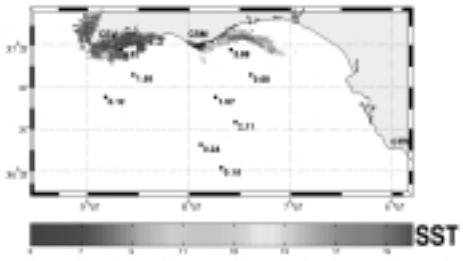

Fig. 3. (See page 109 for original color plate) Climatological map of vertical velocitites (m/d) for Cape San Vicente and Cape Santa Maria zones. The map is based on 311 daily images from 1998 to 2002 between April to September. Black symbols represent the vertical velocities (m/d) based on nitrogen demand to hold new production in the photic zone.

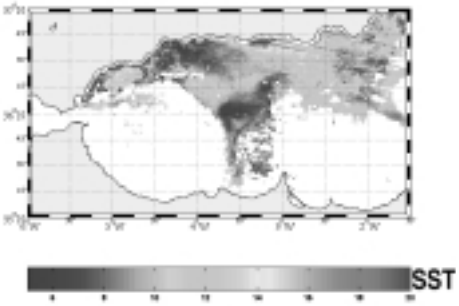

Fig. 4. (See page 109 for original color plate) Climatological map of maxium vertical velocitites (m/d) estimated for the Alborán Sea. The map is based on daily images from 1998 to 2002 for the period between March to September. The maximum estimated w for each pixel along this period is plotted in the figure.

This approach combines the main processes that generate advective inputs of nutrients to the photic zone in the region and associates them with a vertical velocity. These vertical velocities occur at coastal upwellings and open ocean mesoscale features. They modify the size structure of phytoplankton communities, favouring the permanence of large cells in lit waters (Rodriguez *et al*., 2001). This permanence cannot rely on unstructured flow dynamics at smaller scales, as turbulence increases the settling velocity of phytoplankton cells (Ruiz *et al*., 2004). Therefore,

velocities influence not only the fertilization of the ocean surface but also the composition of the phytoplankton communities after the fertilization. They can be diagnosed by remote sensing images, representing a concrete case where the biology can be implemented to further understand the physics rather than the standard reverse direction approach.

Studies of mesoscale physical-chemical-biological interactions in the Antarctic Circumpolar Current

Volker H. Strass

Alfred-Wegener-Institut fuer Polar - und Meeresforschung, Bremerhaven, Germany

ABSTRACT

Following a short introduction on the peculiarities of the Southern Ocean biological pump and the important role it plays in the global climate system, this paper reports results obtained from *in situ* surveys and open ocean perturbation experiments. These demonstrate the influence of mesoscale dynamics on structuring the regional distribution of biological production and its limitation by the availability of dissolved iron. In conclusion the need to consider the vertical dimension of biogenic carbon export to its full extent in mesoscale studies is emphasized.

INTRODUCTION

The research described below is motivated by the perception that the environment of the marine biota is shaped by physical processes. Physical processes act and influence the marine biota on length and time scales, ranging from the scale of molecular diffusion to the scale of the global ocean circulation. Physical processes regulate ambient temperature and salinity, the availability of nutrients and light, and the displacement and transport of organisms.

Vice versa, the marine biosphere influences the physical realm of the Earth's climate system by virtue of biologically mediated geochemical fluxes. The biological pump of carbon is probably the most prominent example of such an influence. Through primary production carbon dioxide is taken up in the sun-lit upper ocean layer. Part of this carbon is eventually transported to the deep ocean and sediment where biogenic matter precipitates, and then withdrawn from further contact with the atmosphere. Thus, the biological carbon pump exerts a control on the radiation budget of the atmosphere. Primary production also fuels growth at the highest trophic levels, and thus the living marine resources that are harvested by humans.

As regards an influence of the biological pump on global climate, the Southern Ocean is considered as being of particular importance. This view stems from the abundance of plant nutrients nitrate, phosphate and silicate, which are supplied to the surface photic zone in large amounts by the upwelling of deep water masses within the Antarctic Divergence, along the southern rim of the Circumpolar Current. The nitrate concentrations found here are the highest worldwide in the open ocean. Much of the nutrients are however subducted again, as they are left unused by phytoplankton primary production. This surplus of nutrients has prompted a wealth of hypotheses, according to which climatic changes in the Southern Ocean biological pump explain the glacial-interglacial variations in atmospheric CO2 concentrations (e.g. Neftel *et al*., 1982; Barnola *et al*., 1991; Francois *et al*., 1997). Changes in the biological pump might result from changes in stratification and hence light limitation, changes in sea ice cover, and changes in the

flow field affecting the macro-nutrient supply (e.g. Knox and McElroy, 1984; Sarmiento and Toggweiler, 1984; Siegenthaler and Wenk, 1984). The iron hypothesis (Martin, 1990), by which primary production in the open ocean is recently iron-limited but was higher during the dryer glacial periods when more of this micro-nutrient was deposited via wind blown dust, is now receiving much attention.

It was this enigmatic situation, the contrast of high nutrient concentrations to low primary production and phytoplankton biomass, termed Antarctic Paradox (for a review see de Baar, 1994), which caught my interest roughly 10 years ago. What follows below is not a representative review of the state of the art and knowledge, but rather a few aspects, heavily biased by my own experience.

HYPOTHETICAL PHYSICAL CONTROLS OF BIOLOGICAL PRODUCTION

In contrast to the overall low productivity, increased phytoplankton biomass apparently occurs in the lee of islands and along fronts in the Antarctic Circumpolar Current, notably at the Polar Front (e.g. Allanson *et al*., 1981; Lutjeharms *et al*., 1985; Bathmann *et al*., 2000). Production at the Antarctic Polar Front moreover appears accompanied by noticeable particulate downward export flux (Wefer and Fischer, 1991) and is reflected in biogenic silica-rich sediments (e.g. Bareille *et al*., 1991).

The reasons for the enhancement of productivity at the circumpolar fronts are not yet fully understood. Pollard *et al*. (1995) proposed to explain it by advection from possible upstream areas of high productivity. De Baar *et al*. (1995) suggested that the enhancement of primary production is related to the advection of iron-enriched water masses with the frontal jet. Based on ecosystem model results, Mitchell *et al*. (1991) made the case that an additional supply of iron would not significantly enhance primary production without a mechanism for increasing the strength of stratification. The rather systematic increase of phytoplankton biomass at fronts makes it likely that productivity is enhanced as a result of a process inherently linked to the physics of fronts. This view is supported by a closer look at synoptic satellite images of ocean colour, which reveal patterns of enhanced surface chlorophyll concentrations that resemble the typical mesoscale structures, with horizontal dimensions ranging from below 10 to above 100 km, of frontal meanders and eddies.

Earlier work on the influence of frontal physics on primary production has concentrated on mesoscale upwelling (Woods, 1988; Strass, 1994). Mesoscale upwelling was shown to cause patches of high phytoplankton biomass in oligotrophic environments, such as the North Atlantic in summer, by stimulating primary production through the upwelling of nutrients (Strass, 1992). Model studies (McGillicuddy and Robinson, 1997; Oschlies and Garcon, 1998; Spall and Richards, 2000) came to the same conclusion. In the macro-nutrient rich environment of the Southern Ocean, however, it is less likely that the vertical nutrient flux accomplished by mesoscale upwelling has a significant effect on primary production, although upwelling of the micro-nutrient iron could have an influence (Hense *et al*., 2003). For the Southern Ocean, where primary production is potentially light limited due to prevailing deep mixing (e.g. Tranter, 1982; Sakshaug *et al*., 1991), our first hypothesis was that the general enhancement of production at fronts results from stratification of the water column which is caused by mesoscale cross-front circulation related to baroclinic instability.

Although satellite images were extremely helpful in sharpening our hypotheses about the primary-production-controlling physical processes, it was very clear that, because they do not provide any vertical resolution but instead give an integral measure representative of just the top 10 to 20 m, they would not be suitable for a sincere hypothesis testing. Detailed conclusions about the physical processes that can enhance primary production along fronts can, however, be inferred from mesoscale field studies.

MESOSCALE SURVEYS

My first mesoscale survey of the distributions of physical, chemical and biological variables in the vicinity of the Antarctic Polar Front was performed in the austral summer 1995/1996 during

a cruise of R/V *Polarstern*. The basic measurements were made using an instrument package combining a towed undulator (SeaSoar, Chelsea Instruments) and a vessel-mounted acoustic Doppler current profiler (VM-ADCP, RDI 150 kHz NB), which allowed density and velocity to be measured simultaneously with other physical and biological variables down to 300-350 m depth. The SeaSoar was fitted with a CTD for hydrographic measurements of temperature, salinity and density, a Chelsea Instruments fluorometer, a light meter for measuring the subsurface solar irradiance in the spectral range of photosynthetically available radiation (PAR) and an optical plankton counter (OPC-1T, Focal Technologies Inc.). The vessel-mounted ADCP, installed in the ship's hull, measured profiles of horizontal current and acoustic backscatter in the upper 300 m. To complement the SeaSoar measurements in the upper 350 m, the physical structure of the Polar Front at greater depth was investigated with an array of hydrographic stations, at which a CTD was lowered and water samples for biological and chemical analysis were collected with the attached Rosette bottle sampler. To monitor the temporal variations of currents at a fixed position, a mooring was laid for the duration of the cruise. The mooring was equipped with rotor current meters, one acoustic current meter with CTD, and one upward-looking self-contained acoustic Doppler current profiler. (During a later expedition we deployed five moorings in the survey area in order to collect Eulerian time series at different locations relative to the front, on the northern and southern side as well as in meander troughs and ridges).

The mesoscale distributions of the vertical and ageostrophic horizontal velocities, which are usually too small to be measured directly with moored or vessel-mounted current meters, are inferred by combining the measured density and horizontal current fields and solving the ω-equation developed by Hoskins *et al*. (1978) for atmospheric research and first applied in oceanography by Leach (1987). Prior to diagnosis by use of the ω-equation we eliminated, contributions to the measured horizontal current field arising from high-frequency motions that do not relate to the mesoscale dynamics, inertial oscillations and semi-diurnal tides as revealed by the moored current meter records. Furthermore, the horizontal current field after elimination of high-frequency motions was constrained to be non-divergent and in geostrophic balance with the density field. A range of sensitivity tests (Naveira Garabato, 1999; Naveira Garabato *et al*., 2001) revealed that the spatial patterns of the solution of the ω-equation are highly stable, but the magnitude of the diagnosed vertical and ageostrophic motion is associated with an uncertainty of approximately 50%.

The distribution patterns of the physical variables were compared with the distribution of phytoplankton biomass (chlorophyll concentration), which was derived from measurements carried out with the fluorometer and an attenuance meter included in the OPC. The mesoscale distribution of primary production at the Antarctic Polar Front was calculated with a diagnostic model (Strass *et al*., 2002b), which used the measurements of global solar radiation, of the underwater light field, and of the chlorophyll concentration from the survey as input data. The model is based on photosynthesis-light relationships, with parameters taken from *in vitro* incubations performed (Bracher *et al*., 1999; Bracher and Tilzer, 2001) during the survey.

The quasi-synoptic surveys covered a meander structure of the front and a cold cyclonic eddy located to its south. The highest chlorophyll concentrations and primary production rates were found in a band of mesoscale patches aligned with the front and in a crescent-shaped tongue extending southward from the front along the leading edge of a meander ridge. The increased chlorophyll concentrations at the meander edge are explained by confluence of surface water which carrying phytoplankton populations that had developed under favourable light conditions. The crescent-shaped chlorophyll tongue was observed to merge with the band of patches aligned with the front at the up-stream edge of the cold cyclonic eddy. Here, at the site of eddy/front interaction, a characteristic pattern of ageostrophic cross-front circulation related to mesoscale upwelling and downwelling was identified. Consistent with the principle of potential vorticity conservation, upwelling was found to occur on the anticyclonic, equatorward side of the jet and downwelling on the cyclonic, poleward side in the frontogenetic situation. The associated cross-front circulation is characterized by poleward motion of light water at the surface and a reversed flow of dense water at greater depth; thus it contributes to stratification and thereby to a more favourable photic environment for the phytoplankton growing in the shallower mixed layer.

While the cross-front circulation varies on horizontal scales of less than ten to more than hundred kilometres and time scales of days to weeks, it is constrained to sites of available potential energy, i.e. fronts marked by sloping isopycnals. This finding corroborates the hypothesis that the enhancement of primary production is supported by the mesoscale frontal dynamics, in particular the cross-front circulation related to baroclinic instability (Strass *et al*., 2002a).

The mesoscale distribution of physical properties not only correlated with chlorophyll distribution pattern and with primary production, but also with the abundance of zooplankton in various size classes and even with the abundance of sea birds. Zooplankton abundance has been determined on the basis of net catches (Dubischar *et al*., 2002), OPC data (Pollard *et al*., 2002), ADCP backscatter measurements (Vélez-Belchí *et al*., 2002) and bird abundance by visual counts (van Franeker *et al*., 2002). An estimate of the carbon budget (Strass *et al*., 2002b) indicates that the modelled primary production rates are approximately balanced by the measured loss terms: grazing by zooplankton (Dubischar *et al*., 2002), bacterial uptake (Simon *et al*., 1997) and the downward export flux (Rutgers van der Loeff *et al*., 1997; Rutgers van der Loeff *et al*., 2002). The demand of birds and mammals was minor in this context (van Franeker *et al*., 2002). The approximate balance of carbon fluxes was consistent with the observed steady state of phytoplankton biomass during the investigation period.

The observed correlation of different trophic levels in the food web, from physics to top predators, leads to the conclusion that the mesoscale dynamics in the Antarctic Circumpolar Current sets the boundary conditions that determine the magnitude and rate of biological processes and hence ecosystem structure.

OPEN-OCEAN EXPERIMENTS

In order to test the iron hypothesis, we have so far performed two iron fertilisation experiments in the Antarctic Circumpolar Current with R/V *Polarstern*. The first, named EisenEx (after the German word for iron, Eisen), was performed from mid October to early December, 2000 (Smetacek, 2001); the other, EIFEX (European Iron Fertilisation Experiment), from mid January to mid March, 2004. The tests consisted of fertilizing a patch of water in the ACC with dissolved iron, pumped from the ship into the sea, and of monitoring for as long as possible the biological response to the addition of iron.

Both experiments were performed as close as possible to the Antarctic Polar Front, a key region in the global climate system. Since this front is associated with a swift and meandering frontal jet, conducting a controlled *in situ* experiment here is however demanding. A fertilized patch created within the frontal jet could easily be displaced 600 km downstream during a three-weeks experiment and would probably disintegrate along its path because of horizontal shears at the jets flanks and due to frontal instabilities. As a solution to this problem we conducted both experiments within a mesoscale eddy, a strategy that turned out to be successful.

The oceanographic measurements done in the course of the fertilization experiments were aimed at three particular objectives.

Objective 1: To identify a suitable site for the iron fertilization experiment.

The measurements aimed at identifying a stable eddy were made with an instrument package combining the vessel-mounted acoustic Doppler current profiler (VM-ADCP) with either a towed undulator (Scanfish) or a CTD (Conductivity Temperature Depth sonde). The ADCP+Scanfish/CTD package allowed the mesoscale density and velocity fields being mapped simultaneously with other physical and biological variables down to 200-300 m depth.

Using this instrument package, guided by information on sea surface height variability obtained from satellite altimetry before and during the cruise, we succeeded after one or two weeks of surveying to identify and map hydrographic structures which appeared ideal for conducting the experiment. Those structures were cyclonic eddies of 50 - 130 km width, shed by either the Antarctic Polar Front or the Southern Polar Front due to detachment of a northward protruding meander. Due to their origins, the eddies contained in their centres high concentrations of macro-nutrients typical of the Antarctic surface water masses.

Objective 2: To monitor the displacement and spreading of the fertilized water body subjected to advection and diffusion.

For that purpose, different measuring techniques were used in combination.

(a) A surface buoy drogued at 18 – 26 m depth, equipped with GPS receivers and radio as well as ARGOS satellite transmitters, was deployed in the centre of the eddy to aid the ship navigating in a Lagrangian manner while pumping the iron solution into the sea along a spiral-shaped track around the buoy in order to produce a fertilized patch as homogeneous as possible. After iron injection, the drift of the buoy as monitored via radio and ARGOS provided the primary source of information about the movement of the fertilized patch of water.

(b) For mapping the full extend of the moving patch the inert tracer SF_6 (Watson *et al*., 2001) was used as a marker substance during the first experiment, while a helicopter flown chlorophyll-sensitive LIDAR system was employed during the second.

(c) Numerous casts of a CTD sonde, attached to a rosette water sampler, were done for hydrographic profiling from the surface to intermediate and occasionally full ocean depths. The CTD rosette sampler was the major tool for supplying the various scientific groups on board with water samples for chemical and biological measurements. By performing repeated CTD surveys in the area at fine horizontal resolution of a few kilometres it was possible to map the three-dimensional distribution of those variables and their change in time.

(d) Measurements of currents by the vessel-mounted acoustic Doppler current profiler (VM-ADCP) were continuously made throughout the cruise and processed on board to monitor the mesoscale circulation.

(e) A tethered free-falling microstructure probe (MSS) was used for profiling small-scale turbulent motions down to 300 m depth. From these data the vertical distributions of turbulence parameters like overturning scales and vertical diffusivity were estimated (Cisewski *et al*., 2005).

(f) To continue to monitor the fertilized patch after the end of the second experiment, autonomous floats (VS-APEX) were deployed.

Objective 3: To provide a detailed description of the physical environment of the phytoplankton and zooplankton at the experimental site, and to provide the basic measurements needed for estimating fluxes of particulate and dissolved matter.

A three-dimensional combined circulation and ecosystem model with data assimilation was used to support the data analysis.

By using the combined information from different measurements we were able to follow the fertilized patches, which circled several times within the eddies, until we had to depart from our experimental site at the end of the cruise. Despite the motion and spreading of the patch it was possible to perform a controlled experiment. A three-dimensional assessment of the SF_6 inventory of the patch suggested a final content, which compared well to the initially released mass minus the estimated losses to the atmosphere.

Both experiments confirmed the hypothesized fertilizing effect of iron, even in rather deep mixed layers, with an estimated efficiency ratio of biogenically fixed carbon to iron added in the order of 1000. Moreover, the experiments revealed clear differences in the development of the various phytoplankton species, and a reaction of the zooplankton to the increased availability of food.

DISCUSSION: THE IGNORED 4th DIMENSION

The sampling strategies applied to mesoscale surveys (as those described above), are usually designed as a compromise between three opposing demands: first, coverage of horizontal scales as large as possible; second, horizontal resolution as fine as possible; third, a sampling as fast as possible in order to achieve synopticity. The typical result is an area of 100 x 100 nautical miles

squared, mapped with a horizontal resolution of 2 nm along-track and 10 nm between tracks, within 5 days which is far from being ideal. The horizontal coverage is just sufficient to cover one mesoscale feature like an eddy or half a meander. The spacing between tracks is hardly enough to resolve the smaller secondary instabilities, which however tend to be associated with the most vigorous upwelling and downwelling velocities (Strass, 1994; Rixen *et al*., 2003b). The time needed for mapping may be shorter than that needed by major mesoscale features to develop, but rather similar to the development time of smaller structures - the reason why many people are terming such mappings "quasi-synoptic". The vertical dimension is not considered a free parameter in the optimisation of the sampling strategy. So far almost everybody worked on the assumption that it is sufficient for physical-biological surveying to probe the vertical down to, say, a maximum of 500 metres.

However two recent surveys have revealed events of phytoplankton sedimentation that reached down to the ocean floor, at 4000 to 5000 m depth. One was a natural sedimentation event, the other was enhanced by iron fertilization. Both were mesoscale in horizontal extent, and developed on the time scale of days. While these observations are, of course, scientifically very exciting, they reveal a new problem for the mesoscale observer. They suggest that a 4th dimension, the vertical, has to be taken into account to its full extent.

Acknowledgements

More than 100 scientists from many institutes and various nations contributed to the results mentioned above. Foreign institutes also contributed major parts of the equipment used, such as the SeaSoar that was provided and operated by the Southampton Oceanography Centre (SOC) or the Scanfish from the Netherlands Institute for Sea Research (NIOZ). The data would not have been collected without the skilful help from the captain, officers and crew of R/V *Polarstern*.

Strategy to capture the influence of ocean dynamics on pelagic ecosystems

L. Prieur [1], G. Gorsky[1] and Y. Gratton[2]

[1] *L. O. V., CNRS, Villefranche sur mer, France*
[2] *INRS-ETE (Eau, Terre, Environnement), Québec, Canada*

Almofront 2, carried out in December 1997 - January 1998, is a very good example of a multidisciplinary experiment. We describe how this experiment, involving more than 50 physicists, chemists and biologists was carried out on the 85 m French oceanographic ship l'*Atalante*. Almofront 2 was the continuation of Almofront 1 (April-May 1991), carried out with less means but with a similar strategy (see Prieur and Sournia, 1994, and papers quoted within). The general objective of Almofront 2 was to understand why geostrophic density fronts bordering large oceanic jets appear more productive in terms of phytoplankton, zooplankton and carbon export (Lohrenz *et al*., 1988a and b; Olson *et al*., 1994) than their surrounding waters. The idea was to start observing such a mesoscale system at the beginning of the winter in the Eastern Alboran Sea, a region where the Atlantic water jet is known to generally circumvent a more or less developed anticyclonic eddy (Tintoré *et al*., 1988; Folkard *et al*., 1994; Allen *et al*., 2001b; Viudez *et al*., 1998). A major density front is usually observed on satellite thermal images where this system encounters the Mediterranean waters at the Alboran Sea eastern boundary.

Starting with this general idea, more precise objectives were defined within the framework of JGOFS-France. The process begun with a careful review of the mesoscale processes known to be present in the region (e.g. Bower *et al*., 1991; Onken, 1992; Zakardjian, 1994; Zakardjian and Prieur, 1998; Viudez *et al*., 1998). The final constraint was that the means to attain these objectives had to be realistic and deployable within a "reasonable" amount of time. The objectives were the following.

O1- To establish the mean scale of the physical and dynamical fields maintaining the Jet-Eddy Front (JEF) in order to describe the system's internal structure. These fields are: density, currents, potential vorticity and secondary circulation. This description must take into account the temporal evolution at a scale of a few days.

O2- To characterize the levels of primary and secondary productions and the nature of the organic matter export in the frontal system and its adjacent regions, i.e. the Mediterranean and Eddy waters. To determine if the changes in trophic pathways are related to the secondary circulation and/or the internal structure of the JEF.

O3- To describe the relations between the surface and deep ecosystems in terms of carbon export, and to assess the role of the vertical zooplankton migration.

O4- To quantify the organic and inorganic matter fluxes inside the JEF system and to determine the role of the oceanic front on the carbon and nitrogen budgets in the Alboran Sea.

O4 is an end product. It will be reached only after the first three prime objectives have been achieved. To attain the first three goals it was necessary to perform a scale analysis in order to elaborate the data acquisition strategy. O1 led us to sample the density and current fields with a resolution of a few km, i.e. 1/10 of the local internal Rossby deformation radius. This resolution was needed to characterize the potential vorticity and divergence fields, and thus the vertical velocities associated with the secondary circulation. Such a high resolution (~ 1 km) was obtained with the tow-yos. The tow-yo sections also needed to be long enough to sample both sides of the structure.

On the biogeochemical level (O2 and O3), it was decided to deploy means to illustrate the local ecosystem pathways (Figure 1) that will also be used as the building blocks of the post-campaign modelling studies. Long "Lagrangian" stations were selected. These stations lasted at least 48 hours in order to obtain significant measurements of primary production and vertical fluxes.

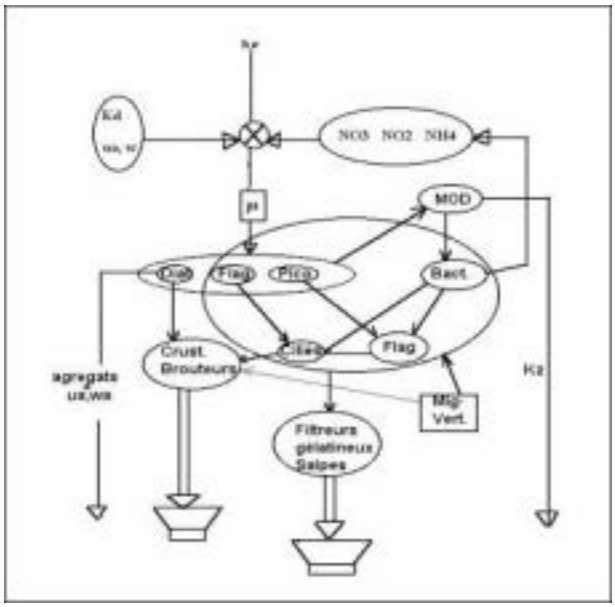

Fig. 1. Foodweb scheme with several trophic paths studied during Almofront2.

Assumptions had to be made to render the objectives attainable. The first assumption was that the JEF system was not unstable on the time scale of the observations (45 days). If the system happened to move slowly, the sampling strategy must be able to follow its displacement in real time. Therefore, it was necessary to divide the ship time into fast, high resolution surveys of a limited number of variables (i.e. tow-yo without nutrients), slower CTD-rosette sections with almost all variables, and much slower operations such as fluxes measurements and incubation experiments. The second assumption was that the secondary circulation is sufficiently effective to disturb the trophic system. That is, it must maintain itself for more than a few weeks as the reaction time of the primary producers and the microbial loop is of the order of a few days, while it is of the order of a few weeks for the secondary producers. To some extent, the trophic systems give the physicists information on the time scale of the phenomena which they seek to understand.

With these assumptions the strategy was to divide the ship time in two different parts or legs. A first leg was dedicated to space-time acquisition of the hydro-bio-geochemical parameters with high spatial resolution while a second leg was dedicated to the long operations of biogeochemical fluxes measurements in specific areas named "sites" inside the JEF system. Quick surveys at 10 knots were programmed to follow (with satellite information, ADCP and thermosalinograph) the evolution of the hydrodynamic structure.

Leg 1 (objectives O1 and O2). We performed an initial survey covering the whole study zone (Figure 2). The measured variables included currents (with an ADCP), temperature (T) and salinity (S) (with a thermosalinograph), and meteorological parameters. Two fixed lines of current meters and sediment traps were also deployed. The last 20 days were shared between two CTD sections with bottle samples (T, S, O_2, nutrients, fluorescence, pigments, alkalinity, pH, Freon, trace metals, bacteriology, bioluminescence, spectrum of the size of small and large particles) and three groups of sections (0-600 m) with our CTD tow-yo system without bottles (T, S O_2, fluorescence, beam attenuation). Another towed, prototype system, the THES, pumped water directly on board during profiling. It was used during three sections in the northeastern part of the JEF to obtain continuous profiles (0-200 m) of nutrients, pCO_2 and size spectra simultaneously, in addition to the classical physical parameters and currents.

Leg 2 (objective O3). This leg was dedicated to "on site" measurements during 36 hours to obtain estimates of the primary production fluxes, export by sediment traps, bacterial production, regeneration rate, while supervising the evolution of the hydrodynamic and chemical structures. A line of two sediment traps was deployed at the beginning of each site. Its drift was followed during 36-48 hours during which CTD and water sampling was undertaken. At the same time primary production (carbon and nitrogen and oxygen) flux experiments were conducted onboard or by deploying another line of incubation bottles. Eight sites were selected, including six along a transect through the JEF system and two others, one upstream and one downstream of the crest of the meander (Figure 2).

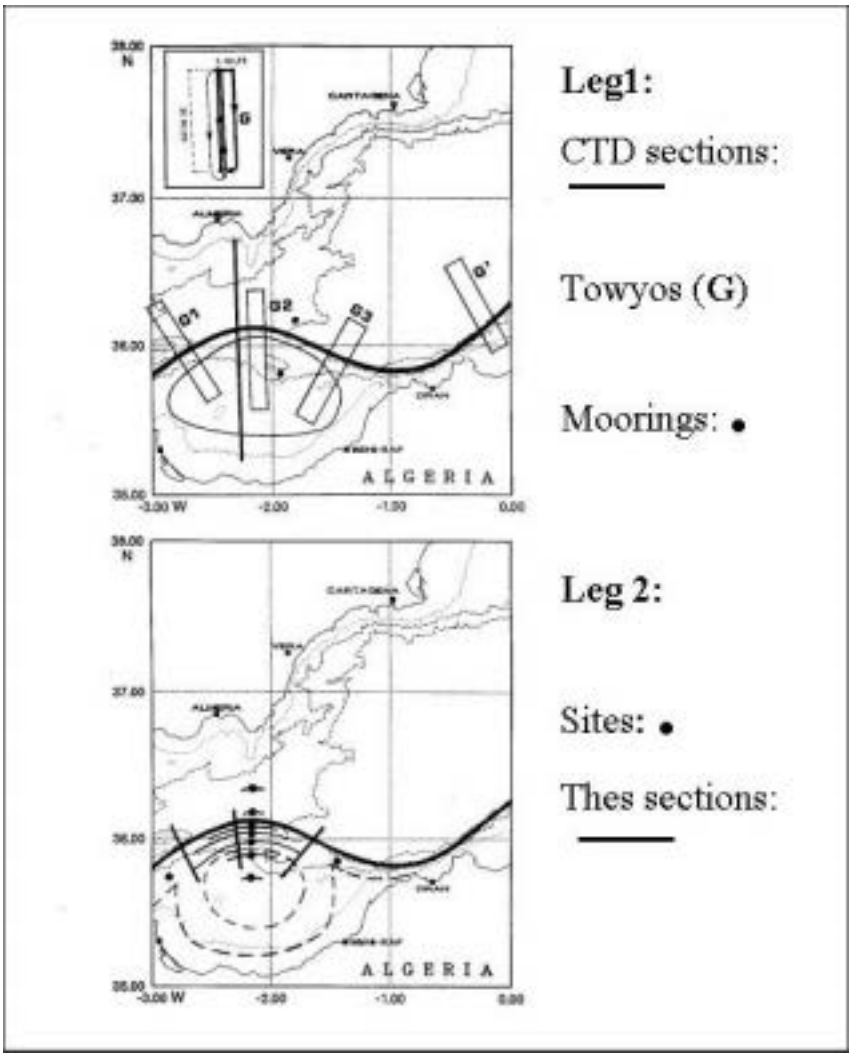

Fig. 2. Location of study sites.

RESULTS

The first survey identified a density front with a jet meandering around a well developed anticyclonic eddy. This structure appeared stationary during all leg 1. However, early in leg 2 the whole system drifted towards the East-North-East with a velocity of approximately 5 cm/s. Thanks to the thermosalinograph, ADCP and imagery surveys, various sites with the desired characteristics could be located. These sites were not simply positioned perpendicularly to the JEF. Using information on current and density fields we positioned each site within a typical dynamic structure corresponding to the stationary JEF system observed during Leg 1. *A posteriori* analysis enabled us to reposition the sites within Leg 1's JEF structure. This analysis also made it possible to highlight the fact that intra-site variability was clearly lower than the inter-site variability (Prieur and Sournia, 1994) and that different zones of the JEF were effectively explored during Leg 2. These sites could also be positioned on the THES section that was carried out across the meander and the eddy at the end of Leg 2 (Figure 3). Finally, it could be confirmed that the sediment traps drifted along streamlines in every instance.

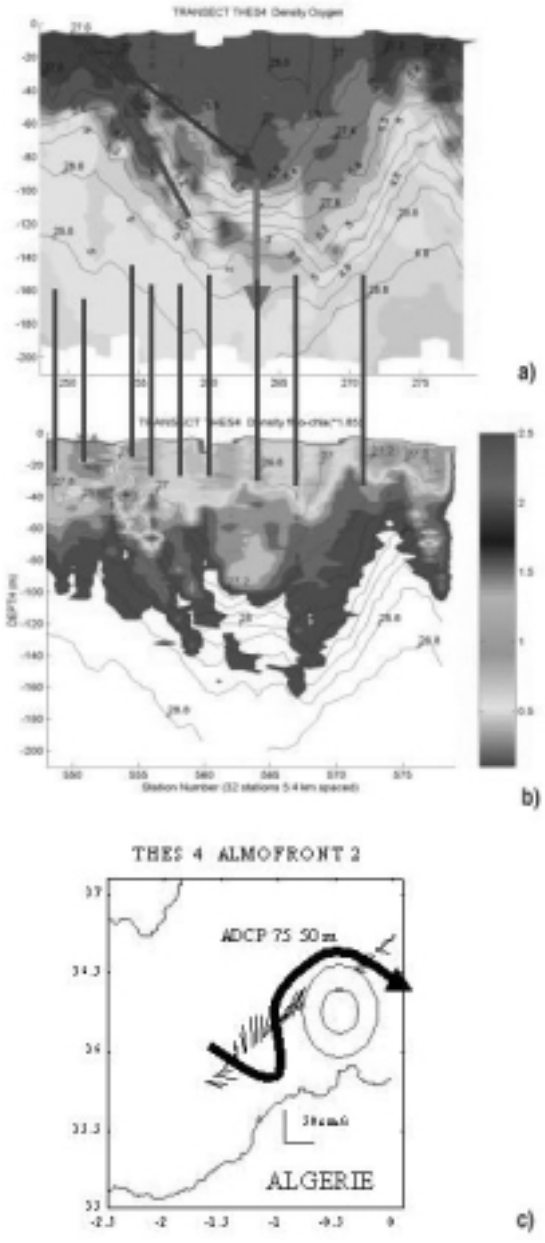

Fig. 3. Oxygen (a) and fluorescence (b) profiles across the eddy structure (c).

Thanks to this strategy we were able to determine that the JEF had similar internal structures in both stationary and moving phases. The cyclonic side of the jet (the left part of the oxygen and fluorescence sections presented in Figure 3) exhibited the strongest autotrophic activity and the largest abundance of micro-phytoplankton represented by diatoms (Leblanc *et al*., 2004). The bacterial growth changed its limiting factor from Mediterranean waters (P limited) to the centre of the eddy (DOM limited, Van Wambeke *et al*., 2004). The herbivorous meso-zooplankton was reproducing and was not food limited in the centre of the jet (Gaudy *et al*., 2002), whereas the gelatinous plankton was more abundant in the eddy. A strong vertical export of particulate organic matter and a very high large particles content was found in the Eddy (vertical arrow in Figure 3) whereas the vertical export was weak on the jet cyclonic side where the primary production was the highest and the nutrients not completely consumed in the surface waters. Other indications (not shown) of that have been observed as well. They are compatible with a rather strong transfer of progressively ageing matter (Tolosa *et al*., 2001) along the slanting isopycnals from the jet cyclonic edge towards the central part of the eddy (the publications on Almofront 2 are available through the following ftp address:

oceane.obs-vlfr.fr/pub/prieur/almofront/almofront2/almofron2_pubrapp/pubalmofront/pub_parues/

or on the Pr

http://www.obs-vlfr.fr/proof/index_vt.htm

All the results confirm the observations reported in Gorsky *et al*. (2002) that surface mesoscale hydrodynamic structures are areas of contrasted export of organic carbon: some zones of very weak export are located close to high export sites due to mesoscale ecosystem activity driven by physical processes and secondary circulations.

This simplified presentation does not take into account the complex fields of various secondary circulations. This secondary circulation will be inferred from the 3D fields of currents and mass by using a complete analysis in Q vector (Giordani and Planton, 2000). Such a Q vector analysis was performed by Allen *et al*. (2001b) using QG approximation on data obtained one year before Almofront 2 in the same area.

PERSPECTIVES

New means are now available that will make it possible to re-examine the strategy of biophysical observations in the future. Operational models are becoming increasingly powerful, as real-time data are provided. However, in order to reach the high resolution necessary to study the processes related to primary production and trophic webs in the open ocean, new or improved instrumentation will have to be deployed: MVP (Moving Vehicle Profiler: a modified tow-yo system), gliders, autonomous systems for exploration of the submesoscale physical structures. Bio-optics, zooplankton counters or imagers should be mounted on these autonomous vehicles. These improvements will greatly increase the efficiency of the information available during the long ship-based stations required to gain sufficient information on the fluxes between the different food-web components. This on the other hand will considerably increase the costs of observational systems and the time necessary for processing the data.

Comparing the time scales of physics and biology in mesoscale dynamics

Maurizio Ribera d'Alcala', Serena Esposito, Mariella Ragni and Vincenzo Vellucci

Laboratory of Biological Oceanography, Stazione Zoologica 'A. Dohrn', Napoli, Italy

ABSTRACT

A proper estimate of the vertical velocities associated with mesocale instabilities in the ocean and the perception of their relevance in biogeochemical processes are relatively recent acquisitions in marine science. Numerical approaches and indirect estimates based on *in situ* data robustly demonstrate that mesoscale instabilities can generate a vertical transport of nutrients which may significantly enhance primary production while displacing organisms over time scales of the same order of magnitude of their physiological responses. Both processes have been analyzed in numerous studies but the extent to which the peculiar dynamics which occur in mesoscale instabilities, through nutrient supply and light field modulation, favour certain taxa versus others has not been addressed so far. An analysis of the rates of biological responses over the time scales characteristic of mesoscale structures, conducted by means of existing mechanistic models of plankton physiology, shows that changes in nutrient concentrations and light availability should not be able to produce the dominance of a specific taxon. By contrast, the very few studies where species information is available for such structures show the presence of species much more abundant than others. Factors determining the species spectrum of phytoplankton communities are still elusive and mesoscale instabilities may be proper systems where addition al insight could be gained.

Any pulse of CO_2 assimilation by marine autotrophs ultimately depends on a photosynthetic event which, in turn, requires light and essential nutrients in quantities so as to satisfy the approximately fixed ratios in the elemental composition of the organisms. Afterwards, the organic material may be channelled through the food web along paths which depend on the space and time covariance of the other components, and their typical response times.

During the last two decades the relevant mechanisms producing nutrient enrichment of the photic zone have been analyzed in much more detail than before, due to the continuous improvement of observational and numerical tools allowing the analysis of key processes with a better resolution both in space and time. This has also been the case of mesoscale processes whose dynamics has been observed by multi-sensor arrays on undulating towed vehicles sampling the tridimensional field of the hydrodynamic variables and reconstructed by fine grid numerical models.

Mesoscale structures, e.g., eddies, fronts, etc., form in many oceanographic contexts and span over at least one order of magnitude in size and two orders of magnitude in lifetime. Depending on the specific scales and patterns of the 3-D distribution fields of hydrographic properties, e.g.,

nutrients, in which they form, they contribute to nutrient injection in nutrient poor surface water, either vertically or horizontally (e.g. Lima *et al*., 2002). However the mechanisms and the quantification of the enrichment process have not yet been conclusively assessed (Lévy, 2003).

In addition of acting as a nutrient pump, mesoscale structures may vertically displace organisms, (Taupier-Letage *et al*., 2003), may generate strong horizontal gradients in the composition of biotic components (Rodriguez *et al*., 2003 and references therein) or may isolate and favour retention of organisms for periods as long as months (Halvorsen *et al*., 2003).

Most studies on the coupling between mesoscale activity and biota have focused on the role of the latter in enhancing primary production in otherwise oligotrophic areas (Martin and Pondaven, 2003), though recent numerical studies suggest that mesoscale and sub-mesoscale processes could play a critical role even in highly productive regions (Lévy, 2003).

For example in the North Western Mediterranean Sea the large scale isopycnal doming due to the cyclonic circulation and the formation, during winter, of deep convection patches drive a highly variable large scale density field. Quite often, at the time of the occurrence of deep convection, a large scale phytoplankton bloom is already in place (Figure 1). Because of the interplay between the eddy field and the surface buoyancy fluxes an extremely complex dynamic evolution originates. The associated vertical velocity field is highly variable and often intense, thereby modulating isopycnal displacement, and vertical mixing. Those, in turn, play an important role in shaping the structure and the functioning of plankton communities.

A non-systematic analysis of satellite data relative to the April 2000 *in situ* survey has revealed the presence in the NWMed of a variety of mesoscale/submesoscale structures: filaments exporting (and perhaps producing) Chlorophyll-rich water toward oligotrophic waters to the south, fast and energetic mushroom-like structures entering the bloom waters from the surrounding areas, frontal meanders and associated instabilities, and finally oligotrophic anti-cyclonic eddies in the order of 100 km originated by the Algerian Current which reach the North Balearic Front (Figure 1).

While the nutrient enrichment due to the winter intermediate convection in the area is the main driver of the bloom, the superimposed mesoscale dynamics is probably a main determinant in modulating the bloom time course, in terms of total production, composition and fate.

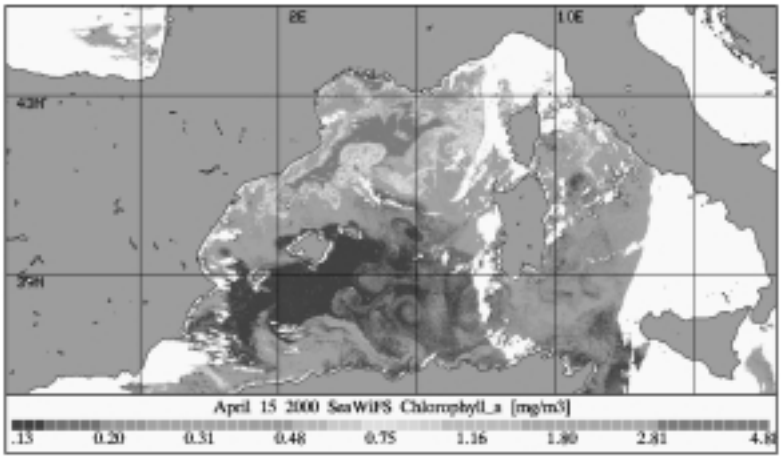

Fig. 1. (See page 109 for original color plate) NW-Mediterranean bloom and deep convection area.

The vertical components of water movement associated with mesoscale and sub-mesoscale dynamics refuel the photic zone with nutrients or dilute it both for nutrients and cells, changing the light environment of autotrophs, increasing or decreasing the average irradiance, eventually modifying its spectral properties, thus imposing highly variable conditions for cell growth. Those changes certainly affect many photobiological and nutritional responses of phytoplankters. As a result mesoscale dynamics not only modulates biomass production but also its specific composition.

As mentioned above, while the first effect has been widely analyzed, the second is still largely unexplored.

If we consider only three biological traits of phytoplankton biology (responses to change in irradiance, nutrient concentration and life cycle), the typical scales span from hours to days, for the first two, to weeks or months for the last one. They all depend on the match-mismatch between vertical velocities and the typical time scales of the biological responses.

Table 1 presents the time scales of some photo-dependent responses of phytoplankton.

Table 1. First order kinetic coefficients for the indicated pigments and processes under different light conditions (LL to HL ≡ transition from Low Light to High Light, HL to LL ≡ reverse transition, 12L:12D ≡ Illumination cycle of 12 hours of light and 12 hours of dark, Dtx ≡ Diatoxanthin, Chl *a* ≡ Chlorophyll *a*, Fucox ≡ Fucoxanthin, Ddx ≡ Diadinoxanthin).

Light regime	Photodependent parameter			Location/species	Reference
	Dtx/Chl a		*Ddx/Chl a*		
LL to HL	0.59 h^{-1}		0.66 h^{-1}	Gulf of Naples	Brunet *et al*., 2003
HL to LL	0.38 h^{-1}		0.27 h^{-1}		
HL to LL			0.52 h^{-1}	Alboran Sea	Claustre *et al*., 1994
	Chl a/cell		*Fucox/cell*		
LL to HL	0.32 d^{-1}		0.32 d^{-1}	*S. costatum*	Anning *et al*., 2000
HL to LL	0.36 d^{-1}		0.36 d^{-1}		
	Chl a	*Fucox*	*Ddx*		
12L:12D	1.11 d^{-1}	1.05 d^{-1}	0.92 d^{-1}	*P. tricornutum*	Ragni, 2005
Natural light	*Photorepair*			Antartic phytoplankton	Cianelli *et al*., 2004
	3.8 d^{-1}				

The synthesis of photoprotecting carotenoids during light transitions (Brunet, 2003; Claustre *et al*., 1994) and/or the repair mechanisms of damaged photosynthetic reaction centers (Cianelli *et al*., 2004) have time scales in the order of hours, which may be appropriate or too slow for vertical speeds in the order of 0.2-2 m/h and attenuation coefficients in the order of 0.05-0.1 m^{-1}.

Changes in the pool of light harvesting pigments (e.g., chlorophyll *a* and fucoxanthin) subjected to light shifts are definitely slower (Anning, 2000). A comparative assessment of the dependence of cell growth rates on changes in the optical cross section versus efficiency in dissipating excess energy has not yet been accomplished. It would be reasonable to assume that in highly dynamic mesoscale systems photoprotective responses should be more important than changes in photocapturing capability.

Adaptation to a variation in nutrient concentration may be equally important. Existing physiology-based mechanistic models show that physiological changes to pulses in nutrient concentration are in the order of a day (Flynn *et al*., 1997). This may be another factor of selection for certain species against others in a phytoplankton bloom according to the time course of environmental variables in that specific site.

Finally, species displaying life cycles which depend on sexual reproduction (e.g., diatoms) after several divisions may be favoured if the time scale of the overall cycle matches the typical scales of the mesoscale structure.

The inferences sketched above cannot be supported by observations because there are few reports describing the species composition associated with an increase in phytoplankton in a mesoscale structure. As a matter of fact, during an intensive study at the Antarctic Polar Front the dominance of one single diatom species (*Thalassiotrix antarctica)* was observed in a cyclonic meander of the front (Smetacek *et al*., 2002; Strass *et al*., 2002a), but the interpretation of that pattern mostly relied on resistance to grazing pressure.

Other mechanisms favouring one algal group versus another may involve sinking velocities of cells. In fact, it has been recently reported that mesoscale processes affect the size spectra of the plankton community (Rodriguez *et al*., 2001) with strong implications on the structure of the

food web. In this context it is worth noting that such processes display an intermittent behaviour that cannot be adequately parameterised by average properties. In other words, there is a wide range of scales that embed the short and the medium term acclimation of primary producers to a variable physical dynamics.

Because most planktonic organisms are microscopic ($<10^{-2}$m), the outcome of processes at the typical scales of the mesoscale, is also affected by processes at '*Sub Grid Scale*', which is the scale proper of those organisms. The interaction among the two affects macroscopic biological processes such as biomass build-up, consumption, species abundance, succession, etc.

To summarize, diverse physiological responses of phytoplankton triggered by the specific spectrum of variance of a mesoscale structure may drive species patterns and succession which are also modulated by the parallel response of grazers to the same spectrum through their relative abundance and selective grazing pressure. Overall, since mesoscale dynamics matches typical times of biotic responses, from short term adaptations to seasonal reproductive cycles, it may select for specific species spectra and communities. A consequence of this is a different flow of energy and matter in the food web, which affects CO_2 withdrawal, the amount of utilizable resources by our society, etc.

It is definitely relevant to analyze evidence of qualitative differences determined by different mesoscale dynamics and to discuss possible techniques to reconstruct what is the impact of the biological controlled spectral window as highlighted by Lewis (2002).